First Principle Study of Ions in water and Ionic Liquids

Dissertation

zur Erlangung des Grades

"Doktor der Naturwissenschaften"

im Promotionsfach Chemie am Fachbereich
Chemie, Pharmazie und Geowissenschaften

der Johannes Gutenberg-Universität

in Mainz

Christian Krekeler

geb. in Holzminden

Mainz, April 2008

Tag der mündlichen Prüfung: 03. Juni 2008

List of Publications

Parts of this thesis lead to the following publications:

1. C. Krekeler, B. Hess and L. Delle Site, J. Chem. Phys. **125**, 053405 (2006).
2. C. Krekeler, L. Delle Site, J. Phys.: Condens. Matter **19**, 192101 (2007).
3. C. Krekeler, L. Delle Site, J. Chem. Phys. **128** (13), online, (2008).
4. B. Qiao, C. Krekeler, R. Berger, L. Delle Site and C. Holm, J. Phys. Chem. B **112**, 1743-1751 (2008).
5. C. Krekeler, J. Schmidt, Y. Y. Zhao, B. Qiao, R. Berger, C. Holm and L. Delle Site, *submitted to J.Chem.Phys.* (2008).

Contents

1 Abstract

In this work the density functional theory in the framework of Car-Parrinello molecular dynamics (CPMD) was applied on the properties of two systems, (1) hydrated ions and (2) ionic liquids. These two systems show a larger number of properties and applications exceeding those from other systems. That is why they are important in our life (water) or of increasing importance (ionic liquids). The method was the multiscale modeling, which combines the results for different length scales. For water the electronic and the atomistic level was described. The results showed that water-water interactions are dominant with respect to the ion-water interactions at the electronic and the atomistic scale, and that the ion influence can be described as geometrical ordering in the first shell. Furthermore from the results one can suggest that standard non-polarizable water models are sufficient to study the hydration of ions. In case of ionic liquids the results showed that the hydrogen bonding was found to be important and the electrostatic description of the classical models has to be adjusted. In general the connection of the microscopic mechanism shown in this work and the large scale properties is particularly useful for further theoretical investigations, on the quantum level (either high level quantum and/or DFT calculations) and on the molecular level (CPMD and/or classical MD). The results for the ion hydration and ionic liquids may play a crucial role for further molecular modeling and simulations.

2 Zusammenfassung

Die beiden in dieser Arbeit betrachteten Systeme, wässrige Lösungen von Ionen und ionische Flüssigkeiten, zeigen vielfältige Eigenschaften und Anwendungsmöglichkeiten, im Gegensatz zu anderen Systemen. Man findet sie beinahe überall im normalen Leben (Wasser), oder ihre Bedeutung wächst (ioinische Flüssigkeiten). Der elektronische Anteil und der atomare Anteil wurden getrennt voneinander untersucht und im Zusammenhang analysiert. Mittels dieser Methode konnten die in dem jeweiligen System auftretenden Mechanismen genauer untersucht werden. Diese Methode wird "Multiscale Modeling" genannt, dabei werden die Untereinheiten eines Systems genauer betrachtet, wie in diesem Fall die elektronischen and atomaren Teilsystem. Die Ergebnisse, die aus den jeweiligen Betrachtungen hervorgehen, zeigen, dass, im Falle von hydratisierten Ionen die Wasser-Wasser Wechselwirkungen wesentlich stärker sind als die elektrostatischen Wechselwirkung zwischenWasser und dem Ion. Anhand der Ergebnisse ergibt sich, dass normale nicht-polarisierbare Modelle ausreichen, um Ionen-Wasser Lösungen zu beschreiben. Im Falle der ionischen Flüssigkeiten betrachten wir die elektronische Ebene mittels sehr genauer post-Hartree-Fock Methoden und DFT, deren Ergebnisse dann mit denen auf molekularer Ebene (mithilfe von CPMD/klassischer MD) in Beziehung gesetzt werden. Die bisherigen Ergebnisse zeigen, dass die Wasserstoff-Brückenbindungen im Fall der ionischen Flüssigkeiten nicht vernachässigt werden können. Weiterhin hat diese Studie herausgefunden, dass die klassischen Kraftfelder die Elektrostatik (Dipol- und Quadrupolmomente) nicht genau genug beschreibt. Die Kombination des mikroskopischen Mechanismus und der molekularen Eigenschaften ist besonders sinnvoll um verschiedene Anhaltspunkte von Simualtionen (z.B. mit klassische Molekular-Dynamik) oder Experimenten zu liefern oder solche zu erklären.

3 General Introduction

Solvents and liquids are essential for our daily life; they are important for a wide range of fundamental processes due to their various properties. These can range from density anomaly (highest density at 4^o), melting (273.15 K) and boiling point (373.15 K) (water) to low melting, nano-structures, no vapor pressure, high conductivity, low viscosity, etc. (ionic liquids) and many more. Solvents/liquids can be studied both with experimental and theoretical methods, which in general focus on single aspects of solvents/liquids (for example structural distribution of water around an ion or the global radial distribution functions). But the interplay between these single aspects, the local ones (electronic and molecular descriptions) and the global ones (the interaction of the local structures with the surrounding molecules) is rarely discussed, even though this interplay is necessary to understand the properties of solvents/liquids like water for instance. We will address two solvents/liquids in this work: (1) one of the most important solvents, water, and (2) the ionic liquids, which is a field of growing interest.

Water is one of the simplest and most relevant molecules in nature, in particular in biology and chemistry its special properties are of great importance. In cell biology all the mechanisms are depending on the presence of water, which solvates the different substances, is involved in the transport of ions through specific channels and delivers protons to store energy (e.g. NADH+H^+). In chemistry water is used as solvent for a wide range of inorganic and organic compounds, while in organic chemistry water is not only a solvent, but instead certain processes for instance depend on the phase separation of water and organic solvents, e.g. the asymmetric epoxidation of allylic alcohols to epoxy alcohols. The solvation of positive ions, which will be presented in this work are also of great importance in biology, chemistry, physics and technology.

This is only a small selected list of possible range of applications. Therefore it is important to have a detailed knowledge about the properties of water by itself and as a solvent. In fact water is a protic-polar molecule, due to the highly

polar oxygen-hydrogen covalent bonds. This leads to a permanent dipole moment and the formation of hydrogen bonds. However, we will discuss the hydration of ions mainly with respect to the changes of the molecular water dipole moments and its components, from the first solvation shell to the bulk and their interplay. The general problem is that experiments cannot provide a detailed description of water properties. Nowadays, it is possible to partially determine the structures of water around an ion, and separately the radial distribution function of the whole system using experimental techniques. Using theoretical methods and combining the different scales will give us the advantage that we can look at properties of the whole system and at the same time in a selected regions.In this way we can reproduce experimental data at the different length scales and at the same time we can study the interplay of the different scales. This will lead to a more detailed description of the system and the mechanisms therein. The disadvantage so far is that the system size is limited, which means the size is much smaller than for classical simulations but still larger than for *ab initio* calculations (like e.g. Møller-Plesset perturbation theory (MP2), couple cluster (CCSD(T))). The goal of this work is to understand the behaviour of the small clusters of the system, the whole system, and the interplay of these two, which will at the end lead to a general scheme for hydration of ions. With this scheme one can get a deeper insight into solvation and one can better understand why certain classical water models are doing well to describe hydration, while others do not. The small clusters are build by stepwise adding water to the ion to reach a full first solvation shell, while the whole system can be studied solvating the ion in a cubic box with a larger number of molecules (up to 128 water). Then the dipole moments, its orientations with respect to the ion-oxygen direction and the electronic (lone pair, bonding pair and oxygen-hydrogen) contributions to it were calculated. The picture emerging from that study then shows that the water-water interaction is dominant compared to the ion-water interaction, starting at the electronic level and continuing at the atomistic level. This is counter-intuitive to the general believe, which is that the ion-water interaction is very strong (depending on size and charge) in the first shell (or better at the local scale).

In the same spirit we use high level quantum, DFT and clasical MD to study the ionic liquids (IL's) or molten salts. The temperature and the structural criterion have been introduced to distinguish between ionic liquids and molten salts. The latter ones are high-melting, highly-viscous and very corrosive. The ionic liquid

instead are low melting (mostly below 100 ^{o}C) and have relatively low viscosity, while another definition also includes the difference between ionic-covalent crystalline structures.

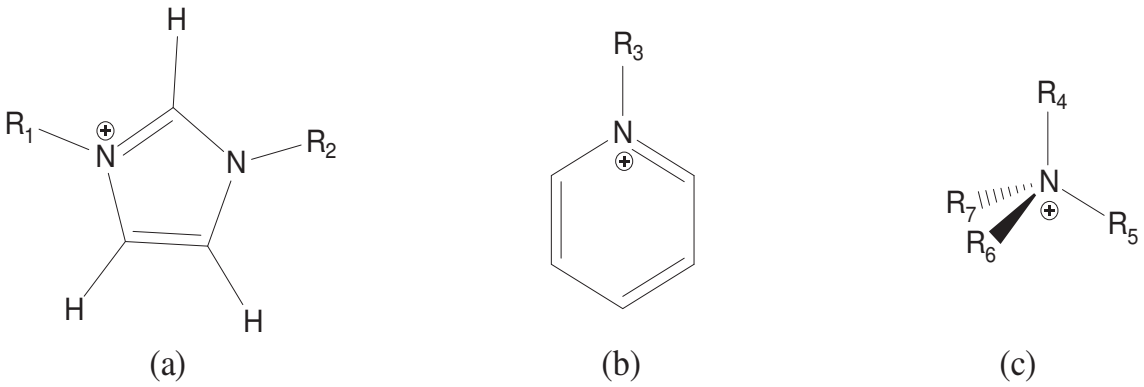

Figure 3.1: Selected examples of quaternary ammonium with two aromatic systems (a): Imidazolium ring (aromatic); and (b): pyridinium cation(aromatic); and the prototype (c): quaternary ammonium. The residues R_i(i=1,..,7) can be chosen, from alkyl-groups to more complex side-groups, such that systems with completely different properties can be designed. Another method to influence the properties of ionic liquids is the choice of the anion, from single halides to very complex anions.

Ionic liquids can be designed/synthesized to show a large variety of properties, even more than normal organic solvents show. They can be tuned by changing the positively charged part (most common IL have the positive charged imidazolium ring as center compound) as well as the anions and side groups. This means the solvent can be designed to match every purpose. Furthermore they are very stable and environmentally friendly, so they can be used in all kind of processes without losses. This leads to a broad range of applications no other organic solvent can access. In the last two decades the ionic liquids became more and more popular out of these reasons. There are several different molecules for which the definition of ionic liquids is true. Most common ones are based on compounds involving quaternary nitrogens; a small selection is given in Fig. 3.1.
The ionic liquid we started to study is the simplest one, 1,3-dimethyl-imidazolium chloride. The final goal of the project on ionic liquids is to have a consistent multiscale description of them using three different methods. On the electronic scale *ab initio* methods will be used along with density functional theory (DFT) and the atomistic scale will be described by DFT (or better the planewave pseudopo-

tential approach of DFT embedded in CPMD) and classical molecular dynamics (MD). The *ab initio* methods are very accurate to describe the electronic level and the local chemistry, but they are computationally very demanding and therefore limited to small molecules or clusters. In case of ionic liquids the effort to even look at a system of two cations plus two anions is tremendous. The DFT calculations cannot compete with the accuracy of the *ab initio* methods but the electronic level can be described with the electronic density and much larger systems can be treated. With this one can capture the electronic and the atomistic scale (to some extend), even though this methods is not as computationally demanding as *ab initio* methods but still not as ¨cheap¨ as classical MD. The MD is using classic force fields, which embedded the electronic description already but cannot capture the insight into electronic description. The MD provides information concerning large scale properties, like conformational and dynamical ones, with much less computationally costs as the two other methods. The best approach is iteratively combine these methods such that at the end a consistent view from electronic to atomistic scale results. However, the goal of this study so far was to provide more insight into the electronic description of the ionic liquids, since little is known until today. Therefore the optimized geometries, total energies and harmonic frequencies of selected clusters of 1,3-dimethylimidazolium chloride were calculated. We found that the results from the density functional theory and the MP2 calculations show good agreement. Furthermore we looked at the electrostatic moments, the dipole and quadrupole moment, of several clusters (one cation plus on anion; two, four and eight cations plus anions). With this we could even link the results from density functional theory and thus also from *ab initio* data with results from classical simulations.

4 Theoretical Details

4.1 Introduction to First Principle Methods

The simplest approach to simulate liquids is treating molecules as classical rigid particles with assigned charges and a given interaction potential. This classical ansatz allows for the description of properties and the physics at macroscopic level. However, interactions based on very strong electronic nature interactions cannot be described with classical mechanics in a proper and accurate way. Therefore quantum mechanical approaches have to be included to describe the physics and behaviour at the electronic scale. Simulations based on quantum mechanics are in general called first principle or *ab initio* methods. They include the quantum chemical approaches, like Hartree-Fock (HF) and those based on its improvement as, e.g. pertubation theory (e.g. MP2), configuration interaction (CI) and coupled cluster (CC) method, [1–6] and more physical method density functional theory (DFT).[7–13] All methods have the same background, the electronic Hamiltonian has to be solved for a given configuration $\{\mathbf{R}_I ... \mathbf{R}_N\}$ with the charges $\{Z_I ... Z_N\}$:

$$\hat{\mathcal{H}} = \hat{\mathcal{T}} + \hat{V}_{el,el} + \hat{V}_{N,el} \tag{4.1}$$

$$= -\sum_{i=1}^{n} \frac{\nabla_i^2}{2} + \sum_{i \leq j}^{n} \frac{1}{|\mathbf{r}_i - \mathbf{r}_j|} - \sum_{I}^{N} \sum_{j}^{n} \frac{Z_I}{|\mathbf{R}_I - \mathbf{r}_j|} \tag{4.2}$$

where:
n = number of electrons
N = number of nuclei
$\hat{\mathcal{T}}$ = kinetic energy of the i-th electrons
$\hat{V}_{el,el}$ = electron-electron interaction
$\hat{V}_{N,el}$ = nuclei-electron interaction

The Hamiltonian here given is in atomic unit (a.u.), i.e. the quantities m_e, $\hbar$, a_0

are set equal to 1. Then the time independent Schrödinger equation Eq. 4.3 for the ground state using this Hamiltonian has to be solved.

$$\hat{H}\psi(r_1,..,r_n) = E\psi(r_1,..,r_n) \tag{4.3}$$

The solution will give the many-body wavefunction $\psi(r_1,..,r_n)$, whose form is known only for a few cases, e.g. the hydrgon atom, He^+ and H_2^+. Based on this equation the electronic density is given as:

$$\rho(\mathbf{r}) = N \int d\mathbf{r_2}...d\mathbf{r_n}|\psi(\mathbf{r}_1,..,\mathbf{r}_n)|^2 \tag{4.4}$$

This is a general formalism, which in principle can completely describe every system in detail. But up to today there is no practical way to solve exactly the equation analytically nor numerically for many-body systems. The above mentioned methods like Hartree-Fock and the so called post-Hartree-Fock methods are solving the eigenvalue equation numerically with the help of a Slater determinant constructed out of a chosen set of one particle orbitals. Another important method today is, besides the HF theory, the density functional theory (DFT). This approach solves the Schrödinger equation in a different way than the HF based methods. In contrast to this the DFT is using the electronic density ρ as the main quantity and the energy is defined as a functional of this electronic density. In the following DFT is refered to be a first principle method. Its advantages are the fact that it is accurate and efficient to describe large systems and (as will emerge later on) its statistical properties. In the past few years DFT was applied to several systems and problems with great success. Whereas the methods based on HF are, even though they are very accurate, still computationally extremely demanding. They can be applied to molecules or clusters with a small limited number of electrons in a very efficient way. Unfortunately large molecules or liquids cannot be treated today by these methods.

4.2 Density Functional Theory

The density functional theory (applied today) has its basis in the Hohenberg and Kohn [9] theorems. The 1^{st} theorem states that a ground state of an N-particle system is completely characterized by the single-particle density $\rho(r)$. This means

that the external potential $\mathcal{V}(r)$, ψ and all ground state properties are unique functionals of the density.[14] The 2^{nd} theorem states that there is a universal energy functional $E_{\mathcal{V}}[\rho]$ for a given external potential $\mathcal{V}(r)$. This functional can be minimized using the variational principle with respect to the electronic density $\rho(\mathbf{r})$. With this ansatz the ground state electronic density ρ_0 and the corresponding ground state energy E_0 could in principle be determined.

$$E_0 \leq E[\rho(\mathbf{r})] \tag{4.5}$$

The energy functional then can be written as:

$$E[\rho(\mathbf{r})] = \mathcal{F}[\rho(\mathbf{r})] + \int d\mathbf{r}\rho(\mathbf{r})V(\mathbf{r}) \tag{4.6}$$

Where $\mathcal{F}[\rho(\mathbf{r})]$ is a universal functional, independent from the external potential, and for a given system it is unique. Furthermore the density becomes much more important than the 3N dimensional wavefunction $\psi(\mathbf{r}_1,\mathbf{r}_2,...\mathbf{r}_N)$, which is in general not known; therefor approximations are required.
Kohn and Sham [10] later on introduced the use of basis sets in DFT, which circumvent the problem in part $\mathcal{F}[\rho(\mathbf{r})]$. They suggested to write:

$$\mathcal{F}[\rho] = \mathcal{K}[\rho] + V_{ee}[\rho] + E_{xc}[\rho] \tag{4.7}$$

$\mathcal{K}[\rho]$ represents the kinetic energy functional of electron gas of density $\rho(\mathbf{r})$. $V_{ee}[\rho]$ is then called Hartree-energy:

$$V_{ee}[\rho] = \frac{1}{2}\int d\mathbf{r}'\frac{\rho(\mathbf{r})\rho(\mathbf{r}')}{|\mathbf{r}-\mathbf{r}'|} \tag{4.8}$$

The exchange-correlation energy E_{xc} includes mainly the electron-electron correlations. With this approach all unknown parts are described by one functional E_{xc}. But the special form, the structure and the analytic form, of this functional is still unknown. However, there is a way to exactly determine E_{xc} in the limit of slowly varying densities.

$$E_{xc} = \int d\mathbf{r}\rho(\mathbf{r})\epsilon_{xc}[\rho] \tag{4.9}$$

One of the first practical attemps to describe the exchange-correlation energy $\epsilon_{xc}[\rho]$ was the local density approximation (LDA),[15] which is based on a homogenous electron gas with density $\rho(\mathbf{r})$. Since some problems in atomic physics, quantum

chemistry, and condensed matter physics could not be described correctly, more advanced exchange-correlation functionals were necessary to improve this approach. This is done by correcting the E_{xc} with the help of the gradient of the density, which is the so called generalized gradient approximation (GGA).[16] The E_{xc} in this case is depending not only on the electron density but also on the gradient of the electronic density $\nabla\rho$ and higher derivatives of ρ. This leads to more realistic description of atoms and molecules. Unfortunately, up to today there is no functional, that allows to capture the long range dispersion interactions. This is a open problem of DFT. Despite this limitation it has been shown that DFT is still a powerful tool.

There are several different functional; the ones used in this work are the BLYP and the PBE functional. The BLYP functional (including the Becke exchange functional and the correlation functional from Lee, Yang, and Parr) was used for the solvation of ions in water, while for the ionic liquids the PBE (Perdew, Burke and Ernzerhof) exchange-corelation functional was applied. [17–20] Regarding the equations so far they give nothing than a general scheme. To apply this scheme to several systems a key is required, which was also introduced by Kohn and Sham.[10] They do not use the density as the general quantity to estimate the ground state; they go one step back and describe this theory with respect to a basis set of orthonormal one-electron wavefunctions. The electronic density then reads as:

$$\rho(\mathbf{r}) = 2\sum_{i}^{N/2} |\psi_i(\mathbf{r})|^2 \tag{4.10}$$

The parts of the general functional $\mathcal{F}[\rho(\mathbf{r})]$ are:

$$\mathcal{K}[\rho] = 2\sum_{i} \langle\psi_i(\mathbf{r})| - \frac{\nabla^2}{2}|\psi_i(\mathbf{r})\rangle \tag{4.11}$$

$$V_{ee}[\rho] = \int d\mathbf{r}' \frac{\rho(\mathbf{r})\rho(\mathbf{r}')}{|\mathbf{r}-\mathbf{r}'|} \tag{4.12}$$

For the form of the exchange-correlation energy E_{xc} see Eq. 4.9. Combining all these parts the energy functional becomes:

$$E[\rho] = \mathcal{K}[\rho] + V_{ee}[\rho] + E_{xc}[\rho] + \int d\mathbf{r}\rho(\mathbf{r})V(\mathbf{r}) \tag{4.13}$$

Solving the Euler-Lagrange problem then gives:

$$[-\frac{1}{2}\nabla^2 + V_{eff}(\mathbf{r})]\psi_i(\mathbf{r}) = \epsilon_i\psi_i(\mathbf{r}) \tag{4.14}$$

with the effective potential:

$$V_{eff}(\mathbf{r}) = \sum_I V_{eI}(\mathbf{r} - \mathbf{R_I}) + \int d\mathbf{r}' \frac{\rho(\mathbf{r}')}{|\mathbf{r} - \mathbf{r}'|} + \frac{\partial E_{xc}}{\partial \rho(\mathbf{r})} \tag{4.15}$$

The equation Eq. 4.14 is the Kohn-Sham eigenfunction equation, which has to be solved in a self-consistent way until the input density $\rho_{start}(\mathbf{r})$ equals the end density $\rho_{end}(\mathbf{r})$. At every step of the geometry optimization of a certain system the density has to be calculated according to the described procedure. In the context of the Kohn-Sham equations eigenstates and eigenvalues are obtained, which have no direct physical meaning; the only quantity determined in this way is the ground state density and total energy.

4.3 Planewave Basis Set

The Kohn-Sham equations rely on the use of basis sets to represent the wavefunction $\psi_i(\mathbf{r})$. This is extremly important for the efficiency of the computational method. There are different types of basis sets available, which are either local, e.g. Gauss type orbitals (GTO's) or delocalized wavefunction, i.e. the planewave basis set, or a mixture of both. The basis implemented in the CPMD code used in this work [21] is the planewave basis set. The expansion of this basis has the advantage of solving the eigenvalue equation via simply a Fast Fourier transformation. Furhtermore the planewave representation is independent of the ionic position of the nuclei. Instead, localized orbitals have the disadvantage that changes of ionic positions lead to a complete different basis with different and/or additional forces acting on the nuclei.
In general, the planewave basis set is defined as:

$$\psi_i(\mathbf{r}) = \sum_G c_{i\mathbf{G}} e^{i\mathbf{G}\mathbf{r}} \tag{4.16}$$

with $\mathbf{G} = \mathbf{k} + \mathbf{g}$ and i=1,..,n (n = No. of electrons),
k: first vector in the Brillouin zone,
g: vector of Fourier space.

The planewave representation is the best choice for translation invariant system like metals or solid state systems. The application on disordered systems is possible with large simulation boxes. The size of the simulation boxes are chosen such that the periodic images do not effect the physical properties of the studied system significantly. The basis set for computational capability has to be truncated to a finite set by using an energy cutoff in the kinetic energy.

$$E_{kin} = \frac{1}{2}|\mathbf{k} + \mathbf{g}|^2 = \frac{1}{2}|\mathbf{G}|^2 =\leq E_{cutoff} \tag{4.17}$$

A limitation of such an approach is that, while in case of localized orbitals the description of core electrons is simple, the required set of planewaves will be quite large. To overcome this problem, the pseudopotential approach is used, where core electrons are included into an effective core potential, and thus the number of planewaves can be significantly reduced.

4.4 Pseudopotential Approach

As already mentioned the core region of an atom cannot be represented by a reasonable amount of planewaves. A new effective potential has to be constructed which treat the core and valence electrons in an accurate way. The pseudopotential approach is the simplest way to overcome this problem. The core region of an atom is not involved in chemical interactions and should be the same as for an isolated atom. Therefore the Kohn-Sham equations have to consider the valence electrons only. This takes place in the new potential which replaces the nuclear potential. The description of the core region is included in the effective potential. For this approximation three criteria have to be considered to achieve a consistent description; (a) the eigenvalues from all electron calculations of the isolated atom have to reproduce the eigenvalues of the occupied states in the pseudopotential approach; (b) the wavefunction of the pseudopotential outside a certain core radius r_c has to match the all electron calculations in that region; (c) the logarithmic derivatives of the eigenfunctions (to test the scattering properties of the atom) have to fullfill the same criterion as the wavefunctions. With the criteria from above the pseudopotential represents only the valence electrons. Moreover the electrostatic potential for the valence electrons is the same as for the all electron calculations, while the third condition ensures that the derivatives of the eigenfunctions with respect to the energy of the two different approaches (pseudopotential and all

electron) coincide. The potentials can be produced using experimental data or all electron calculations at the DFT level. In general the pseudopotential for a certain atom has to be applicable to a various number of systems. Unfortunately this is mostly not the case and for each system the pseudopotentials have to be tested.

4.5 Car Parrinello Molecular Dynamics

In classical molecular dynamics, the description of molecular systems via rigid bodies, classical Coulomb and dispersion interactions, can give a valid idea of the behaviour and the physics of macroscopic systems. But with upcoming non trivial electronic interactions, in systems with e.g. chemical reactions, the classical molecular dynamics (MD) is no longer valid. Thus a more appropiate method to deal with electrons is needed and quantum mechanics has to be included. In classical molecular dynamics simulations, the nuclei move according to forces based on effective potentials, which have to be generated with respect to electronic interactions. The advantage of involving quantum mechanics is the direct description of the effective potentials, from which the Hellmann-Feynmann forces F_I for the I-th nuclei, which correspond to the forces on the ions, can be calculated. [8]

$$F_I = \int \rho(\mathbf{r}) \frac{\partial V_{el,I}(\mathbf{r}, \mathbf{R}_I)}{\partial \mathbf{R}_I} d\mathbf{r} \tag{4.18}$$

The Car-Parrinello scheme is combining all the advantages at the different methods. While the ionic dynamics is treated at classical level the wavefunctions of the corresponding quantum systems evolves with them, i.e. the electronic system is always assumed to be in the ground state. The problem of this scheme is that there are two different time scales involved: one for the nuclear and one for the electron motion. Specifically, the integration of the equation of motion is on the time scale of the nuclear dynamics and the electrons are propagated pseudodynamically, using the smoothness of the time evolution of the wavefunction. This can be done because the electronic motion is of the order of three magnitudes faster than the nuclear motion. In classical MD the forces, governing the nuclear dynamics, are determined by the derivatives of the Lagrangian of the particular system with respect to the nuclear positions. The derivatives of an appropriate Lagrangian with respect to the atomic orbitals then leads to the classical forces on the wavefunctions. The following Lagrangian is proposed by Car-Parrinello for this purpose.

$$\mathcal{L}_{CP} = \sum_I \frac{1}{2}\mathcal{M}_I \dot{R}_I^2 + \sum \frac{1}{2}\mu_i \left\langle \dot{\phi}_i | \dot{\phi}_i \right\rangle - E_{el}(R_I, \rho) + \sum_{i,j} \Lambda_{i,j}(\langle \phi_i | \phi_i \rangle - \delta_{ij}) \quad (4.19)$$

With $\mathcal{M}_I$ defined as the masses of nuclei and μ_i is the fictitious mass associated with the electronic degrees of freedom. The first two terms describe the kinetic energy of the nuclei and the electrons. The last term is introduced to guarantee the orthonormality of the wavefunctions.
The Born Oppenheimer approximation is the standard simplification for solving quantum mechanics many-body problems, which allows to separate the movement of nuclei and electrons, due to their relative masses. This approximation allows the separation of the nuclear and electronic degree of freedom. The following equations of motion then characterize the CP-scheme.

$$\mathcal{M}_I \ddot{R}_I(t) = -\frac{\partial E_{el}(R, \rho)}{\partial R_I} \quad (4.20)$$

$$\mu_i \ddot{\phi}_i(t) = -\frac{\delta E_{el}(\phi, \rho)}{2\delta \phi_i^*} + \sum_{i,j} \Lambda_{ij} \phi_j \quad (4.21)$$

These two formulas have to be solved. They are coupled via the ionic positions, while $\mathbf{R}_I$ is changing ϕ changes accordingly, then $\mathbf{R}_I$ moves again etc. Thus, for every configuration $\mathbf{R}_I$ one calculates the electronic ground state.[8]
All practical calculations for the water systems herein were performed in the frame of the most popular Car-Parrinello molecular implementation [21]. The wavefunctions are expansions in a plane wave basis set with a cutoff criterion based on the kinetic energy, see Eq. 4.16,4.17. In this work we used this scheme to optimize structures of small clusters and the dynamics of liquid like systems.

5 Ion Hydration

5.1 Introduction

In organic chemistry solvents can be separated into several groups, which range from polar-protic, e.g. water, primary alcohols etc. to apolar-aprotic, e.g. aliphatic molecules. Water is the prototype of a polar-protic solvent, which means: protic solvents show hydrogen bonding, can donate acidic protons and are able to stabilize and solvate ions; cations by non-binding electrons and anions by hydrogen bonding. Water is one of the simplest molecules in nature, but in its liquid state it forms one of the most complex fluids, which is directly related to the complex hydrogen bonding network. The properties of water depend also on the polarization of the oxygen hydrogen covalent bonds, with a formal negative charge at oxygen and the formal positive charge in between the hydrogens, which leads to the permanent dipole moment and the protic behavior. Due to these properties water and especially hydration of ions play an essential role in many day life processes in chemistry, biology, and technology.[22] The description of liquid water and hydration with experiments [23–25] and theory [26–46] has revealed several crucial aspects already but yet still many problems remain unclear. The state of the art of experimental and theoretical work, and comparison of them, is extensively discussed in review by Asthagiri et al.[46]. The recent experiments of water and the solvation of ions can determine the structure around the ion, by monitoring the changes of the vibrational frequencies; for example in case of anions, which are connected via hydrogen bonding. Most of the experiments show limitations, but in general these techniques allow to distinguish the first solvation shell around ions. Other experiments for determining the solvation structure around ions are x-ray diffraction and neutron scattering experiments, which determine the position of the atoms; they are technically challenging because of the preparation of the samples, therefore the experimental results of structural properties even in case of the number of water molecules in the first shell can differ (in case of water molecules

around a single sodium cation in liquid the number is ranging from four to eight molecules [25]), but the overall global structure can in principle be measured. The experimental parameters, however, are essential for parameterizing classical force fields, and these limitations lead to problems in this kind of parametrization, and in turn to rather large differences between classical models [47]. To overcome these limitations it is necessary to study water systems with first principle methods. Because the classical simulations, as already announced, are not sufficient to cover the whole range of interactions in water. Instead first principle methods can link the atomistic with the electronic scale and therefore the general principle of solvation can be accessed by regarding (a) the water molecules around ions; (b) the general behaviour of liquid water around the ion;(c) the interaction of water molecules in these different environments and in particular (d) the basic electronic interactions. In literature the points (a) and (b) are treated mostly as isolated topics, and there are some approaches to also include (c) in the description of hydration. [36–38, 42] The problem with these approaches is that they are concentrating only on specific systems, single types of ions. These might be: one single ion [36–38] or a set of different monovalent ions [42]. However, studies on single ions or even on ions with the same charge and different size only reveal a limited picture in water. But to understand the principle mechanism behind hydration it is important to study (a),(b), and (c) for a large variety of ions. This is done in this work; as the first approach we study the monovalent anions F^-,Cl^-, and Br^-; the monovalent cations Li^+, Na^+, and K^+; and at the divalent cations Mg^{2+}, and Ca^{2+}. The first step was to study the small cluster of these ions with surrounding water to get an inside into local effects, those effects of the ion on water in the first solvation shell. Therefore the structures of several clusters have been optimized and the dipole moment was calculated. The effects which occur in the ion-water clusters are important, since they are still present in liquid systems. After having studied the ion-water clusters we move on to hydrated ions. This enabled us to also study the more global effects, the interaction of the first shell water molecules with the surrounding bulk water; and the general behaviour of liquid water around the ion. Following this strategy the local effects, i.e. the direct polarization of water due to the interaction with the ion and the water-water interaction among the molecules in the first shell, can be separated from more global effects, i.e. water-water interaction of the first shell water with the surrounding bulk and the bulk behaviour. The final step was to look at the electronic scale (d) of all the available configurations.

The following procedure has been applied: first we have studied the several ions (Li^+, Na^+, K^+, Mg^{2+}, Ca^{2+},F^-, Cl^-, Br^-) in small water clusters from 1-8 water molecules, depending in the size and charge of the ion; then the cations have been solvated in larger systems of water, 32, 64, and 128 water molecules. The study was performed using the Car-Parrinello code CPMD [21]. Then the mechanisms were analysed by localizing the charges in space using the maximally localized Wannier scheme, see Section 5.2.1 for further details. Then the dipoles were calculated using these Wannier centers and the classical description $\mu = \sum_j q_j \mathbf{r}_j$; where, q_j is the charge, negative for the centers representing the electrons, and positive, corresponding to the valence electrons, in case of the nuclei. The vector $\mathbf{r}_j$ is the vector of the charge coordinates with a reference point, which is the oxygen atom in case of water. The dipole moments for the water molecules around the ions in the small clusters and in liquid like systems the dipoles corresponding to the several shells were collected. With this we described the local chemistry around the ions and the interaction of the first solvation shell with the surrounding shells and the bulk. As result we found that the water-water interactions are more relevant than the ion-water interaction for the solvation properties. The ion-water interaction only contributes to the local geometrical structure of the first shell, while the water polarization due to the ions is neglectable. However this analysis is true only for cations, while in the case of the anions there is a hydrogen bonding formation of water with the anion, the resulting hydration is different but the overall water-water interaction for the molecular water dipoles must be still present. This study so far included more generic properties, but the very basic electronic level was not approached. This was done by regarding the different contributions to the dipole moment and the Wannier functions, which represent the Boys like localized orbitals. The contributions to dipole moment are divided into lone pair, bonding pair and oxygen-hydrogen bond parts. The Wannier functions were collected for selected water molecules in selected ion-water clusters (Na^+, Mg^{2+}, Ca^{2+} with up to 6 water). For the liquid system only the bare influence of the ion was considered. With this approach we found that besides the lone pair contribution, the bonding pair contribution has to be taken into account in the description of the dipole moment. Furthermore we found that even in small clusters the water-water orbital cloud repulsion hinders the ion-water interaction.

Combining the results from the more atomistic and the more electronic point of view a general mechanism emerges. In case of one ion and one water molecule

the ion-water interaction is present and the only quantity; the interactions already shifts towards water-water interactions in the presence of one additional water molecule. This effect clearly gets stronger with increasing amount of water, due to the repulsion of the non-binding valence electrons of water. This leads in case of water to more or less predictable structures of the water molecules around the ion. In liquids the additional effect of hydrogen bonding arises. On the local scale, around the ion, the water-water repulsion is competing with the hydrogen bonding formation within the shell (only for monovalent ions) and the hydrogen bonding with the surrounding shells. In case of divalent ions there is no hydrogen bonding within the first shell and only the hydrogen bonding of the molecules of the first shell with those of the second shell. Thus the ion in principle only directs the geometric structure of the molecules surrounding it.

5.2 Technical Details

In general for all the calculations we used a planewave pseudopotential approach of density functional theory, i.e. the wavefunctions are expanded into a planewave basis set, while the atoms are represented by pseudopotentials. All simulations for the water clusters are performed using this approach within the Car-Parrinello Molecular Dynamics code [21] with the BLYP exchange-correlation functional [17–19]. Troullier-Martins norm conserving pseudopotentials [48] have proven to describe the atoms quite good, thus they were chosen for the different ions (Li^+, Na^+, K^+, Mg^{2+}, Ca^{2+}) and oxygen; for hydrogen a local pseudopotential was employed [49]. The alkali and earth alkali metals have no valence electrons in the cationic state, which can be described by two approaches either a non linear core corrected or a semicore approach, i.e. either a positive core is remaining and the effective core-potential is corrected or the electrons in the second highest shell (e.g. in case of Na: the 2s 2p orbitals) are treated explicitly. We have tested both cases and the semicore approach proved to be more accurate and transferable to other systems, see also Refs. [50, 41]. Lithium is a special case. While only the doubly occupied 1s orbital will remain in the cationic state, the non linear core correction had to be used. The addition of an electron to the outer shell is not that problematic as the subtraction of one, the halides (F^-, Cl^-, Br^-) could be represented by usual norm conserving Troullier-Martins pseudopotentials.
As the first step to approach local effects, small clusters are build, which contain

one ion and a small number of water molecules. The building scheme is rather simple, to the ion water molecules are systematically added to fill the first hydration shell. The studied ions are the monovalent cations Li^+, Na^+, K^+, the anions F^-,Cl^-,Br^-, and furthermore the divalent cations Mg^{2+} and Ca^{2+}. The number of water around the specific ion is varying from 5 (Li^+, Na^+, K^+,F^-), 6 (Cl^-,Br^-,Mg^{2+}) to 8(Ca^{2+}), while the small ions have only up to five molecules in the first shell, the bigger ions are surrounded by up to 8 water, which is only true for the calcium cation. The other large ion K^+ has only five water in its first shell, due the fact that the shell with a higher number of molecules was unstable. The clusters were optimized using the Car-Parrinello code [21] and as convergence criteria for a structure the Hellmann-Feynamnn forces on the nuclei had to be lower than $1{\cdot}10^{-3} a.u.$. The small clusters in vacuum provide an insight into the local structure around an ion in liquid water, the next step is to consider the non-local bulk effects, that is the interactions which arise from surrounding water. Therefor larger water systems, with 32, 64 and 128 molecules, have to be simulated. The initial configurations for the Car-Parrinello molecular dynamics simulations have been provided by classical molecular dynamics simulations at 300K for 100ps with the SPC/E water model. The main focus was on the cations Li^+, Na^+, K^+, Mg^{2+} and Ca^{2+} in water, with *ab initio* MD simulations carried out at 300K. The box sizes of the cubic cells are, according to reproduce the density of water, around 9.5 Å, 12 Å and 15 Å for 32,64 and 128 water molecules, respectively. The time step was chosen to be 3 a.u. (1 a.u. = 0.024 fs)and the electron mass was set to 400 a.u.. In case of the 128 water molecules the electron mass was changed to 600 a.u. and a new time step of 4 a.u. was employed, due to the highly demanding computational cost of such a system. Also because of this the equilibration of the 128 water was done only for 3ps, and data was collected for 2ps. The other systems were equilibrated for 5 ps and data were collected for another 5ps, and in case of $Ca^{2+}(H_2O)_{64}$ 14 ps. The length of the equilibration can be compared with the 3ps from a recent simulations of the solvation of methane in water which is clearly a more complex system than we have treated here[51].

5.2.1 Wannier Centers and Dipole Moments

A powerfull method to study changes in the electronic structure is the maximally localized Wannier scheme, which is embedded in the CPMD code [21]. In gen-

eral the planewaves are localized via a unitary transformation to get the Wannier functions, which are local in **k** and in **R** space. The criterion for the degree of localization is similar to the criterion Boys' used for finite systems.[52]

$$\Omega = \sum_n \left(\langle \mathbf{r}^2 \rangle_n - \langle \mathbf{r} \rangle_n^2 \right) \tag{5.1}$$

The resulting localized functions are equivalent to Boys' orbtials, which in principle are also called hybrid or canonical orbitals. To properly study the changes due to polarization the Wannier centers were calculated out of the localized functions, therefore, they have the special properties, which are: (i) they contain two electrons, (ii) they can represent the electrons of binding and non-binding electrons, and (iii) the changes of the electronic structure due to interactions can be studied by changes of their geometrical structure. Having described the electrons in a molecule in that way the changes due to other molecules can be studied. In the present work the Wannier centers have been used to determine the dipole moment of water in presence of one ion. Furthermore the properties of the geometrical structure of these centers were used to investigate the mechanism of polarization at the electronic level, see Fig. 5.1.

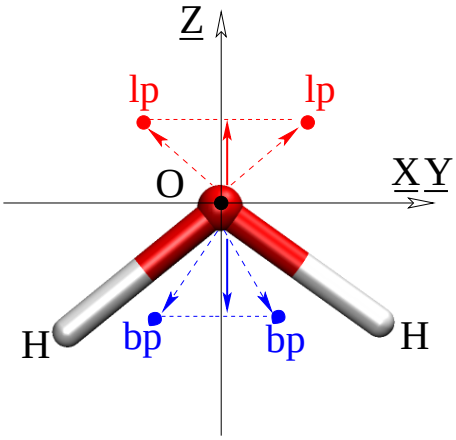

Figure 5.1: Schematic representation of the projections of the Wannier centers along the molecular axis **Z**. O-lp is the vector from oxygen to the Wannier center position for the lone pair electrons. bp and OH are defined in the same way.

The dipole moment is then determined within the classical aproach: $\mu = \sum_j q_j \mathbf{r}_j$; with q_j as the charge, negative in case of the point charges representing the electrons, positive in case of nuclei, and the vector $\mathbf{r}_j$ connecting the charge coordinates

with the oxygen as reference point. The reference point can be arbitrary chosen for neutral molecules, in our study we have chosen to be consistent with literature [53, 54] and uses the oxygen as a origin of the system (see Fig. 5.1). The localization of charge is not unique [55–57, 49] but we are interested in relative (by comparison) values of the molecular dipole for different systems. This means the absolute value is not crucial, and therefore the dependence on the localization technique is also not crucial. In a further analysis the Wannier functions have been used to determine the changes in water polarization. The Wannier functions are calculated for the water, in the presence of the ion and then without the ion; the differences are then plotted with respect to different cluster sizes, see Fig. 5.15, 5.14, 5.13, and will discussed in section 5.4.

The data collected include the Wannier centers, calculated on the fly for every 10 time steps *ab initio* MD, while they were calculated for all clusters separately as well. The centers represent the maximally localized Wannier functions, which are analogous to the Boy's orbitals (hybrid or canonical orbitals), for a more details see chapter 5.2.1. The obtained centers have been used to calculate the molecular dipole moments for the individual water molecules in the small clusters as well as in the liquids. Furthermore the dipoles can be analysed with respect to different shells in liquid systems. We focused on the direct comparison between the first shell dipole with those from the clusters, this also implies that the absolute value of the dipole moment is not important; rather the relative comparison plays the crucial role. As convergence criteria the gradient in the calculation of the Wannier function is used with the threshold of $10^{-10} a.u.^2$.

5.2.2 Test of Setup

As mentioned in the theory section above, a specific pseudopotential for one element should in general be sufficient, unfortunately there are many different potentials for one element available, which are only working for some specific setups. Therefore the pseudopotentials we have used had to be tested on well known compounds and also on the system we want to apply them on. As a test several compounds were taken from literature and the optimized structures were calculated. As the reference we used data from Herzberg provided for several chosen compounds. [62] As table 5.1 shows the agreement in all cases is rather good, LiF is the only combination given a larger (below 10%) than the other combinations

Technical Point 5.1: *Localization Methods*

Besides the used Wannier scheme there are several other localization methods for DFT, e.g. the Bader analysis [49, 55–57] and the electron localization function (ELF) [58–60] and the Mulliken analysis[61]. The Bader analysis allows to separate atoms in molecules and can be extended to separate molecules in condensed phase. This is done by considering the electronic density around the single molecules. This local density is then used to derive the average molecular dipoles moments of water. With this method the dipole moment 2.6 D of water was derived. The next method is the ELF scheme, which is calculating the probability to find paired electrons around a molecule. With this scheme the electron shell structure can be determined.

$$ELF = \frac{1}{1 + \frac{D}{D^o}} \tag{5.I}$$

with the electron localization D and D^o (the uniform electron gas with spin-density equal to the local value of $\rho(\mathbf{r})$)

$$D = \sum_i^{\rho} |\nabla \psi_i|^2 - \frac{(\nabla \rho)^2}{4\rho} D^o = \frac{3}{5}(6\pi^2)^{2/3}\rho^{5/3} \tag{5.II}$$

The last method which was mentioned above is the Mulliken analysis. This method rely on the electron density from which the net population and overlap population is determined, which lead to the gross population and in the end to the net atomic charges. With all these methods the dipole moment of water in principle can be determined more or less accurate and the values can differ. Thus to describe the polarization in an unique way one has to consider the changes of the dipole moments and not at their absolute values. The other difference to the Wannier scheme, which was used, is that one has to do this for selected configurations. But to achieve good statistics the dipole moments have to be collected for a larger number of configurations, thus the on the fly calculation, like in the implemented Wannier scheme is quite useful.

listed in table 5.1 (below 5%). As a further test we compared the ion-water clusters, with the alkali metals Li^+, Na^+, K^+ and the earth alkali metals Mg^{2+}, Ca^{2+} and in case of sodium even the neutral atom-water clusters (see table 5.2), for all ions with literature, if data was available, see tables in Appendix 8.

dist	calc.[Å]	lit.[Å][62]
Li_2	2.69791	2.6729
Na_2	3.0788	3.05584
K_2	3.90003	3.9051
F_2	1.48138	1.41193
Cl_2	1.987	2.09570
Br_2	2.34991	2.28105
LiF	1.77536	1.563764
LiCl	2.02273	2.020673
KF	2.23870	2.17145
KCl	2.69335	2.66665
KBr	2.86203	2.82078
NaF	2.02258	1.92594
NaCl	2.36078	2.40689
NaBr	2.55828	2.50203
MgO	1.70709	1.749
Mg_2	3.890	3.890
CaO	1.85755	1.8221
Ca_2	4.2773	4.2773

Table 5.1: Comparison between structural data available from spectroscopy and those obtained from our calculations for several compounds. Exception: LiF, with a disagreement of ca. 10%; all others show differences within 5%, which is a quite good aggreement.

n	1	2	3
r(Na-O_1)	2.3094(2.35)	2.247(2.333)	2.2781(2.302)
r(Na-O_2)		2.257(2.333)	2.2883(2.302)
r(Na-O_3)			2.2938(2.302)

Table 5.2: Distances (in Å) between Na and O for interior $Na(H_2O)_n$ clusters. The used pseudopotential has been the semicore potential for sodium with the LSDA/BLYP approach. The literature values are in parentheses. In literature DFT/LSDA-BLYP (Ramaniah et al.[50]) have been used.

Another important factor for our setup have been the accuracy of the simulated results, since we apply semicore pseudopotentials we had to be sure that the energy cutoff was chosen correctly and high enough. Extended test with 80, 90, and

100 Ry as energy cutoffs showed us no differences in the cluster structures and differences in the molecular dipole moment remain below 5% compared to the results obtained with 70 Ry as cutoff. In order to check also the setup of the *ab initio* MD (AIMD), it is not only important to have the correct pseudopotential, the choice of the time step and the electron mass is also of importance. For all the liquid systems we compared the obtained radial distribution functions with those published in literature (from classical MD, AIMD, and experiments) and found good agreement, with this we could also check if equilibration was reached, see section 5.3.1. [34–39, 41, 42, 45, 63, 64]

5.3 From Microscopic to Macroscopic Scale

5.3.1 Water Structures and Comparison with previous work

As a first step towards hydration we have studied small clusters, up to the size corresponding to the first hydration shell around an ion. The starting point have been the solvation of monovalent ions M^+ (M=Li, Na, K), A^- (A=F, Cl, Br) and of the divalent ions M^{2+} (M=Mg, Ca). The aim was to find the local molecular properties of ion hydration. For the optimized structure, Wannier centers have been calculated to obtain the average molecular water dipole moment in the first shell. As mentioned already in the technical section, some of the structures were optimized as a check for our technical setup. The starting configurations for Na^+ water clusters were taken from geometry parameters given by Ramaniah et al.[50]. These structures are the prototypes of the structures we used in the following, with different ion-oxygen distances, for the other cations. The set of used structures is shown here with the help of the calcium-water clusters, see Fig. 5.2. The structures for 1-5 water molecules was used for the monovalent cations, while for the divalent ions; clusters contain 1-6 (Mg^{2+}) and 1-8 water (Ca^{2+}). The quadratic-pyramidal and trigonal-pyramidal structure only occur in the case of divalent ions, in case of the monovalent ions these structures had been unstable.

We reproduced the structures of neutral sodium-water clusters of Ramaniah et al.[50], structures of the Li^+ clusters of Müller et al. [33] and and Lyubartsev et al.[65] (see table 8.1); then structures of Na^+ clusters (see table 8.2) also provided by Ramaniah et al.[50], Schulz et al. [66] and Bauschlicher et al. [67], and for the K^+ clusters (see table 8.3) geometries we found good agreement with the

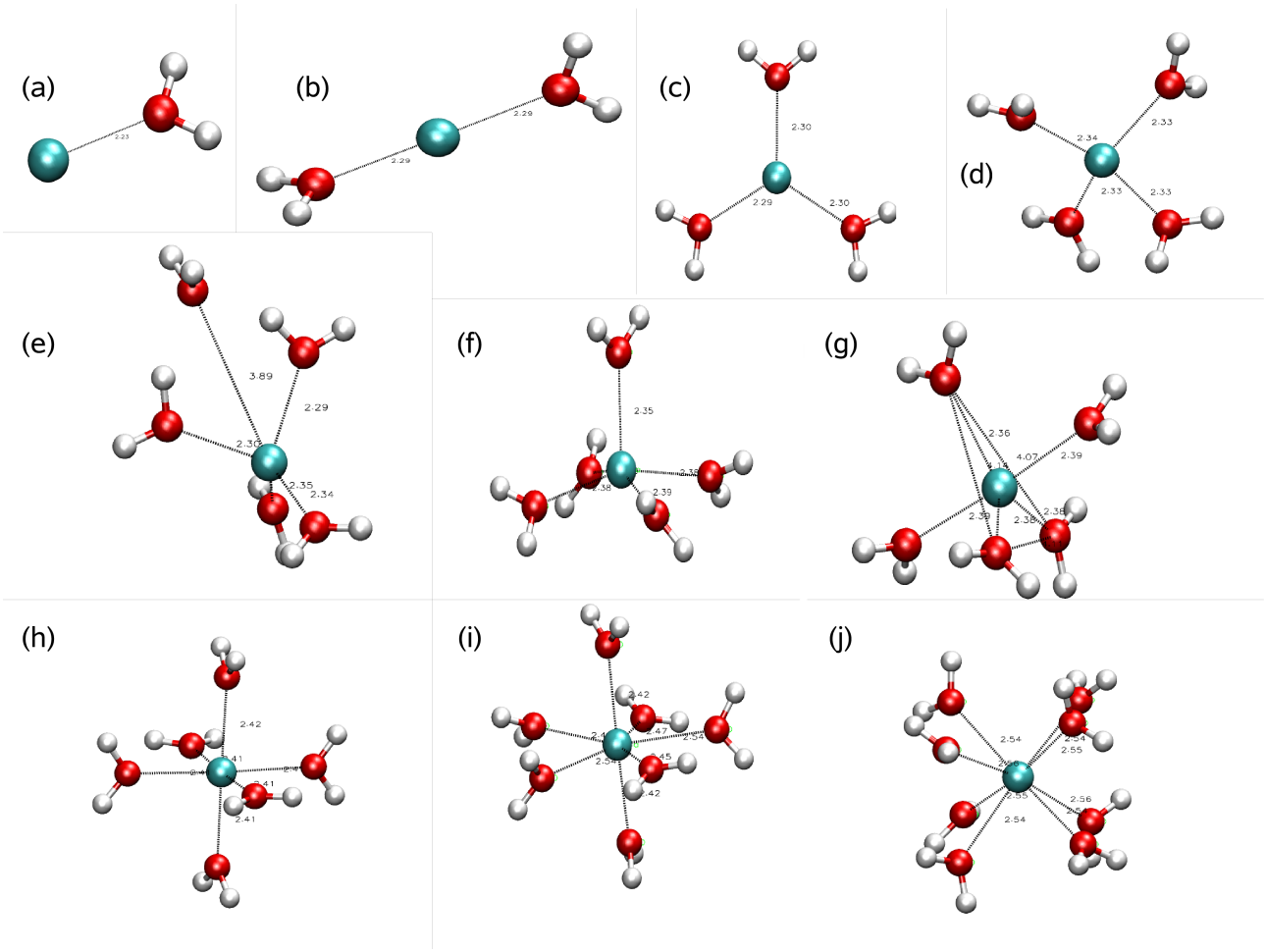

Figure 5.2: An example of the structure of cations surrounded by water in the case of Ca2+ water clusters (a)-(j); the structure (a)-(e) are also used for the monovalent ions-water clusters, while (a)-(h) were the structures simulated for Mg^{2+} in small water systems.

experimental K^+-O distances given of Glending et al.[68] and Džidić et al. [69] and those predicted by Lee et al. [70].

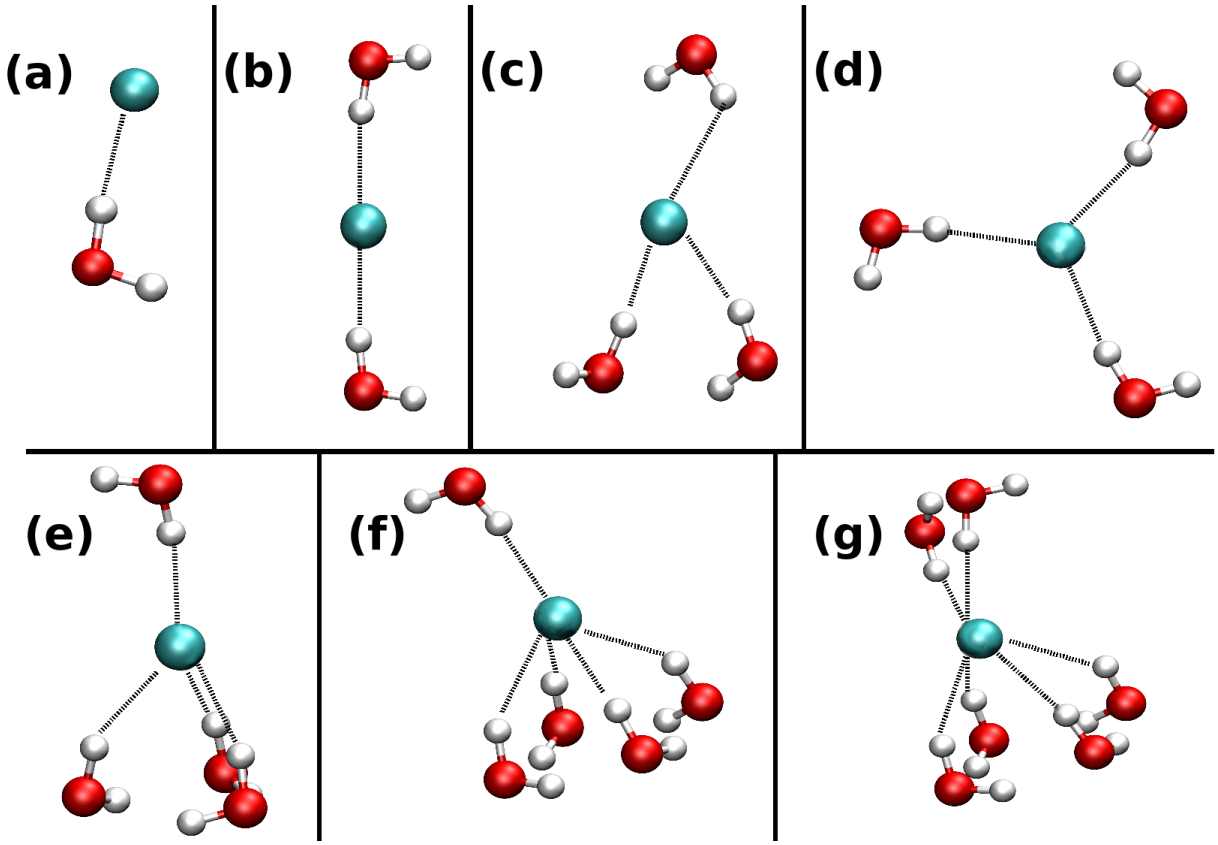

Figure 5.3: Example of optimized structures for $Cl^-(H_2O)_n$ clusters. a) $A^-(H_2O)_1$; b) 1+1 structure, i.e. 1 water molecule on each side of the chloride; c)2+1 structure, i.e. 2 water molecules on one side and only 1 at the opposite side of chloride; d)structure 3, equidistant distribution of water around chloride; e)3+1, analog of b); f) 4+1, analog of b); g) most stable solvation structure extracted from a 31 water molecules system [71].

For the divalent cations magnesium and calcium water clusters were optimized and compared with the structures given by several work on Mg^{2+} [27, 28, 30] and Ca^{2+} [29–31, 34, 35, 37]. The same procedure, same geometrical setup but different ion-oxygen distances, was applied for anions, with the chloride water clusters providing the general geometrical setup. The clusters of the monovalent anion Cl^- with water are compared with the results of Gora et al. [72] and Kim et al. [73]. Also those reported in the table of Combariza et al. [74] show good agreement. The F^-, and

Br^- water clusters are generated according to the chloride water clusters. The results we got are in good agreement with literature, for F^-: see Ref. [75, 73] and for Br^-: see Ref. [73, 76]. In principle the structures we obtained are not larger than maximally 5%, the anion structures are only 3% larger than the one from literature.

With the small clusters the local effects, which are the ion water interactions are studied; this is the microscopic scale. On a molecular scale there are global effects, which are the water-water interactions of the surrounding water molecules. Since the interplay of both effects is of interest, we studied in a further step the solvation of the cations in liquid systems containing 32, 64 and 128 water molecules. The molecular dipole moments are collected concerning the microscopic and the macroscopic surrounding.

To simulate the liquid like states, the ions are solvated with 32, 64 and 128 water molecules. The obtained radial distribution functions M^{n+}-O (n=1, 2; M=Li, Na, K, Mg, Ca), M^{n+}-H, and O-H, O-O are collected and compared with literature. We found good agreement with published radial distribution functions there.[34–39, 41, 42, 45, 63, 64] So far the cluster calculations and the simulations of the liquid systems reproduced previous results rather well. This ensured us that the technical setup we used for describing ion-water systems is accurate enough. The connection of the results, especially in combination with the dipole moment analysis, and the basic electronic analysis will then allow to describe the general trends in ion-water systems. In the following sections this will be discussed in more detail.

5.3.2 Molecular Dipole Moments

The analysis of the electronic properties is based on the calculation of the molecular dipole moments as illustrated in section 5.2.1. The molecular dipoles found in the first shell are compared with the ones obtained for the clusters. We analysed the results in terms of the interplay between the local, ion-water, and the global effects, due to the water interactions all over the system from the solvation shell to the bulk. The dipole moments of individual molecules in liquid systems cannot be measured directly with experiments, and as underlined before even in *ab initio* methods it is not possible to determine individual molecular dipoles in condensed phase in a unique way. One way to determine the molecular dipole is the electronic density like in the Bader analysis [56, 55], the problem with this method is to choose

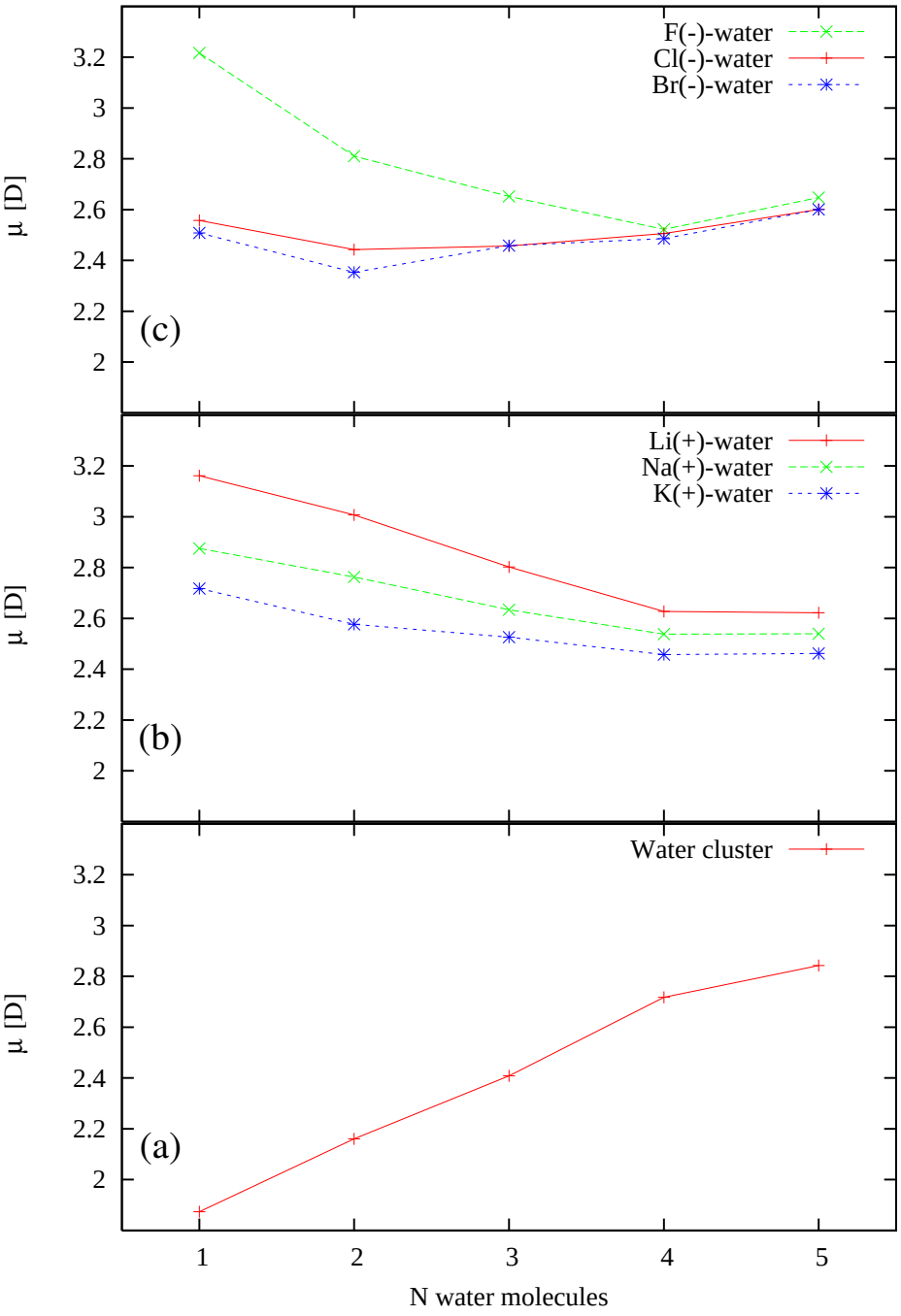

Figure 5.4: Averaged water dipole moment $\mu = |\underline{\mu}|$ as a function of the number N of surrounding water molecules. The structures for the clusters of pure water, were taken from [53] and from [77] and reproduced, via geometry optimization.

the correct cutoff to separate the molecules from each other. Another method is the previously presented Wannier analysis, as already mentioned above the Wannier centers represent the localized orbitals derived from the plane wave basis set. The centers are point charge like particles including two electrons. Then the dipole moment is calculated (as decribed in section 5.2.1), and as discussed before our study does not depend strongly on the localization procedure (e.g. definition of simple molecules in a condensed phase).

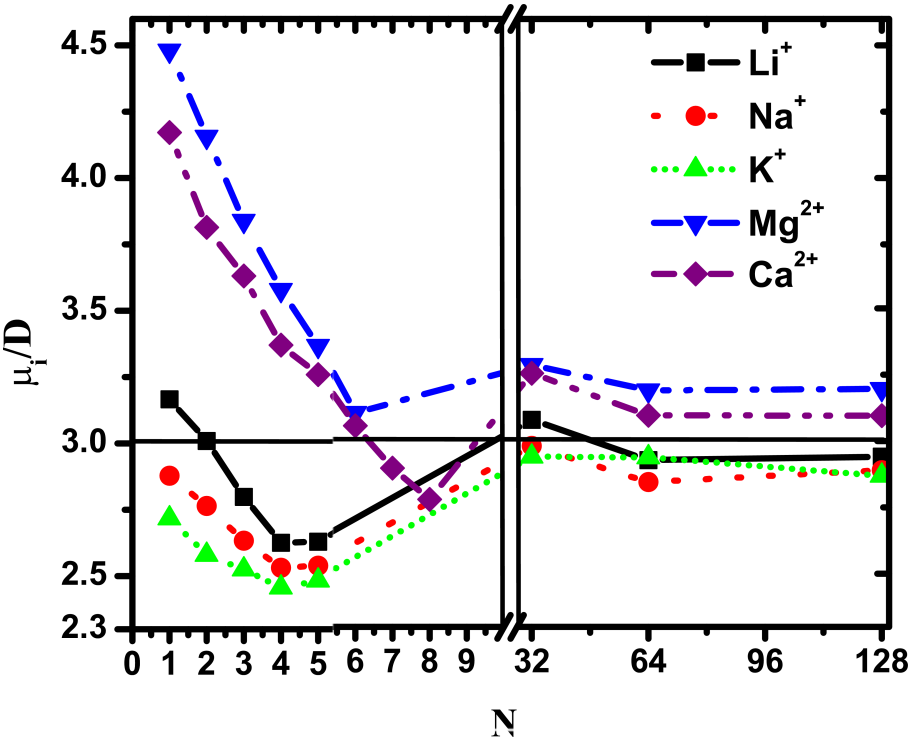

Figure 5.5: Average molecular dipoles for different systems (clusters of increasing size), from a single molecule up to the characteristic coordination number of the ion considered (left), and the average dipole moments of the water molecules in the first solvation shell around the ions of extended systems of different size, 32, 64 and 128 molecules (right). Full polarization is reached for the molecular dipole in one water systems. This strongly depends on the ion. In extended systems the molecular dipole is found to be close to the value of pure water, which is the general feature of all ions.

First we compared the resulting dipole moments of monovalent clusters with similar pure water clusters [77], to investigate the straight influence of the ion on the surrounding water molecules (see Fig. 5.4). The dipole moments of water in presence of divalent ions are collected as well (see. Fig. 5.5). The pictures show

that there is a general trend for all kind of clusters, which is depending on the amount of water in the cluster. As one can immediately see the dipole moment of pure water is rising with increasing amount of water molecules. In liquid water Silvestrelli et al.[53, 54] found a molecular dipole moment of **3.0 D**. The trend of pure water is approaching this value, with a monotonic increment, and would most certain reach it, considering an increasing amount of water molecules in the cell. Regarding the positive ions one can observe a high starting value of the molecular water dipole, but with additional water molecules the dipole moment decreases (even below 3.0 D). For the hydrated ions (in the first shell) a value close to the one of bulk water is reached. In case of the anions the water dipole is staying more or less constant around 2.6 D.

It seems the water-water interactions are getting more important when the number of water molecules is increased. For this reason we did a small test with bromide and chloride in water clusters corresponding to their clusters in liquid. Raugei et al. [71] had simulated bromide in 31 water, they suggested a first solvation shell around bromide, which consists of six molecules. They have found a dipole moment of water around 3.0 D in that shell, and also claimed that the polarization is mainly driven by the water-water interaction with the outer shells. We cut out the structure of the first solvation shell around bromide. We used this bromide-water cluster as initial configuration, optimized it and calculated the average water dipole moment and with that setup we found an average dipole of only 2.55 D. This result shows that indeed it is likely to be the interaction of the molecules of the first shell with those in the second shell which are responsible for increasing the value to 3.0 D. In fact we have the same first solvation shell of Raugei et al. but we have no further shells. The same trend occurs for the $Cl^-(H_2O)_6$ cluster; we took a similar structure as for $Br^-(H_2O)_6$, and the dipole we finally obtained had a value of 2.57 D. The electrostatic moments we observed here showed that the global effects are crucial in the description of the ion hydration. Apparently this is true in case of monovalent anions. The influence of divalent anions in water cannot be studied, because they tend to react with the water and breaking up the water molecule into OH^- and the weak acid HA^-. To study the general influence of bulk water on the polarization of the first solvation shell also different cations (in size and charge) had been considered. Li^+, Na^+, K^+, Mg^{2+}, and Ca^{2+} had been solvated in 32, 64, and 128 water molecules, the latter one was employed only as a further check of the general tendency of the electrostatic moments. We

found a particular competition between the polarization of water due to the direct influence of the ion and the influence of other water. The questions were, which of the two aspects is dominating the polarization and how far does the ion presence influence the system. These questions could be answered regarding the right part of Fig. 5.5, which presents the average dipole moments of the first shell water molecules around the several cations. Here the influence of the second and further shells can be seen, despite the different sizes and charges of the cations the dipoles have values around 3.0 D, or more exact 2.9 D for the monovalent ions (Li^+, Na^+, K^+) and maximally 3.2 D for the divalent ions (Mg^{2+}, Ca^{2+}), i.e. they are close to the dipole calculated for pure water. Since the dipoles of water molecules in the first solvation shell around the divalent cations are only slightly larger and the ones around the monovalent cation are only slightly smaller than the pure water dipole (see Fig. 5.5) this implies a small ion-specific effect contributing to the average molecular water dipole. The two extreme cases are Mg^{2+} and K^+ the strongest and weakest polarizing ions. If one compares the dipole values for $Mg^{2+}H_2O$ and K^+H_2O the difference is almost 2.0 D, while in case of the hydrated ions the difference is around 0.3 D. This implies that the underlying mechanism is general and valid for all cations; that is water-water dominates.

The results above suggest that the water-water interactions are dominating the polarization process and the specific properties of specific ions are less important. Even though the ions polarize the water according to its size and charge, the effect is large with only one ion and one water. As the number of water molecules increases the ion specific water polarization is decreasing, due to the increase of the water-water interactions. For large clusters the effect of the cations can be neglected, this becomes even more evident in the liquid. The water dipole is completely determined by the water-water interaction and only a small offset is present due to the presence of a strongly polarizing divalent cation. For the monovalent anions there is a negative offset, because the water around the monovalent ion is forming a cavity and thus the water in the first shell have less possibilities to be fully involved in the hydrogen bonding network. Another aspect mentioned very shortly above, was the question of how far does the ion influence the water molecules, not only in the first shell but also in further shells. In order to answer this question one has to chose another property to look at, because the values of the dipole moments of the first and further shells showed no significant differences. In order to answer this question properly, we looked at the dipole orientation with

respect to the ion-oxygen vector (see Fig. 5.6) in the first shell and the further shells, as described in section 5.3.3.

5.3.3 Structural Analysis

The dipole vector was defined as pointing from the positive to the negative partial charge, i.e. for cations the dipole is pointing towards the ion, while for the anions the dipole is pointing outwards.

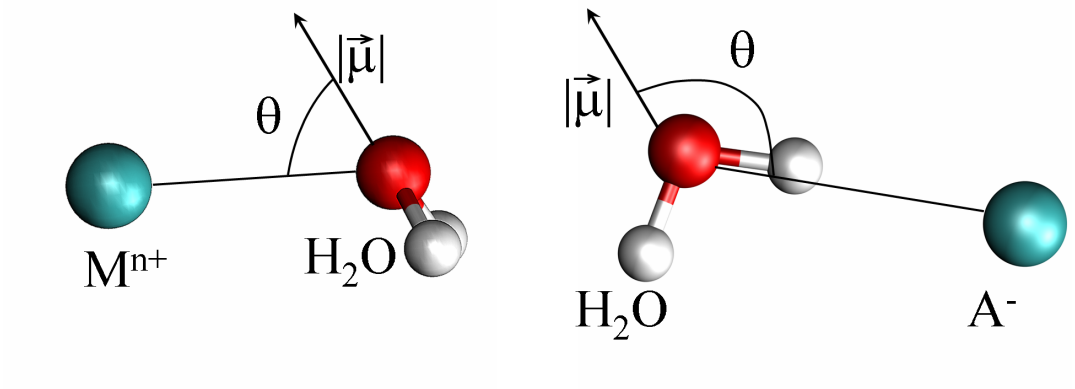

Figure 5.6: Definition of the direction of the water dipole vector for M=Li,Na,K and A=F,Cl,Br. The calculated angles θ are between the M^+/A^--O axis and the dipole vector $\underline{\mu}$.

The study is divided into two part; as before, the clusters were studied, then in the next step the large ion-water systems are considered, in particular the distribution of angles in different shells. The results for anions and cations show a similar trend, given in table 5.3 and in Fig. 5.7. The tilt angles in case of anions is determined mainly by the hydrogen bond from the water to the halide. The results obtained from the cation water clusters were not surprising as well, they are all aligned along the oxygen-ion vector. With increasing number of molecules in the clusters the standard deviation of the tilt angle (in the case of the anions and the cations) is growing, this supports the conclusion, that water-water interactions are getting dominant with the increasing number of water molecules.
So far we have covered the molecular charge deformation and the microscopic orientation of water around ions in case of small systems. The question for the liquid systems is now about how far the ion influences the structure of the liquid. Water creates a cavity around an ion, due to the ion size and charge as a consequence

n	θ	$\Delta\theta$	θ	$\Delta\theta$	θ	$\Delta\theta$	θ	$\Delta\theta$	θ	$\Delta\theta$
	$Li^+(H_2O)_n$		$Na^+(H_2O)_n$		$K^+(H_2O)_n$		$Mg^{2+}(H_2O)_n$		$Ca^{2+}(H_2O)_n$	
1	0.7	0.0	0.5	0.0	0.7	0.0	1.1	0.0	0.1	0.0
2	1.1	0.3	1.8	0.1	1.4	1.3	0.4	0.1	0.3	0.1
3	1.0	0.6	0.4	0.3	0.3	0.1	0.2	0.1	0.4	0.1
4	4.8	3.6	2.6	2.2	1.6	1.0	2.0	1.3	3.0	1.9
5	9.7	7.4	8.4	6.0	9.8	7.9	3.5	2.6	3.7	2.9
6							3.0	1.0	0.9	0.4
7									4.7	3.6
8									11.3	1.0
	$F^-(H_2O)_n$		$Cl^-(H_2O)_n$		$Br^-(H_2O)_n$					
1	148.5	1.1	156.9	0.0	152.9	0.0				
2	147.8	0.5	153.5	0.3	147.1	2.6				
3	152.9	8.7	146.5	3.7	159.9	17.1				
4	145.0	0.6	146.5	1.2	144.3	0.4				
5	141.8	4.4	143.8	1.2	145.0	10.2				
6			140.3	4.4	137.5	4.3				

Table 5.3: The table shows the average orientation θ of the water dipole vector with respect to the oxygen-ion direction (see Fig. 5.6) for the small water clusters with n number of water molecules. θ and its mean square deviation $\Delta\theta$ are in degree.

the surrounding water has to adapt to this geometry. In the cases of cations the dipoles tend to align along the oxygen-ion direction. Since we were interested in the question how far the ion affects the water, it is important to have more than just one shell. The two systems of 64 and 128 molecules are sufficient for this study. The probability distribution of the cosine of the angle between the oxygen-ion direction and the dipole vector was then collected (see Fig. 5.7).

The alignment along the oxygen-ion distance is observed for water molecules in the first shell of small clusters, see (a) (left and right panel of Fig. 5.7). The arrangement of water molecules around the divalent cations is more ordered than the one of molecules around the monovalent cations. More surprising is the fact that in the second shell the ion induced order is evidently disappeared, and this is true then for all further shells. This behaviour is independent of the nature of the ion, which clearly determines the parameters, size and order, of the first shell. This shows that the water has the ability to encapsulate an ion and to solvate it, while the complexity of the liquids remains untouched.

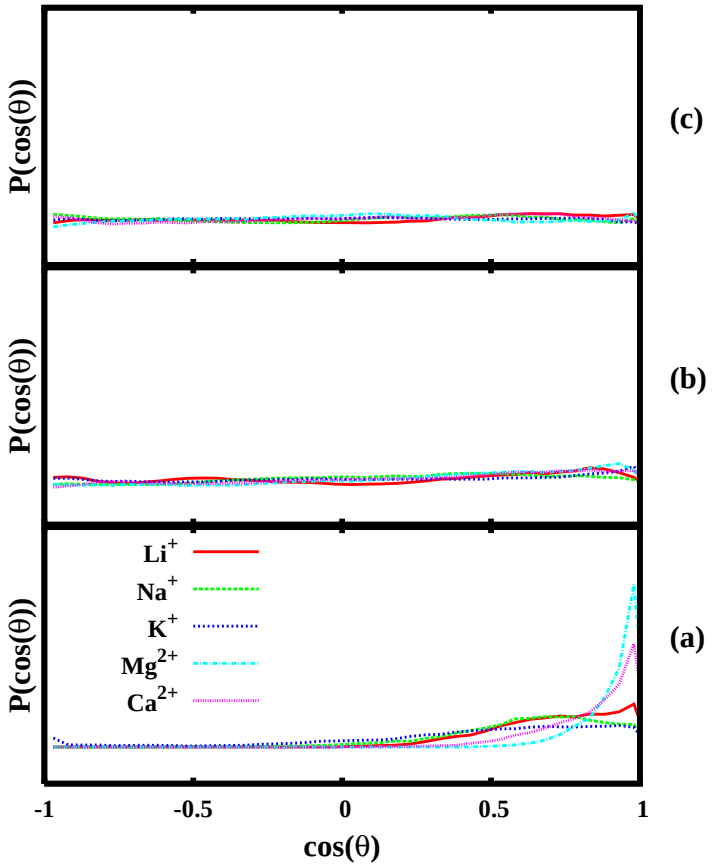

Figure 5.7: Dipole orientation with respect to the oxygen-ion direction for the case of 64 water molecules: (a) only molecules in the first solvation shell are counted; (b) only molecules in the second solvation are counted; (c) only molecules in the third solvation are counted. To be noticed that while in the first shell, local structures are ion dependent, beyond this shell this dependency vanishes in all cases.

5.4 Electronic Mechanism of water polarization: Basic Analysis

The effects of electronic polarization on the microscopic and the molecular scale have been shown, by studying small ion-water clusters and fully solvated ions. We have calculated the average molecular water dipole moments, which is an average molecular quantity and a direct measurement of the polarization due to electronic changes. As the studies of the microscopic and the molecular scale suggest, the water-water interaction is the most relevant process, even within the first solvation shell and independent from the nature of an ion. One question

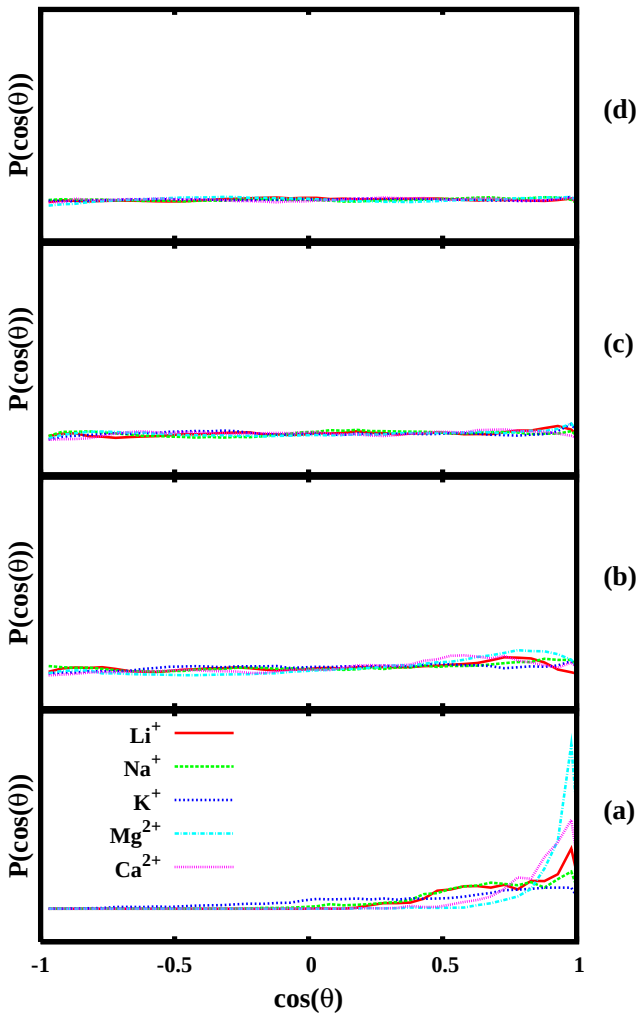

Figure 5.8: Dipole orientation with respect to the oxygen-ion direction for the case of 128 water molecules: (a) only molecules in the first solvation shell are counted; (b) only molecules in the second solvation are counted; (c) only molecules in the third solvation are counted and (d) only molecules in the forth solvation, i.e. bulk molecules are counted. To be noticed that while in the first shell, local structures are ion dependent, beyond this shell this dependency vanishes in all cases.

is still open, why is the water-water interaction so dominant. To answer this question we have to go more in details into the study of electronic properties, i.e. we have also to consider the electronic contributions to the dipole moment (see Fig. 5.9 and section 5.2.1). The direction of the dipole moment vectors,

in this work, is chosen to point from the positive to the negative charge. This choice implies that the dipole vector from the positive charged center (between the hydrogen atoms) towards the oxygen and the one from the oxygen to the negative charged center (between the lone pairs) are additive. The vector from the oxygen towards the negatively charged center (between the bonding pairs) is pointing in opposite direction. Thus this contributions is counter-balancing the lone pairs and OH ones. And the simplest way to consider the electronic contributions is to calculate the projection of these on the molecular axis of the water molecule (see Fig.5.1). The main component of the projection is along the **Z** molecular axis, the components projected on the **X**, **Y** molecular axis are collected as well, however they are negligible small compared to the **Z** contributions. The results of the projection of the localized negative charge and the positive charge along the **Z** axis are presented in Fig. 5.9. From this picture some general trend are emerging: (1) the O-H contribution is in average constant, and (2) the lone pair contribution decreases, with increasing number of water molecules around the ion, while the bonding pair contribution increases or approaches a constant value of bulk water. Case (1) is independent from charge and size of the ion. In case (2) one has to consider, that the decrease of the lone pair contribution is true for all ions, though less pronounced for monovalent cations, but extremely important for divalent ions. This decay is in contrast to recent concepts, which suggest that the lone pair elongation along the cation-oxygen direction should be dominant with respect to any other possible electronic polarization, thus this elongation should remain constant as the number of molecules increases.

Instead, the average dipole moment of water molecules around the selected cations results from a significant competition between the lone pair elongation/compression along the ion-oxygen direction and the bonding pair shift along the internal O-H bonds. The possible mechanism is the following; in case of the cation and one water molecule the lone pair contribution is dominant, and therefore the dipole is very large. When water molecules are added to the shell, they repel each other, due to the repulsion of the valence electrons, and this leads to a decrease of the lone pair ion polarization (see Fig. 5.11) and thus the lone pair contribution to the dipole decreases. Instead the contribution from the bonding pairs due to the shift back (towards the hydrogens) of the electronic charge (less polarization along the ion-oxygen direction) increases and thus balancing further the effect of the ion-lone pair polarization. This mechanism clearly applies in case of divalent cations,

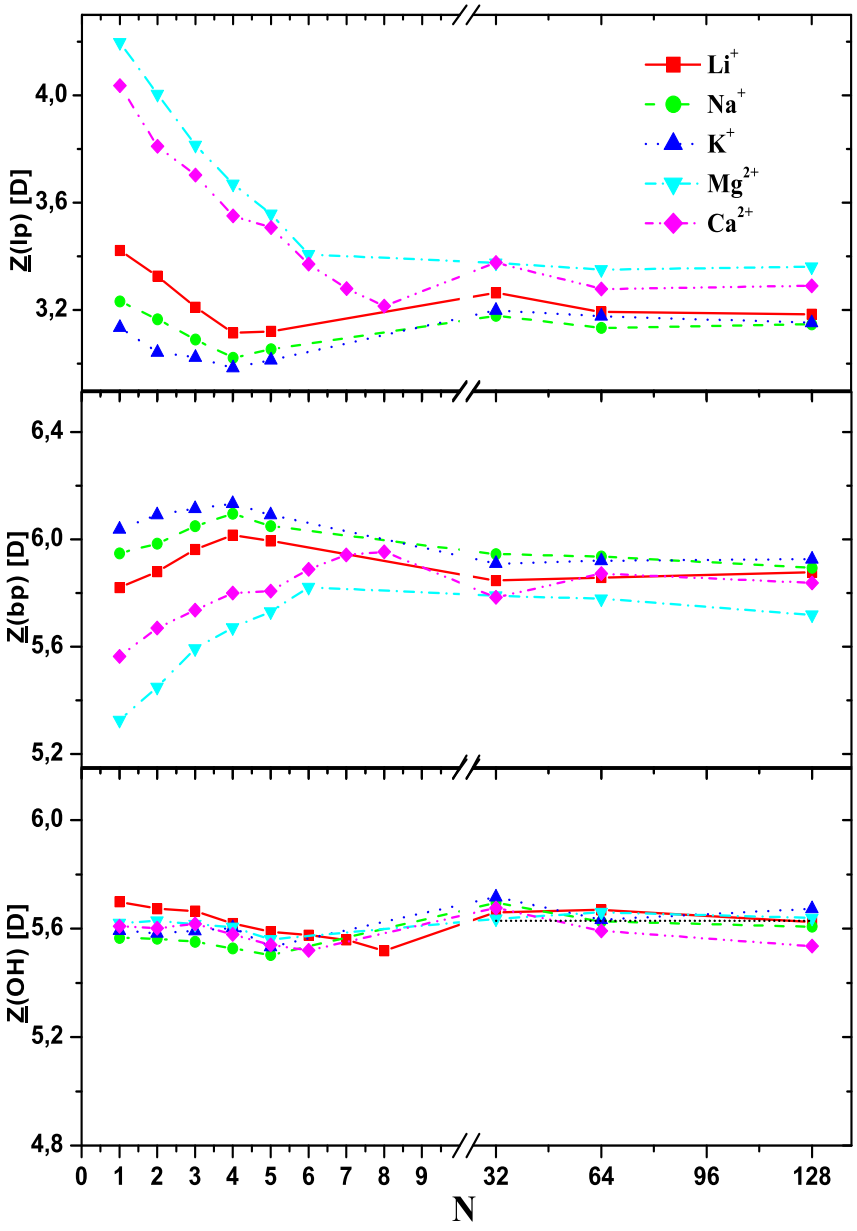

Figure 5.9: Projection of the oxygen-Wannier-center vectors (times the charge) along the molecular axis of water (in Debye); the lp stays for lone pair and bp for bonding pair. The lone pair contribution is decreasing, while the bonding pair contribution is increasing with increasing amount of water. Both contributions are approaching a constant level for sovalted ions. This shows the counter balancing effect, crucial for divalent ions, of the bonding pair against the lone pair in determining dipole moment in the first solvation shell of the ion

in case of the monovalent cations this effect is significantly reduced. And there the water molecules are already forming hydrogen bonds for clusters of $N = 5$. This leads to small increase of the lone-pair contribution and a small decrease of the bonding pair one, since they can act as both hydrogen bond acceptor (lone pair orbital shift) and hydrogen bond donor (bonding pair orbital shift). This effect cannot be found in the treated clusters of the divalent ions, since there are no hydrogen bonds present. This particular difference is based on the different strength of the ions inducing a certain alignment of the dipole moments along the ion-oxygen direction. This strength is larger for divalent ions, thus the alignment is more ordered; in the case of the monovalent ions the strength is weaker which leads to a less ordered alignment.

Additionally the angles $\theta(lp-O-lp)$ and $\theta(bp-O-bp)$ between the oxygen-lone pair vectors and also the angles between the bonding pair vectors were collected (see Fig. 5.10 and sub-figures within). The electronic structure of water in the small clusters is compared to the electronic structure of a single water molecule in vacuum. The liquid like solutions are compared to the values for liquid water in literature. As references the values for $\theta(lp-O-lp)$ and $\theta(bp-O-bp)$ given from Silvestrelli et. al. [53] were used. The general trend is: the $\theta(lp-O-lp)$ is increasing and since the lone pairs and bonding pairs are correlated, $\theta(bp-O-bp)$ is decreasing. This is complementary to the results from the projection of the different dipole contributions along the molecular axis. The increase of an angle then leads to a shorter projection along the molecular axis, which means that the projection for the lone pair contribution is decreasing and the projection for bonding pairs contribution is increasing.

The discussion of the projection of the different electronic contribution on the molecular axis above suggests, that in general the water-water interaction plays a crucial role (see also [78]) and the question is about how exactly this interaction enters into the polarization process. There are two possible reasons: (1) Figs.5.11,5.12 show that additional molecules lead to larger water-ion distance; which implies that the ion-water interaction is strong but only short ranged. (2) Or the orbital cloud interaction hinders the ion-water interaction. These two possibilities could be checked by studying the changes with respect to the ion-oxygen distance and with respect to the changes in the electronic density. The ion-oxygen distances are definitely correlated with the repulsion (short distance equals strong polarization and vice versa) but how strong is this effect? The larger

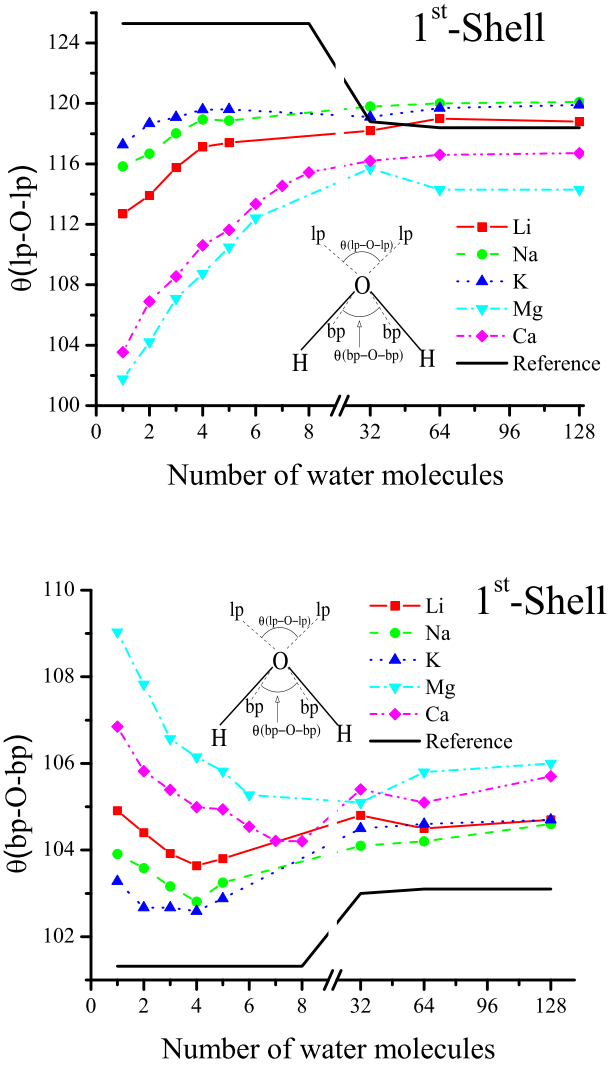

Figure 5.10: upper panel: Average lp-O-lp angle between the two lone pair orbitals with oxygen in the first shell around the ion for different systems; The cluster size is increasing from single water up to a complete first solvation shell. Then in the next step the water like system with 32 to 128 waters are given. It should be noted that the analogous to the behavior of the dipole moment, the polarization in the clusters is strongly depending on the ion while in the solutions the value (117 degree) is close to the one of liquid water (118 degree) with only small influence, which is left from the ion. Lower Panel: Same as left panel, but only for the binding electron pairs in the first water shell around the ion; the bp-O-bp angle is compensating the effect of the ion on the lone pairs; the balance of the WFC-O-WFC angles is determining the dipole moments.

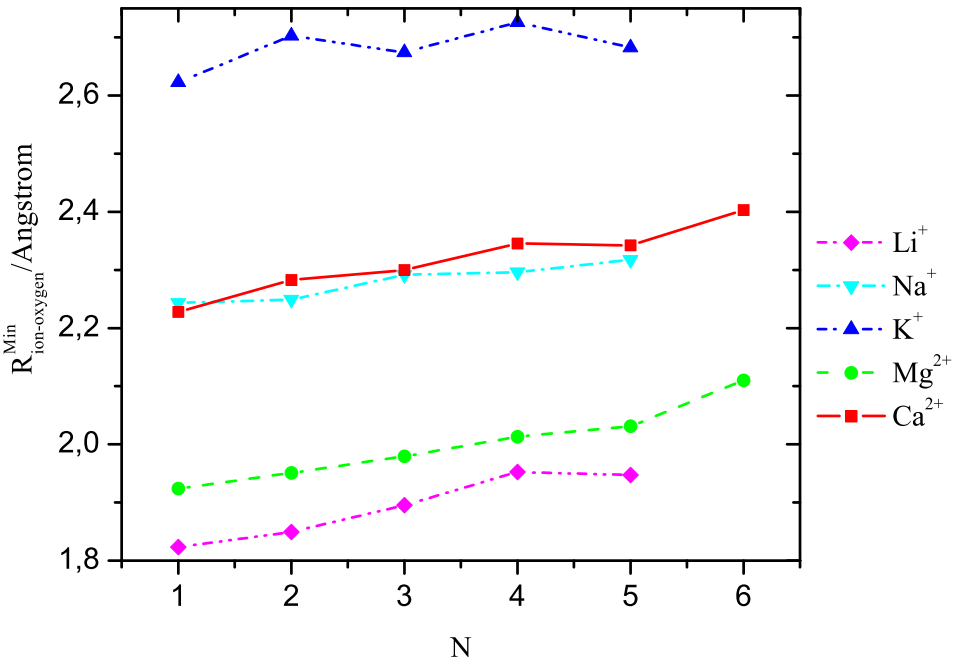

Figure 5.11: Minimum ion-oxygen distance for the clusters up to five molecules (monovalent ions) and six water molecules (divalent ions). The increase in the distances is due to water-water repulsion. This is due to the water-water repulsion for small clusters to which must be added the hydrogen bond formation in case of liquid systems.

distances would lead to a weaker attraction of the lone pair by the cation and therefore the bonding pair contribution is stronger. The way of testing this was to simulate a configuration with Ca^{2+} and one water molecule at the ion-oxygen distance found in the $Ca^{2+}(H_2O)_2$ cluster (which will be called as $Ca^{2+}(H_2O)_1^{(new)}$ in the following). For this cluster ($Ca^{2+}(H_2O)_1^{(new)}$) the dipole components were calculated; the lone pair vector projection along the molecular axis has a value of 4.02 D compared to 4.04 D of the standard configuration, and a value of 5.58 D for the bonding pair vector projection compared to 5.56 Debye of the standard configuration. This shows that the changes in the ion-oxygen distance are not relevant, and the water-water interaction is basically the repulsion of the electronic clouds of each molecule which directly influences the lone pair and bonding pair orbital changes (lone pair contraction and bonding pair elongation). This one can

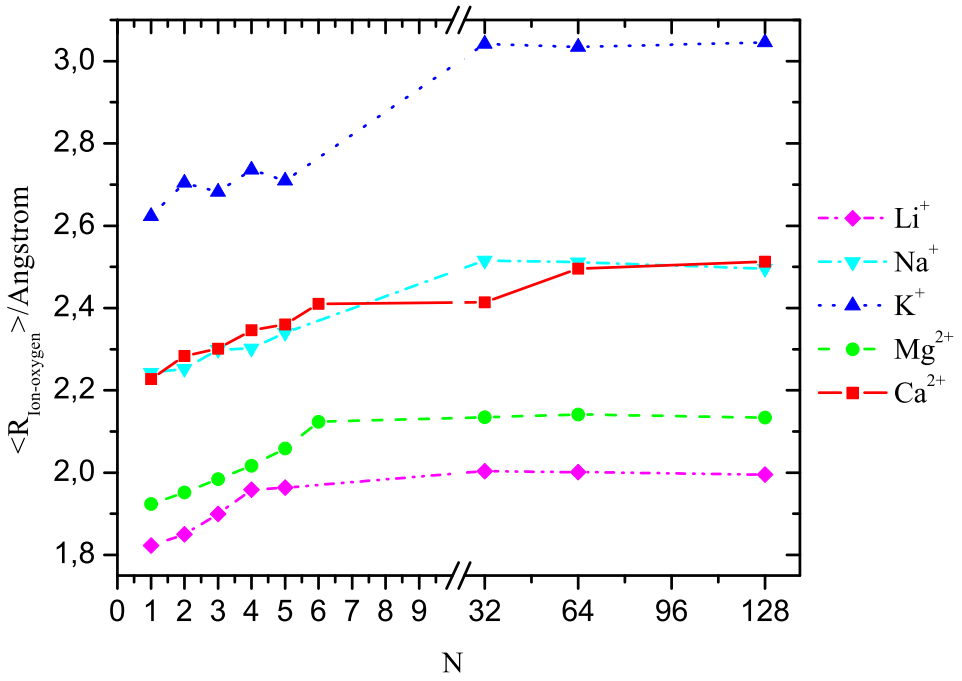

Figure 5.12: Average ion-oxygen distance in the first solvation shell for small clusters and for the liquid system. In general, the distances are increasing beginning from small clusters to an ion specific average distance in liquid. This is due to the water-water repulsion for small clusters to which must be added the hydrogen bond formation in case of liquid systems.

immediately see if the dipole contributions obtained for $Ca^{2+}(H_2O)_1^{(new)}$ cluster is compared with those from the $Ca^{2+}(H_2O)_2$ cluster. The comparison show that the lone pair contribution is about 0.2 D higher in case of $Ca^{2+}(H_2O)_1^{(new)}$ and the contribution of the bonding pair is about 0.1 D higher in case of $Ca^{2+}(H_2O)_2$. The only difference between the two cluster is the electron cloud repulsion in the $Ca^{2+}(H_2O)_2$ cluster, which confirms the idea that this kind of repulsion is the key element in the process of compressing the lone pair and stretching down the bonding pair orbitals. This effect is true in case of the two compared clusters but going towards larger clusters the effects becomes even more pronounced (see Figs. 5.9). This we explicitly show with Figs. 5.13, 5.14, 5.15 by looking at the differences of the perturbed (water in presence of the ion) with the unperturbed (single water

molecule in vacuum, and in the liquid case: the water system without the ion) electron density. This was done for Na^+, Mg^{2+}, and Ca^{2+} to prove if in all cases the orbital cloud interaction hinders the ion-water interaction. This is indeed the case as directly shown by the contour plots. The excess of charge with respect to the isolated water is given in blue colors, while depletion of charge is shown by brown colors. The polarization of the single water in the case (a) in Figs. 5.13, 5.14 is the largest (which is represented by dark blue in the Figs. 5.13, 5.14); the different strength of polarization caused by Mg^{2+} (stronger polarization; larger area of dark blue) and Ca^{2+} is due to the ion size and therefore the distances between ion and water are different (see Fig. 5.11, 5.12). While the number of water molecules increases the polarization effect is decaying very fast to reach a constant level (to a lighter blue or decreasing amount of dark blue), which is almost the same for Mg^{2+} and Ca^{2+} (as already shown by the projection). Fig. 5.15 is given to shown that the orbital repulsion also holds but it is much less pronounced for monovalent ions.

5.5 Discussion and Conclusions

The water molecules around the ion were described by the small clusters and then expanded towards the liquid system. The interplay of the different shells could be discussed and the electronic properties behind this behaviour could be determined. With this study new details about the hydration of ions were found, since the hydration is present in almost every biological and many chemical/physical processes this knowledge can be transfered to understand several other systems. This understanding then will cover the effects on various levels, the local (the ion is acting on the water and the present polarization due to the ion can be discussed) and the global ones (water-water interaction coming from the bulk and acting on the first solvation shell). This is of particular interest in the case of computer simulation, since the recent classical water models are depending rather on theoretical than on experimental results.

We have studied small ion-water clusters and ions hydrated in 32,64, and 128 water molecules. Reasonable geometries and initial structures from literature for the small ion-water clusters have been optimized. The range of ions is from monovalent positively and negatively to divalent positively charged atoms. For the positively charged atoms larger systems were treated; we accumulated several pico-seconds

for each system. The idea was to study the local effects and then link these results to the global effects. For this reason the dipole moments of the clusters have been determined, since this quantity can describe the ion induced polarization directly. We reproduced the single water dipole moment of previous work and found that by increasing the number of water molecules the dipole moment decreases and then approach the value of bulk water[53, 54], independently from the ion. We have also studied the orientation of the dipole moments with respect to the ion-oxygen direction for systems with 64 and 128 water molecules. The divalent ions have a stronger impact than the monovalent ions, which means the dipole moment are stronger aligned along the ion-oxygen direction. But the orientation of the average water dipole moments towards the ion showed that the effect of the ion is only present in the first solvation shell and is vanished already in the second solvation shell. This is interesting because, it is in contrast to the general opinion, that the ion affects the water polarization in the first shell more than the remaining water does. Thus it is believed that the high dipole moment is mainly due to the ion. Regarding our results the influence of the ion on the water polarization is negligible and basically results in the geometrical arrangement of water around the ion, and vanishes immediately in further shells. This analysis at the atomistic level showed that the water-water interactions are dominant for ion-water systems with low ion concentration. To understand why the water-water interaction is so crucial even at ion-water local scale we looked at the various electronic contributions to the water dipole moment in case of the cation-water clusters, e.g. the lone pair one, bonding pair one and O-H contributions. The data collected for the small clusters and the larger clusters then showed that similar to the average dipole moment each contribution started at an initial value (individual for each ion) and ended at the bulk value, except the O-H contribution which remains constant. The mechanism behind this behaviour was then studied looking at the electronic orbitals of water in the different clusters and systems. The differences of the perturbed water (water in presence of the ion) and the unperturbed molecule (water alone) were calculated. The results show that the non-bounded water-water cloud orbital interaction hinders ion-lone pair full polarization, which in turn pushes the lone pairs towards the oxygen and the bonding pairs shift along the O-H bond. In conclusion then the results prove and explain why the water-water interaction is dominant with respect to ion-water interactions.

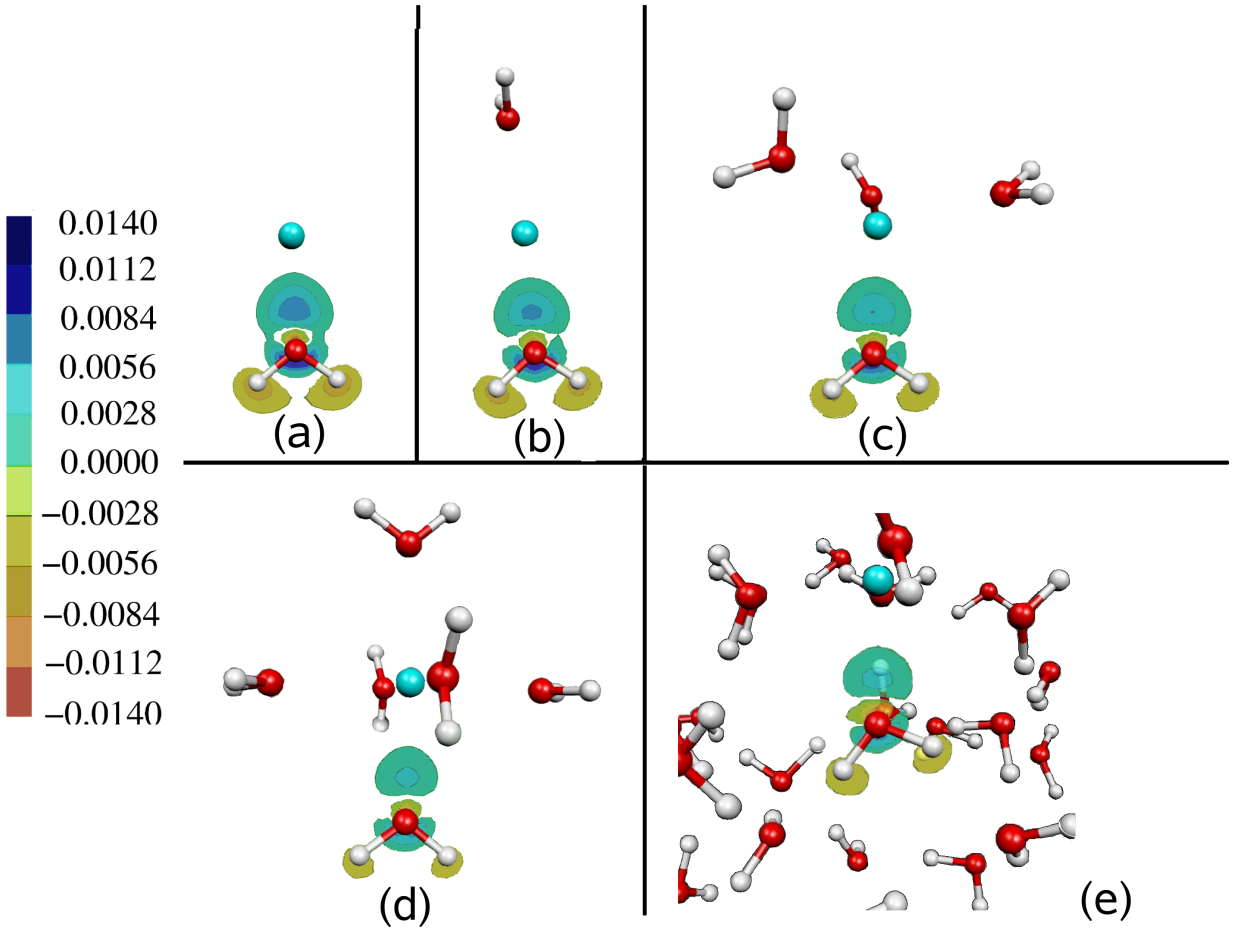

Figure 5.13: A planar section of the density difference (measured in $\frac{e}{au^3}$), with respect to the isolated water molecule, projected onto the Wannier functions (for $Ca^{2+}(H_2O)_1$ (a), $Ca^{2+}(H_2O)_2$ (b), $Ca^{2+}(H_2O)_4$ (c); and $Ca^{2+}(H_2O)_6$ (d) and $Ca^{2+}(H_2O)_{64}$ (e)) is shown. In the $Ca^{2+}(H_2O)_1$ cluster the electrons are pulled towards the ion (excess of charge with respect to the isolated molecule is the shown in dark blue; depletion of charge is pictured as light brown to red), while with the additional molecule the electronic density is pushed back towards the region below the oxygen towards the bonding region. The repulsion between the water molecules induces a shift in the electronic density which lowers the molecular dipole. This is also shown for the $Ca(H2O)_{64}$ system in (e). Here the difference is done with respect to the case of the same liquid configuration excluding the ion; (e) shows similarities to (d), but the density fluctuation is due to the interaction with the second solvation shell. This figure directly shows that the strong ion-water interaction is decreasing due to additional molecules, even in the smaller clusters.

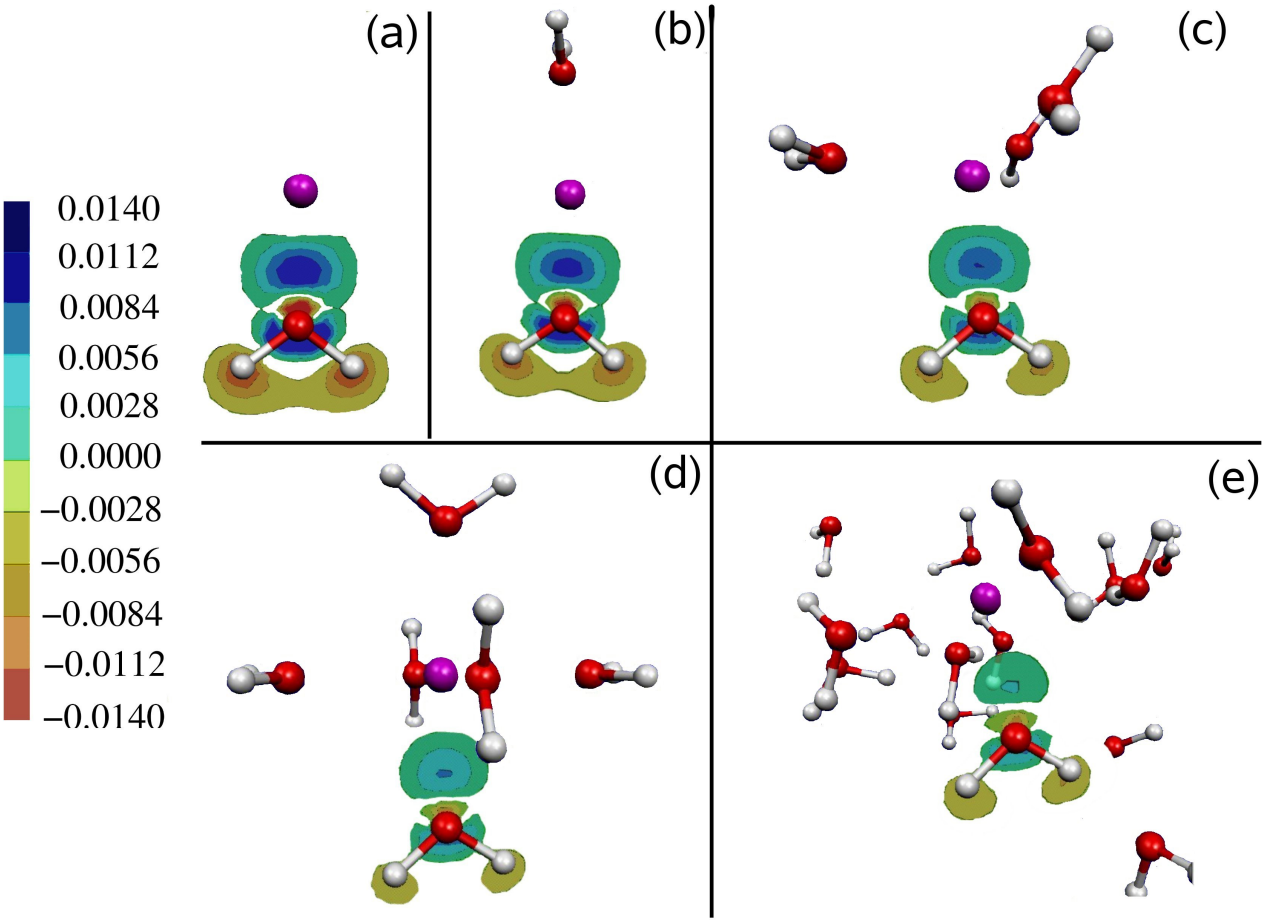

Figure 5.14: As the figure 5.13: A planar section of the density difference, with respect to the isolated water molecule, projected onto the Wannier functions (for $Mg^{2+}(H_2O)_1$ (a) to $Mg^{2+}(H_2O)_4$ (c); and $Mg^{2+}(H_2O)_6$ (d) and $Mg^{2+}(H_2O)_{64}$ (e)) is shown. Even though Ca^{2+} and Mg^{2+} are of different size, the general trend already described in the previous picture still holds. The only difference is the shorter distance in the Mg^{2+}-water clusters (see Fig. 5.11, 5.12) which leads to a more intense polarization along the ion-oxygen direction.

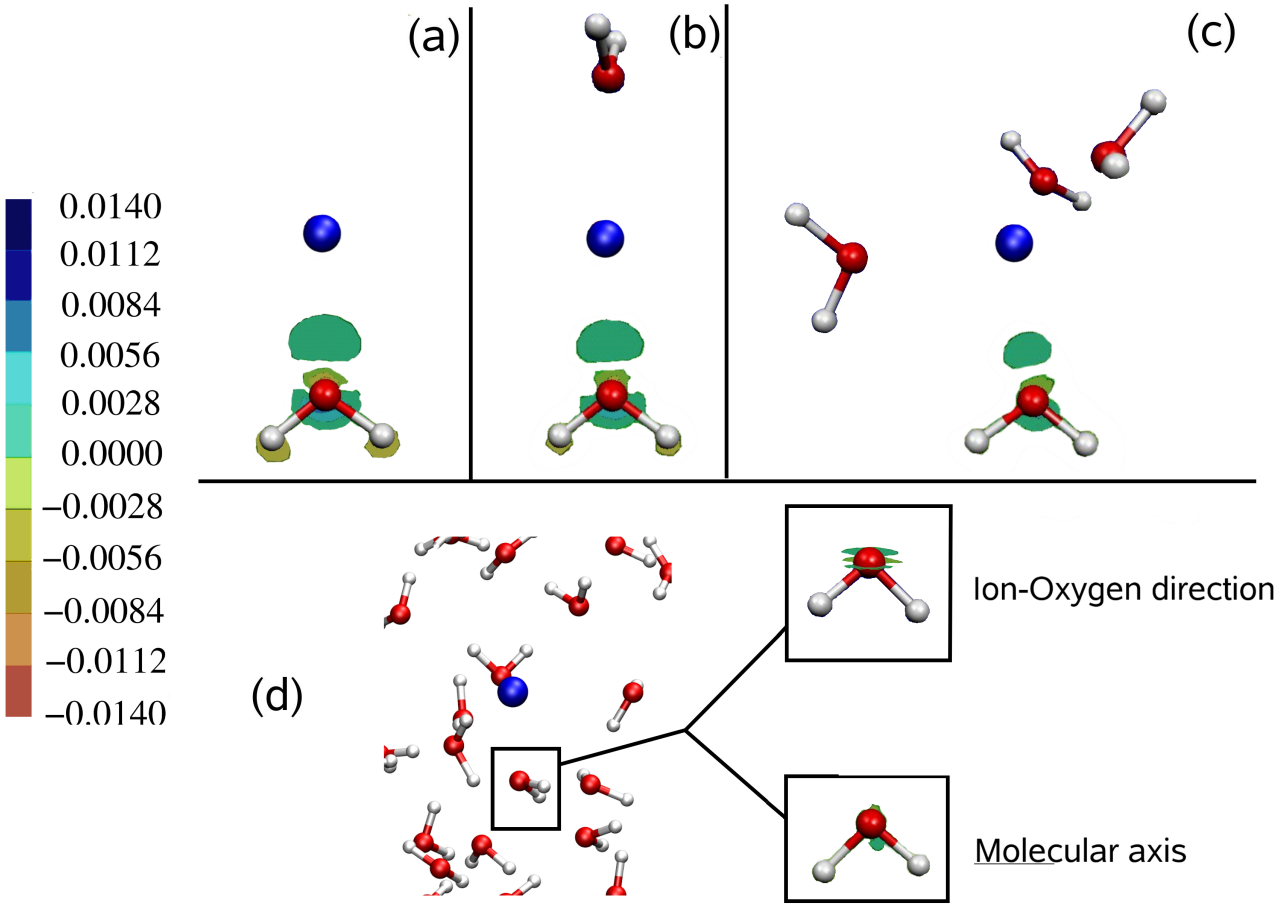

Figure 5.15: As the figures before: A planar section of the density difference, with respect to the isolated water molecule, projected onto the Wannier functions (for $Na^{2+}(H_2O)_1$ (a) to $Na^{2+}(H_2O)_4$ (c); and below $Na^{2+}(H_2O)_6$ (d) and $Na^{2+}(H_2O)_{64}$ (e)) is shown. Here the polarization of the water molecules is much weaker than the one shown in the previous pictures. In the case of the larger clusters the effect of the ion on the water is negligible, since almost every initial polarization vanished.

6 Ionic Liquids

6.1 Introduction: Ionic Liquids

Ionic liquids (IL) are becoming increasingly popular subjects of study for chemical, industrial and technological reasons. Ionic liquids have many properties that extended beyond the ranges of any other organic solvent, due to the possible variations of the molecular structure. Examples are non-volatility, non-inflammability, solvation capabilities to cite a few. Ionic liquids must be distinguished by molten salts for this a temperature criterion must be introduced. Molten salts are high-melting, highly-viscous and very corrosive, while ionic liquids are low melting (mostly below 100 ^{o}C), have relatively low viscosity. Of particular interest are those ionic liquids based on quaternary ammonium or phosphonium salts, which show a wide range of properties like electrochemical stability, good electrical conductivity, high ionic mobility, low melting points, almost no vapor pressure, furthermore chemical and thermal stabilities, and many more properties. Due to these properties the applications range from electrochemistry technologies (as electrochemical solvent) to media in physical-chemistry spectroscopy. Furthermore they are of importance in organic chemistry for synthesis, catalysis, extraction processes, and even for pharmaceutical purposes [79–103]. Ionic liquids can be designed for fitting the individual requirements of an application by: (i) the attached side chains to the cation can be alkyl-groups or other charge stabilizing groups; (ii) the anion can be a simple chloride or even larger and spatial challenging; (iii) one can also choose between a variety of basic structures for the positively charged ion and (iv) by adding functional groups to the side-chains of cations and/or to the anions.
In general, the properties of IL's are well known experimentally, however there is not yet a robust theoretical framework which allows for understanding the reason behind their interesting properties and those are still under investigation [104–109]. For this reason the intention in this work is to approach ionic liquids at the very basic levels, the electronic and the atomistic one (see multiscale model-

ing section 6.2) by combining the different levels of theory to describe different aspects of ionic liquids. The linking motif will take place in form of the multiscale modeling scheme (see Fig. 6.3). At the electronic level we use high level quantum chemical calculations, which give accurate results, but are limited to smaller systems like 1 and 2 ion pairs. Then the density functional theory (DFT) is used to describe the electronic and atomistic level, for one to eight ion pairs (1 ion pair= 1 cation and 1 anion). The DFT, describing the electronic and atomistic level, does not have the limitation as *ab initio* calculations but to ensure that the small clusters are described correctly and accurately, such that larger systems can be addressed, it is important to test DFT with Møller-Plesset perturbation theory (MP2) calculations. The DFT results of the small systems (1 and 2 ion pairs) will be compared to the *ab initio*(RI-MP2) calculations. The comparison is done by checking the structures, the harmonic frequencies and the energetic order of the different structures. The first step to approach ionic liquids and to employ the multiscale modelling scheme is: to start from a known and simple ionic liquid, this means to start with the basic element, the cation, of most common quaternary ammonium salts is 1,3-di-alkyl-imidazolium (see Fig. 6.5), with a variety of different alkyl-groups and anions. In particular the focus of the study presented here is 1,3-dimethyl-imidazolium chloride as the simplest room-temperature ionic liquid, which is known and studied on both experimental and theoretical levels.

The imidazolium ion can be synthesized and modified very easily, see Fig. 6.1. In Fig. 6.1 one possible reaction pathway is given, which in detail is specified in Fig. 6.2. The residues R_i (i=1,..,7) in Figs. 3.1, 6.1, 6.2 can be everything, e.g. alkyl groups or side chains including functional groups. The basic idea of these residues is to stabilize the positive charge of the central ring/atoms (e.g. (c)). There are two ways for doing that: (1) the charged center has to be shielded, i.e. the residues have to be chosen such that nucleophile particles cannot attack due to the spatial hindrance of the side-chains; (2) the side-chains can formally induce charge into the system via the so called +I-effect (electrons are pushed towards the positive charged center) or the +M-effect (mesomeric effect, which can stabilize the charge by distributing it over several atoms). The ionic liquids given in Fig. 3.1 most commonly have large and electron inducing side-chains, but in principle no mesomeric effects.

For different one ion pairs the structures, energies and harmonic frequencies from DFT and MP2 calculations will be discussed, while in case of the two ion pairs

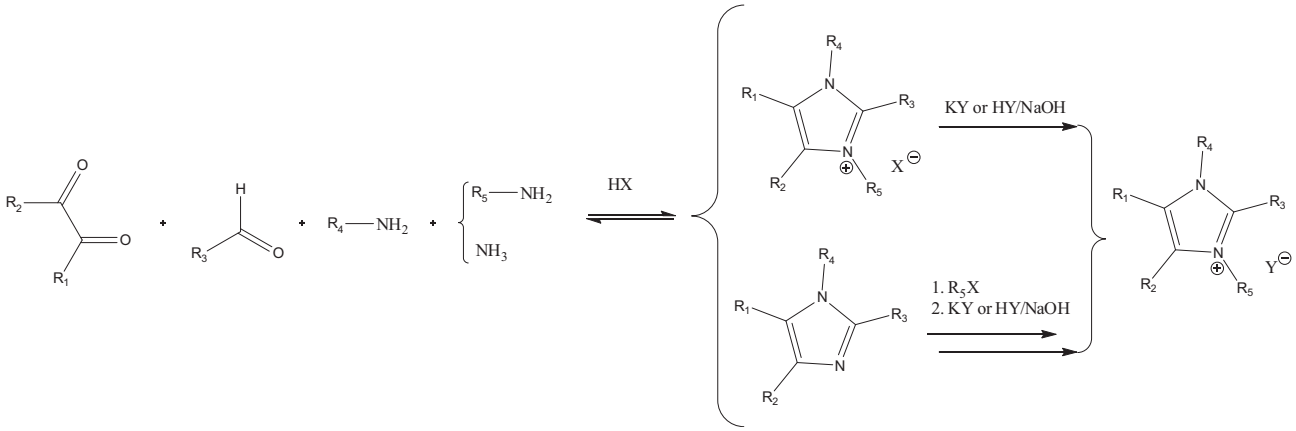

Figure 6.1: One possible reaction pathway from simple organic molecules to the basis compound for imidazolium based ionic liquids. The residues R_i (i=1,..,7) can be chosen freely, which leads to a large variety of different systems of symmetric imidazolium cations or anti-symmetric ones. Another advantage is the easy control of this reaction, see Fig. 6.2.

only the structures will be compared. To study the different kinds of interactions taking place in ionic liquids (from small to large clusters) and to have a link from the electronic to the more atomistic description (via classical MD) the dipole and quadrupole moments have been calculated via the maximally localized Wannier scheme.[11–13] On the DFT level the Wannier centers [11–13] have been collected to calculate the different dipole and quadrupole moments of each cation and in case of the different one ion pairs also of the total dipole. Next the DFT based dipole and quadrupole moments and the MD based ones were directly compared with each other. The dipole moments calculated with DFT show a very broad distribution, while the values classical force fields display a very narrow distribution.

This chapter is organised as follows: in the next section the technical details will be discussed, providing information about the *ab initio* and the DFT setups. Then in the second section the direct comparison of the high level quantum chemistry RI-MP2 and DFT calculations is given; which will be followed by the discussion about the electrostatic moments and the comparison with the classical force fields.

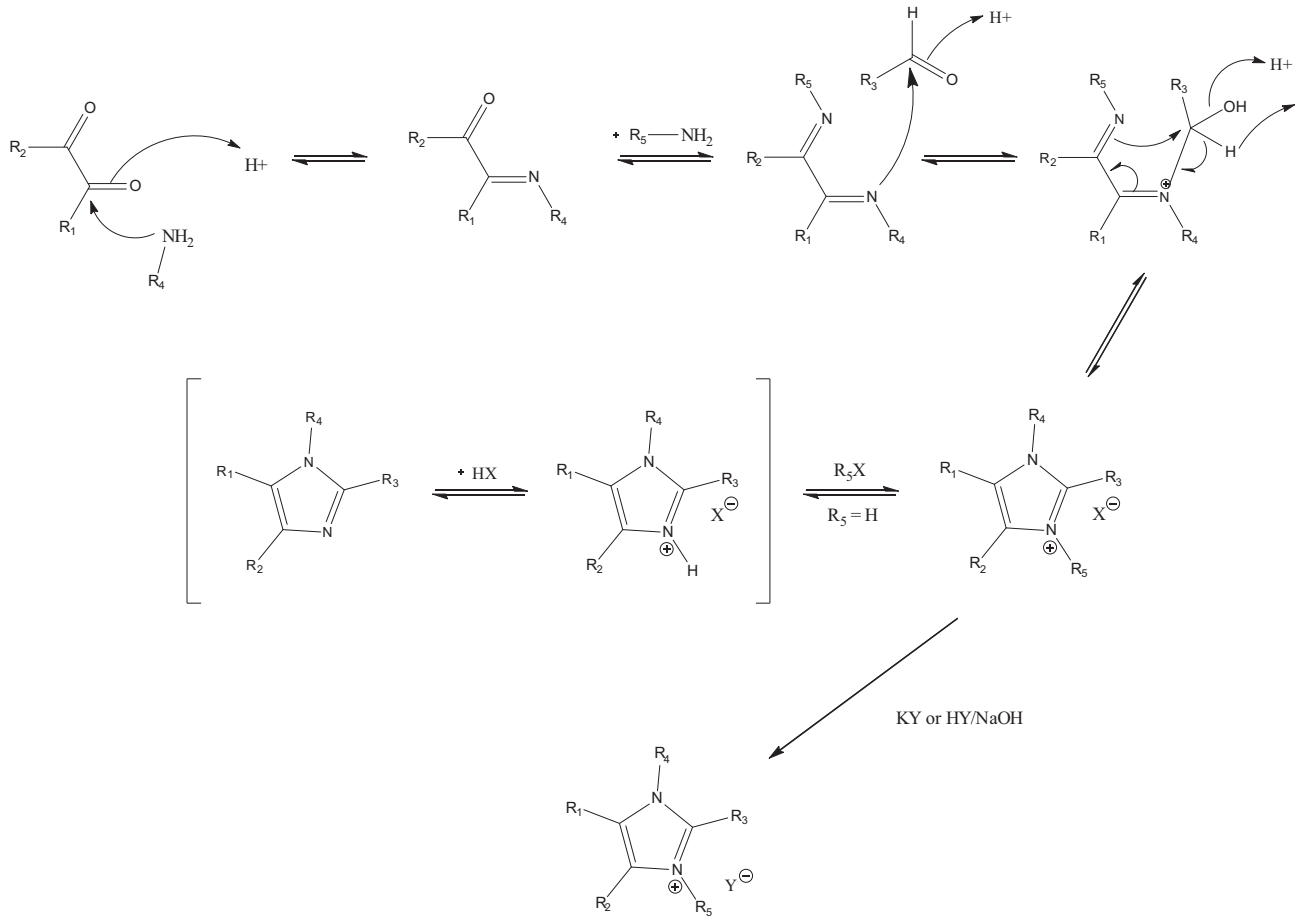

Figure 6.2: One possible pathway to synthesize imidazolium based ionic liquids is shown here to demonstrate how easy these systems could be generated and modified.

6.2 Multiscale Modeling Scheme

Every process/system can be described on different length scales, from the electronic over the atomistic to the macroscopic scale. The macroscopic behaviour is based on the underlying levels; and therefore the changes occurring there may have dramatical effects also on the macroscopic properties. The *post* Hartree-Fock methods are highly accurate and can completely describe a system on the electronic level, but the computational costs are extremely high, concerning RAM and hard disc space. Thus the application of these methods is possible only for relatively small systems, but the advantage is that there the local electronic effects can be explicitly described. These highly accurate description cannot be accessed via DFT calculations, but the system can be described with the help of the (less

accurate) electron density based quantities. The computational costs are also not that small but the interplay of the electronic scale and the atomistic scale can be described. The cheapest method (in terms of computational costs) is the classical MD, there the force fields describe the atomistic properties at classical level. A combination of these methods properly done allows for a detailed study of the different aspects occurring at different scales. Fig. 6.3 shows the general multiscale modeling approach towards the IL. Three level of theory will be applied. On the electronic level the post Hartree-Fock methods (MP2, CC2) are applied on small systems (one ion pair and two ion pairs) with different basis sets from aug-cc-pVDZ to aug-cc-pV6Z; on the atomistic and macroscopic level classical simulations are used; and finally these two theories are bridged/linked to the DFT level implemented in CPMD. The results on each level of theory can be compared to experiments if available.

6.3 Technical Setup

The Car-Parrinello molecular dynamics program (CPMD) and the PBE exchange-correlation functional within the planewave pseudopotential density functional theory approach has been used for the study of the ionic liquids. [112, 20] They have been approached in the same way as had been done for the solvation of ions in water. [113, 78] We started with a small system including only one cation and one anion (for simplicity we refer to them as ion pair (IP)) and then increase (from two ions pairs over four IP's to eight ion pairs) the size of the clusters. The one IP's have been manually constructed according to what is suggested in literature.[104] The two to eight ion pairs have been provided by classical molecular dynamics simulations with two different force fields and optimized afterwards with DFT and RI-MP2 calculations. The two to eight ion pairs are calculated by classical molecular dynamics simulations with (a) the Lopes force field [114] and (b) the Wang force field [115] at 425 K,which is above the melting temperature of

$$DMIM$$

Cl. The structures from the Wang force field have been minimized with respect to the energy (at 0K) afterwards.[111] Four configurations, for each cluster size, were picked out of a box with 239 ion pairs and then the simulation ran for 4ns totally each. The structures of clusters which have been used for the DFT study are taken

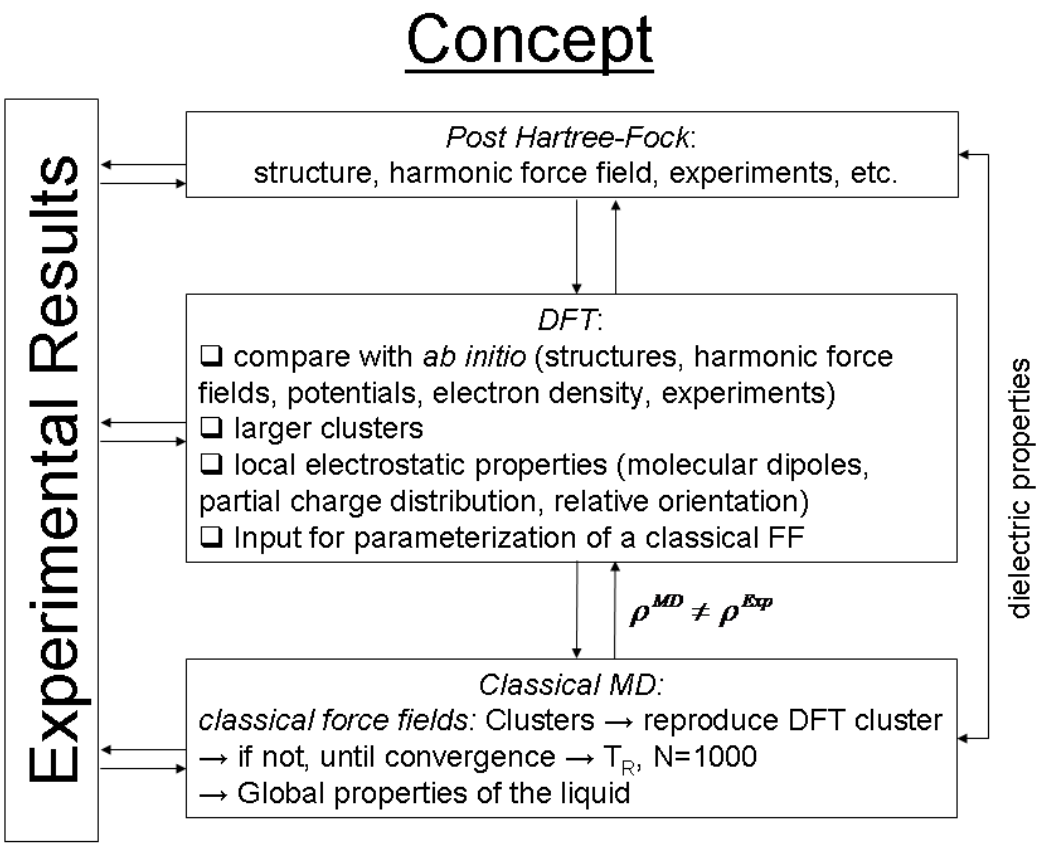

Figure 6.3: The multiscale modeling idea: All scale's are accessed separately and compared to experimental results, furthermore they are compared with each other and improved until consistency is reached. The high level quantum mechanical calculations must be reproduced by DFT calculations in order to have the correct technical setup; then in the next step the classical atomistic simulations and DFT are used to prove the consistency between classical based force fields and quantum description. The post Hartree-Fock calculations [110] and the classical parts [111] are done by our collaborators in Frankfurt. We will link the post Hartree-Fock and the classical part using DFT embedded into CPMD.

from these MD simulations, i.e. uncorrelated local structures after 1ns, 2ns, 3ns, and 4ns. Thus we could average the results over eight different configurations for each ion pair (in total 24 different configurations). Each structure was optimized with this DFT approach providing a energy cutoff of 70 Ry. As convergence criteria the atomic forces had to be either below/around 10^{-3} and/or a constant level of energy was reached. The later criterion was necessary only in case 8 ion pair systems since the number of degrees of freedom was quite high. Then the structures (optimized with RI-MP2/aug-cc-pVTZ) were used as input for further DFT calculations and the geometries were re-optimized and also the harmonic frequencies were collected. The structures and harmonic frequencies obtained for the ion pairs were compared with those obtained after high level quantum mechanical calculations on isolated one IP's [110]. The total energies were obtained as well, and thus the energetic order of the ion pairs can be found (and also compared). The DFT calculations provided the optimized structures of one and two ion pairs as input structures for the high level quantum chemical Møller-Plesset perturbation theory (RI-MP2) calculations. Using RI-MP2 first with aug-cc-pVDZ and afterwards with the aug-cc-pVTZ basis set [116] the structures were re-optimized and the harmonic frequencies were collected. With the optimized structures further single point calculations have been done; (a) with the more extended basis sets aug-cc-pVQZ and aug-cc-pV5Z and (b) also by applying the more accurate coupled cluster theory (RI-CC2, CCSD(T)) and performing single point calculations. Having shown that the DFT results for the two ion pairs are not far off from *ab initio* results the next step is done by optimizing the 4 and 8 ion pairs. For the optimized structures the dipole and quadrupole moments were calculated by using the maximally localized Wannier scheme [11–13], implemented in CPMD. In this scheme the electron density is localized around single molecules by localizing the plane-wave basis to orbital like functions localized around the single molecules. These orbitals can be represented by centers, for a given molecule, which are spatial locations of point-charges, each corresponding to an electron pair. The dipole moment is described in the standard way as: $\mu = \sum_j q_j \mathbf{r}_j$; where, q_j is the charge, negative for the centers representing the electrons, and positive, corresponding to the valence electrons, in case of the nuclei. The vector $\mathbf{r}_j$ is the vector from a reference point (for the ionic liquids we chose the center of mass of the cation) to the charge coordinates. The trace-less quadrupole moment is described as: $\theta_{\alpha\beta} = \frac{1}{2}\sum_{j=1}^{N}\left(3\mathbf{r}_{j,\alpha}\mathbf{r}_{j,\beta} - |\mathbf{r}_j|^2\,\delta_{\alpha,\beta}\right) q_j$ (with the same definitions as above,

but taking into account the different directions $\alpha, \beta = x, y, z$). The dipole and quadrupole moments were collected for all clusters, and compared with literature. Additionally, the dipole and quadrupole moments were calculated using classical methods (MD and the Lopes and Wang force fields) to compare them with the results from DFT calculations. The optimized structures from DFT calculations were taken as initial configurations and optimized with MD.

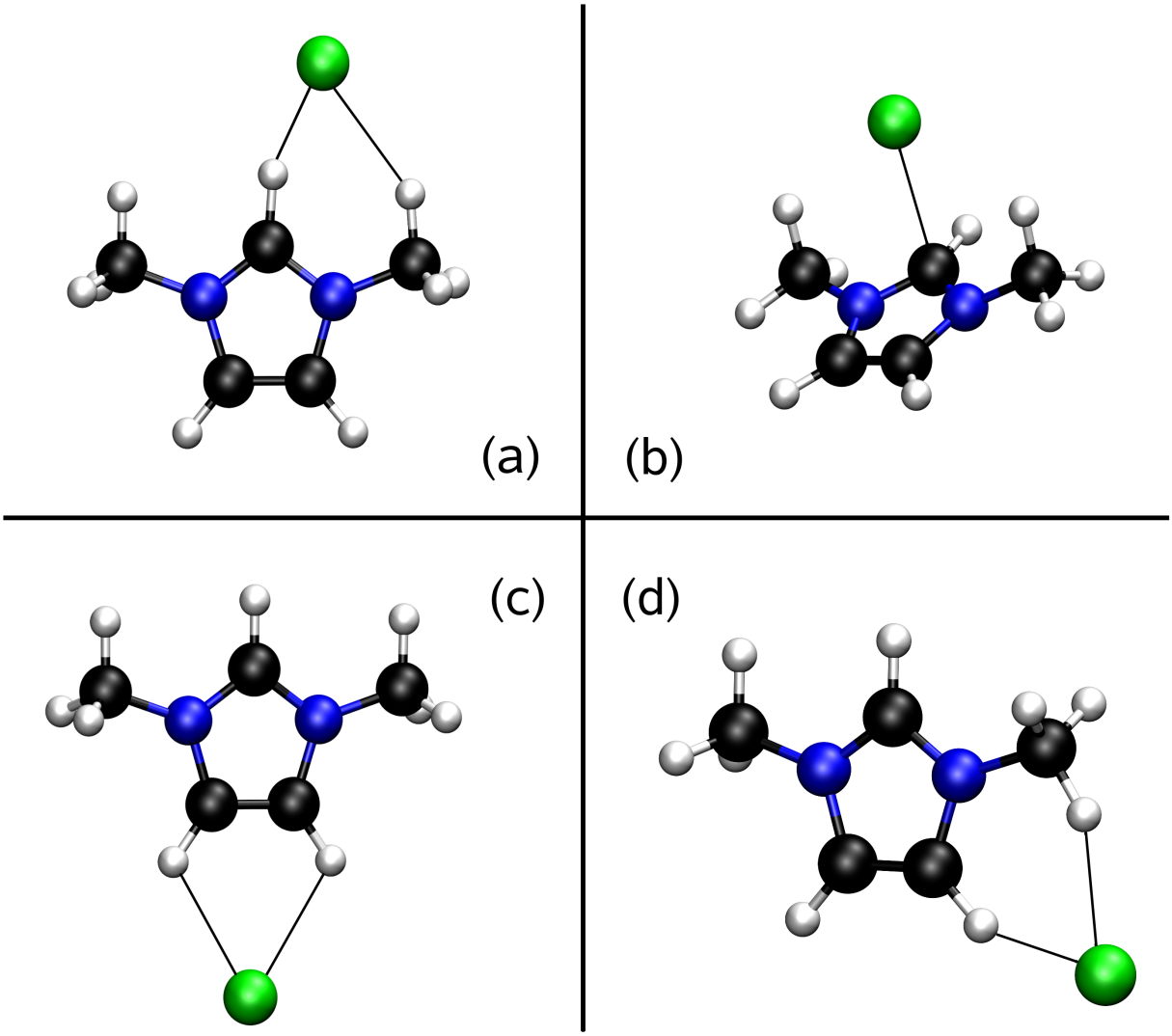

Figure 6.4: The four minima structures for one ion pair of 1,3-dimethylimidazolium chloride have been constructed according to literature [104]. They were used as a starting point for the comparative study of MP2 and DFT for ionic liquids. We could reproduce them with good agreement using DFT/PBE/70Ry and MP2/aug-cc-pVTZ, see table (right panel) in Fig. 6.1.

6.4 Results and Discussion

6.4.1 *Ab initio* versus Density Functional Theory

At the beginning we took the structures from previous work [104] as initial configurations for the optimization of the structures via DFT. In the next step the results were then inserted into RI-MP2 calculations, where the geometry, energies and the frequencies were obtained. The results were input structures for another DFT run. The structures of the one ion pairs are given in Fig. 6.4. With this benchmark test we compared the two methods (MP2 and DFT) with each other. The reason is that we want to know if our setup is correct and that the results we obtain are consistent, such that we can proceed to study larger systems (in case of DFT calculations). But more important is that we calculate very accurate data for our study of the electronic scale with two different methods.

		Calculations		Literature[104]	
Geometry		RI-MP2	DFT	MP2	DFT
1	$d_{H^{14}-Cl^-}$	1.967	1.955	2.006	1.919
	$d_{H^{13}-Cl^-}$	2.468	2.522	2.565	2.573
	$d_{H^{14}-C_2}$	1.119	1.140	1.111	1.152
	E_{rel}	0.0	0.0	0.0	0.0
2	$d_{C^2-Cl^-}$	2.626	2.575	2.697	2.518
	$d_{N^3-Cl^-}$	3.105	3.184	3.132	3.140
	$d_{C^4-Cl^-}$	3.681	3.896	3.634	3.825
	E_{rel}	-.7531	1.8253	-1.2	0.2
3	$d_{H^{15}-Cl^-}$	2.463	2.504	2.525	2.496
	E_{rel}	13.6	14.2	13.6	15.3
4	$d_{H^{16}-Cl^-}$	2.276	2.296	2.355	2.305
	$d_{H^{12}-Cl^-}$	2.094	2.118	2.152	2.076
	$d_{H^{14}-C^2}$	1.075	1.082	1.076	1.087
	E_{rel}	7.3	6.3	7.5	7.9

Table 6.1: Structural properties of the four minima structures of the one ion pair (shown in Fig. 6.4) optimized with RI-MP2 and DFT. DFT and RI-MP2 calculations are consistent and show good agreement with literature and with each other.

Then the structures from the ion pairs obtained from the two different methods were compared and the results for geometrically properties are given in table 6.1. From that table two aspects emerge. First, the RI-MP2 and DFT calculations are consistent and show good agreement with maximum 5% difference (the values in

literature show 7% difference compared to each other). Very good agreement with literature is achieved; all the deviations for the distances are below 4% compared to the data available.[104] Next the order of the total energies from MP2 and DFT were compared with that from Bühl et al. [104] The observed differences are due to the used method and basis set, Bühl et al. used a smaller and less accurate basis set as the ones used in the current study. And as shown in table 6.1, we can reproduce not only the structure in good agreement but also the energetic order of the different geometries.

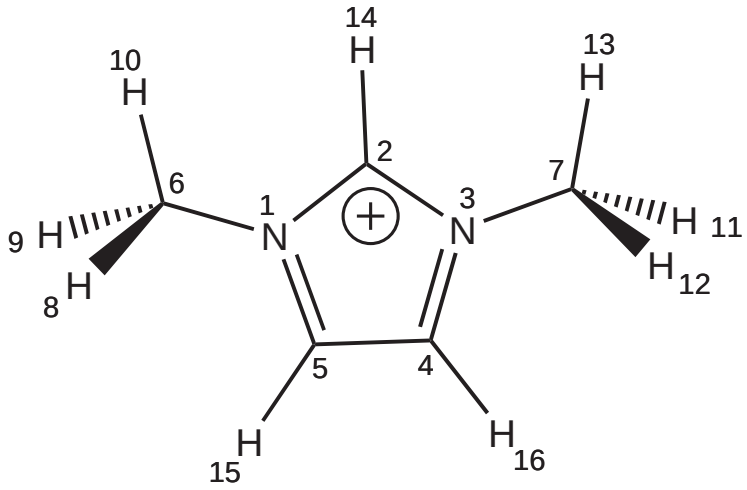

Figure 6.5: Pictural structure of the cation of the studied ionic liquid.

Additionally the normal modes of structures 1 and 2 obtained by DFT and RI-MP2 were compared (see Fig. 6.6 and Ref. [117]) and the main components of eigenmotions could be identified. Due to the complexity of the cation, several mixed or combined motions are included, thus the analysis is restricted only to the high frequency modes; in fact modes with frequencies below 500 cm^{-1} cannot be clearly identified uniquely by the two methods. The largest one around 3300 cm^{-1} belongs to the C_2-H stretching mode for structure 2 (for structure 1 this mode has 2650 cm^{-1}), while around 3000 to 3200 cm^{-1} the other C-H stretching modes are located. Then the C-C and C-N stretching modes are following, around 1300 to 1500 cm^{-1}, while the in-plane or wagging motions can be found to have frequencies around 1000 to 1200 cm^{-1}. And every mode between 500 to 1000 cm^{-1} is corresponding to out-of-plane motions. This is true for the harmonic frequencies obtained by both methods and for all cations in the different configurations. The sub-figure in Fig. 6.6 directly compares the frequencies from MP2 with those from DFT. With

these two pictures one can show that the modes calculated by the two different methods show rather good agreement. But there are small differences between the two methods, which become relevant as the frequencies become smaller. MP2 and DFT are using different techniques (different basis sets (atomic orbitals versus plane waves) and arising from this: different numerical methods) to obtain the frequencies, which might be also a reason that DFT results do not have perfect agreement for small frequencies where the decoupling of the frequencies is very sensitive to the technique used.

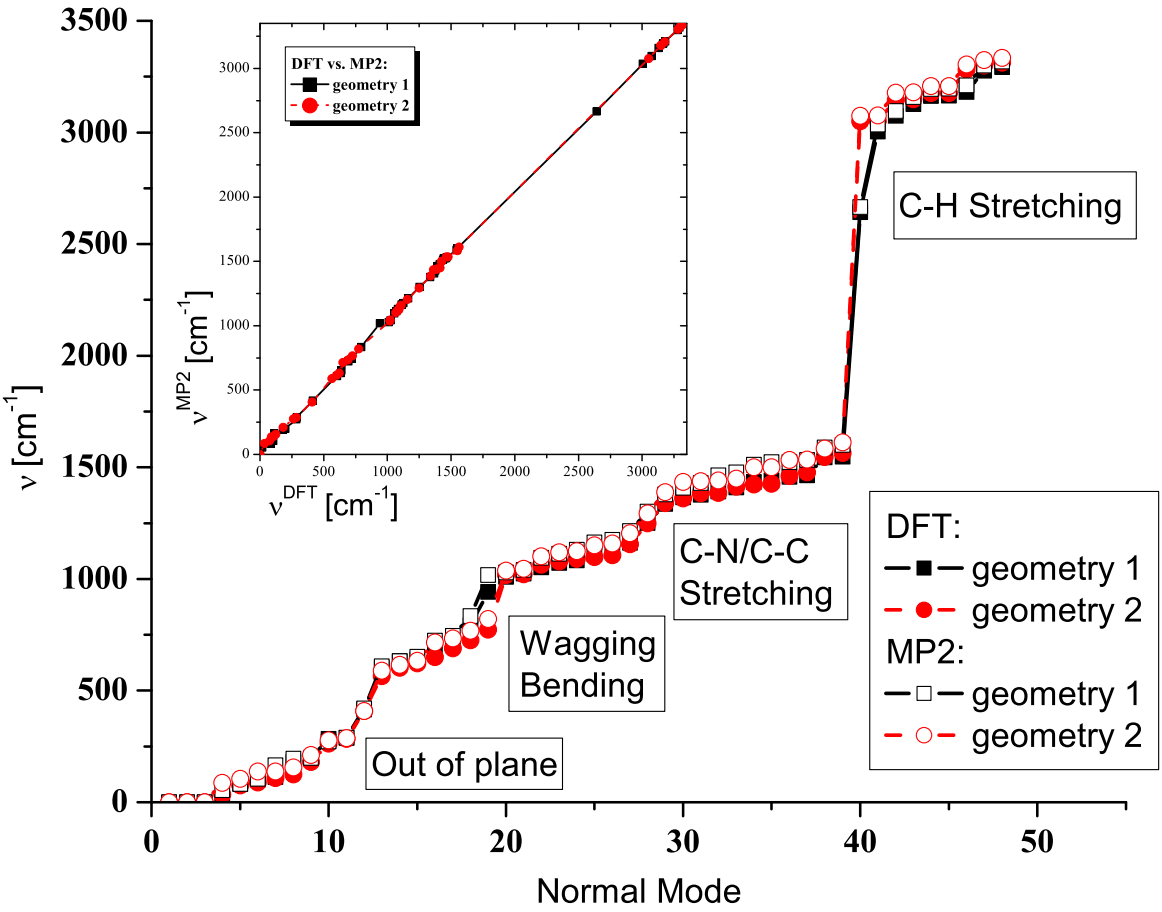

Figure 6.6: Harmonic frequencies (in cm^{-1}) for 1,3-dimethylimidazolium chloride calculated by different levels of theory. They were obtained at the level of RI-MP2/aug-cc-pVTZ and DFT/PBE/70Ry and plotted against the number of modes; the vibrational motions (the main components) are indicated in the figure. In the inset the frequencies obtained by these methods are plotted one versus the other; the slope of 1 shows that the MP2 and DFT calculations are consistent.

6.4.2 Larger Clusters and Electrostatic Moments

Having shown that the DFT reproduce MP2 structures and harmonic frequencies the DFT setup proved to be valid and larger clusters could be addressed. In the following section the structures, dipoles and quadrupoles of 1 to 8 ion pair systems will be discussed. These values will be compared with the values (at least of the dipole moments) available from literature, from which classical force fields were designed. The initial structures (2-8 IP's) were taken from classical MD simulations using the Wang and Lopes force fields and all of them were optimized using DFT. To show that the two methods (RI-MP2 and DFT) are consistent even in case of two IP's the results of two selected conformations were optimized (see Fig. 6.7); and they show good agreement. The larger ones (4 and 8 ion pairs) were exceeding the capabilities of the high level quantum chemical methods, due the expensive computational costs.

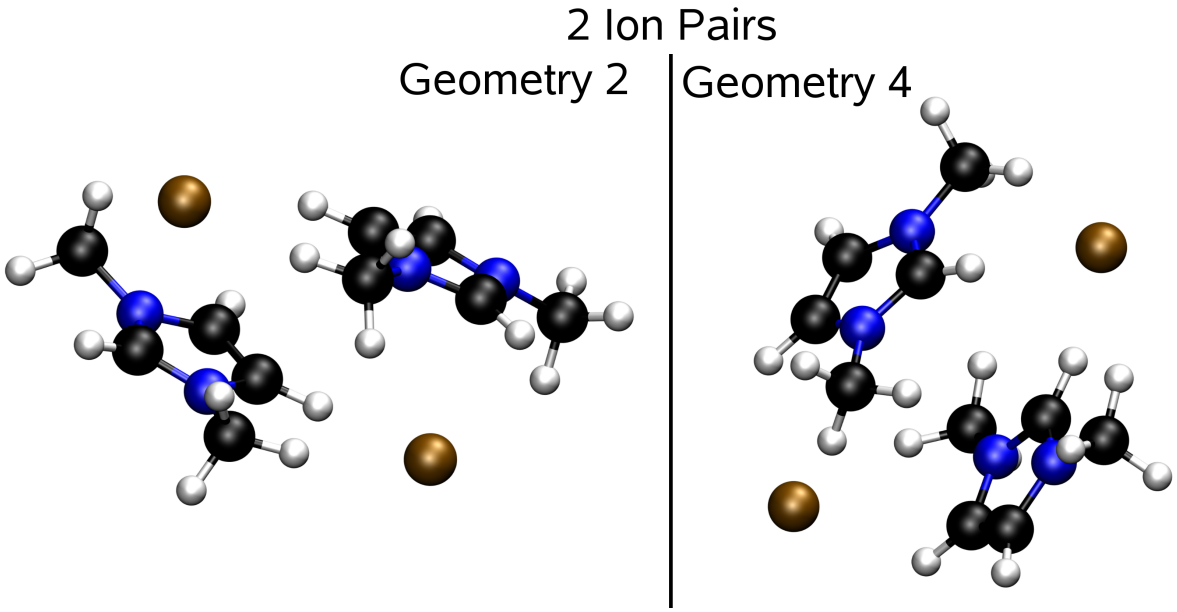

Figure 6.7: Optimized structures of two ion pairs from DFT/PBE/70Ry and RI-MP2/aug-cc-pVTZ calculations to test if the larger cluster can be accessed with DFT as accurate as the one ion pairs.

The dipole and quadrupole moments were then calculated. These are important in building the structure of the liquids. In order to determine electric moments, one has to chose a reference points, which can be: the center of mass (COM), the center of the ring (COR) and the center of charge (COC). The different reference

Calculations		
	Dipole Moments [D]	
Structure	IP_{total}	$IP_{Cation(DFT)}$
pure cation	0.834 (1.03[115])	0.834[2.194]
Geometry 1	12.4 (12.4[107])	4.20[5.518]
Geometry 2	8.3 (8.4[107])	3.47[4.712]
Geometry 3	16.4 (16.2[107])	2.19[1.577]
Geometry 4	16.5 (16.7[107])	2.81[2.573]
2 IP(Lopes)		2.406[3.378]
2 IP(Wang)		2.308[3.068]
4 IP(Lopes)		2.605[3.421]
4 IP(Wang)		2.383[3.206]
8 IP(Lopes)		2.234[3.002]
8 IP(Wang)		2.296[3.160]
Literature		
DFT(liquid)		[2.2-2.67[109]]
HF/6-31G+(d)		1.03[115]

Table 6.2: The dipole moments (in D) are shown for the whole ion pair (in case of the one ion pairs (IP's)) and then for the cation alone. The structures for the larger IP's were taken from classical MD (from the Lopes and Wang force fields as noted in the brackets) and optimized with DFT. The values given in the square brackets are with respect to the center of the ring, while the others are with respect to the center of mass. In case of the larger clusters the dipoles of the cations are given, because the chloride could not be assigned to a specific cation. The comparison of the one ion pairs with literature [107] show excellent agreement; the comparison of larger clusters with literature [109] show agreement within the range of dipole moments given there (1.5-4.5 D).

points lead to different values for the dipole moment of the cation. Considering the lack of uniqueness throughout literature the center of mass was chosen as reference point. And to compare possible values with available data in literature the dipoles with respect to the center of the ring were also considered. In table 6.2 the values for the dipole moment are presented with respect to the center of mass and in square brackets the dipoles with respect to the COR are given.
The values of the dipole moments are collected for several different systems, for the one ion-pair systems for both: the total IP's and the molecular dipoles for the cations within the different IP's were calculated. For larger clusters the assignment

Calculations	
Structure	Dipole Moments [D] $IP_{Cation(MD)}$
2 IP(Lopes)	0.811[2.102]
2 IP(Wang)	1.263[2.553]
4 IP(Lopes)	0.779[2.055]
4 IP(Wang)	1.215[2.504]
8 IP(Lopes)	0.765[2.051]
8 IP(Wang)	1.151[2.434]
Literature	
DFT(liquid)	[2.2-2.67[109]]
HF/6-31G+(d)	1.03[115]

Table 6.3: As figure 6.2: But the dipole moments (values in Debye) are calculated regarding the classical force fields. Initial structures (taken from DFT) were optimized with classical MD and the two different force fields from Lopes and Wang (noted in brackets; first column). The values given in the square brackets are with respect to the center of the ring, while the others are with respect to the center of mass. The values for the dipole moments are about 1D smaller than the ones from DFT calculations.

of anions to a specific cation is not possible, because they are shared by several cations, thus the total dipole moments of one ion pair cannot be determined. Therefore only the average values of dipole moment of the cations were considered. There are several aspects emerging from the comparison of these dipole moments. First, the average values for the one ion pairs obtained in this study are in very good agreement with the ones from DFT/B3LYP calculations [107](see table 6.2). Second, the average values (now considering the $|\vec{\mu}|$ w.r.t COR) for the dipole moments of the cations are within the range given by literature [109]. The changes of the average dipole moment are rather small, but the distribution of the single cation dipoles for each cluster is rather broad ($\pm$ 0.4 D in case of the two ion pair systems; around $\pm$ 0.8 D in case of the four and eight ion pair systems). The next step was to compare these values with the dipole moments obtained for the clusters with assigned charges from the classical force fields. The obtained average values are more than 1 D smaller than the values from DFT calculations. The dipole moments with respect to the classical force fields also show a very narrow distribution of $\approx$0.05 D for the cation dipole moments around the average value. This is because the classical models though flexible are parametrized on single

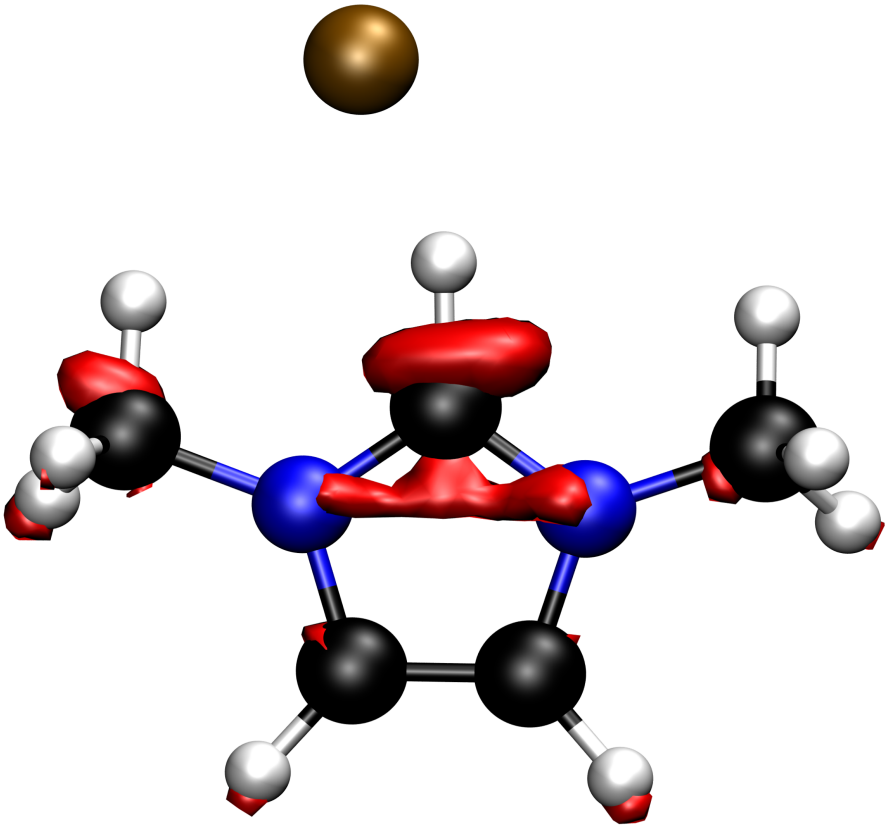

Figure 6.8: As example for the influence of the anion on the electronic density of the cation the geometry 1 is given; it shows a significant shift of the density along the y-axis (parallel to the molecular axis; along the c2-H14 axis) and along the x-axis and none along the z-axis (perpendicular to the ring). This shift coincide with the shift in the quadrupole moment given in table 6.4.

cation calculations in vacuum.

As next step the quadrupole moments of the cations for the different systems were calculated with DFT and classical MD (regarding the two different force fields from Lopes and Wang) with respect to the center of mass. The z-axis is defined perpendicular to the aromatic ring, and the y-axis is parallel to molecular axis (along the C2-H14 bond, with origin at the COM) of the imidazolium. The averaged absolute values of the quadrupole moments for the cations in the ion pair systems are given in table 6.4.

The changes of the θ_{ii} (ii= xx, yy, zz) are due to shifts of the electronic density. This

DFT			
	Quadrupole Moments [D Å]		
	θ_{zz}	θ_{xx}	θ_{yy}
cation	-24.7	4.1	20.6
Geometry 1	-24.0	7.5	16.4
Geometry 2	-20.6	4.9	15.7
Geometry 3	-25.6	7.7	17.9
Geometry 4	-26.4	1.6	24.8
2 IP (Lopes)	-24.0	4.5	19.4
2 IP(Wang)	-24.9	3.2	21.7
4 IP (Lopes)	-24.7	4.1	20.9
4 IP (Wang)	-25.3	4.7	20.7
8 IP (Lopes)	-25.3	3.7	21.6
8 IP (Wang)	-25.5	3.8	21.8
Classical force fields			
2 IP (Lopes)	-17.3	-0.7	18.0
2 IP(Wang)	-18.0	0.9	17.1
4 IP (Lopes)	-17.3	-0.8	18.1
4 IP (Wang)	-18.0	0.8	17.3
8 IP (Lopes)	-17.3	-0.8	18.2
8 IP (Wang)	-18.1	0.8	17.3

Table 6.4: The absolute values of the quadrupole moments (in D Å) of the imidazolium cations in the different ion pair systems are given. The initial configurations were taken from classical MD with the Lopes and Wang force fields (noted in brackets: first column) and optimized with DFT. The lower part of the table shows the quadrupole moments (in D Å) for the different ion-pairs from classical MD and the two different classical force fields (Lopes and Wang; noted in brackets: first column). The quadrupole moment is sensitive to the position of the anion around the cation because of the electron shift caused by the presence of the anion. The quadrupole moments (the absolute as well as the fluctuations) regarding the classical models show a large disagreement compared to the values from DFT calculations.

shifts can be caused by interactions of the quadrupole moment with other electric moments like monopoles, dipoles, and quadrupoles. The monopole-quadrupole interaction is the strongest interaction. The chloride ions can be regarded as monopoles, thus the changes of the quadrupole moments can be linked to the anion-cation interaction. As an example the shifts of the density of Geometry 1 is given, where the pure influence of the anion is shown and the electron density is shifted along the C2-H14 bond, which connects the chloride via hydrogen bonding. The one ion pairs can be regarded as representative example to explain the changes of the quadrupole moments. As mentioned in the previous section, the structures (Geometry 1, 3, 4) are also connected with the chloride via hydrogen bonding. The significant changes of the quadrupole moments occurs along the xx- and yy-direction only, which is connected to this structural properties. In case of Geometry 2 the anion is interacting with the ring, which causes a shift along the zz-direction. The values of θ_{xx}, and θ_{yy} in the larger clusters (2, 4 and eight ion pairs) show more fluctuations than θ_{zz}, which indicates that the hydrogen bonding in larger clusters is an important factor. The fluctuations of θ_{zz} are rather small, which suggest that the Coulomb interaction of the anion with the positive charged ring are small but still present, see Fig. 6.9.

The values for θ_{ii} (ii= xx, yy, zz) with respect to the classical force fields do not show this behaviour. The absolute values of the quadrupole moments obtained by these two methods show large disagreement. Also the fluctuation of the quadrupole moments discussed for the DFT results cannot be captured by the two classical models. These discrepancies and the differences in the dipoles might give some idea as how to refine the classical models to more flexible, polarizable force fields, which might capture the large variation of the electrostatic moments.

Regarding these results one can suggest that in those systems the hydrogen bonding is more important than the C2-anion interactions. This finding is consistent with results collected by previous work [118], which studied the properties of 1-ethyl-3-methyl-imidazolium with chloride Cl^-, tetra-fluoroborate BF_4^-, and bis((tri-fluoromethyl)sulfonyl)imide TF_2N^- for the Lopes force field and conclude that the hydrogen bonding is an important factor in building of the complex structures of ionic liquids.

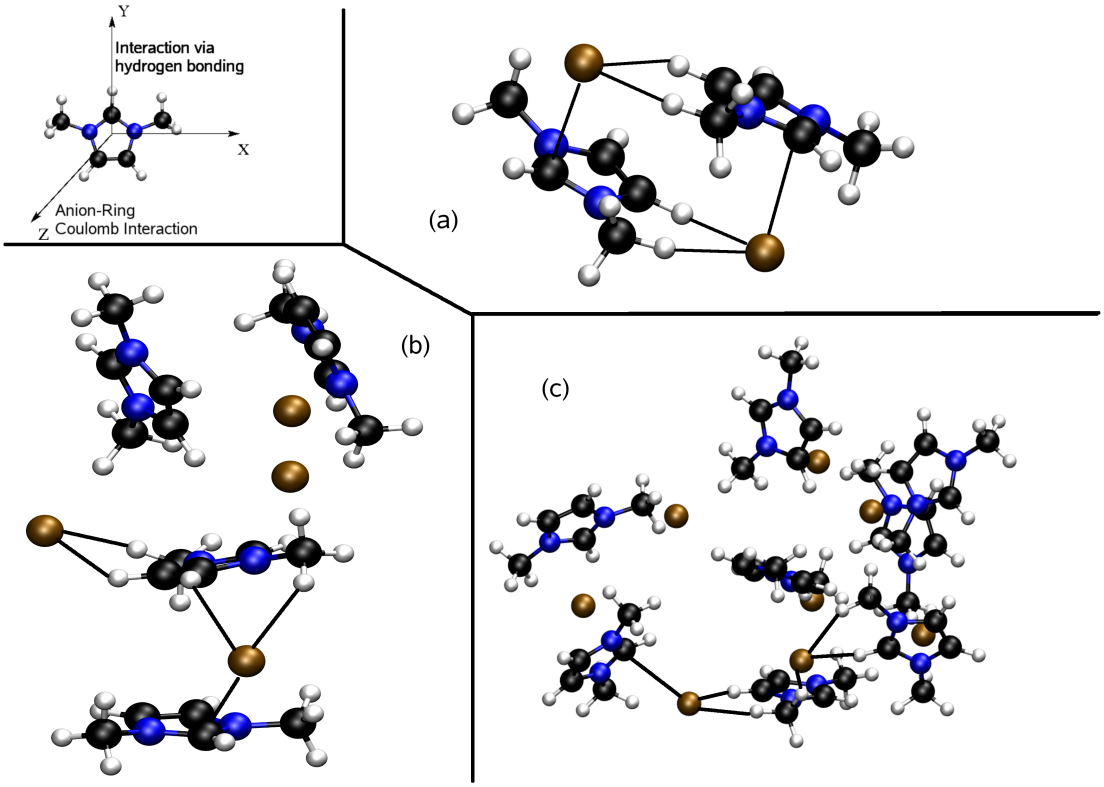

Figure 6.9: Shown are selected structures for (a) 2, (b) 4 and (c) 8 ion-pairs. In the right upper corner a coordinate system for a single cation is shown. The structures show that the hydrogen bonding is crucial and located mainly in the xy-plane, regarding the given coordinate system. The direct anion-ring interaction are also shown in this picture (along the Z-axis), but they are not that numerous. These interaction can be related to the shift of the electron density, observed via the quadrupole moment. The values of θ_{xx}, and θ_{yy} fluctuate much more than the ones from θ_{zz}.

6.5 Discussion and Conclusion

With this setup of comparing DFT with MP2 on one hand and with MD on the other hand we have found interesting insights into the electronic level and partly of the atomistic level of the 1,3-dimethylimidazolium chloride. As a first step towards multiscale modeling we compared structures from DFT with those from MP2, on the level of geometric properties, energetic order and harmonic frequencies. The overall structural agreement is very good, the structures are maximally 4% off from literature and the energetic order could be reproduced as well. In addition we calculated the harmonic frequencies (which might be also of

interest for expermimentalists to measure) of the one ion pairs with both methods and achieved again very good agreement. Then MP2 and DFT structures of two ion pairs have been optimized and also at this level there was good agreement found. With this study the first goal of the work was reached: the comparison of high level quantum chemistry with DFT at different systems and therefore a step towards a deeper understanding of the ionic liquids on electronic level was done. This was also a test for the DFT setup, because to approach the more atomistic scale it is necessary to analyze also larger clusters. Therefore larger clusters (4 and 8 ion pairs) have been taken from classical MD and then optimized with DFT. Since the electric moments are important parameters in ionic liquids, the dipole and quadrupole moments have been calculated. For the comparison of the dipole moments two reference points were considered, the center of mass and the center of ring. The values obtained with DFT are consistent and in good agreement with literature. Furthermore they were compared with the values obtained with classical force fields. The values are more than 1.0 Debye smaller than the DFT results, which is due to the fact that they have been parametrized on single cation calculations in vacuum. Next the quadrupole moments of the cation were calculated, they are more sensitive to changes in the electronic density. Regarding the changes of the quadrupole moments from the DFT calculations one can conclude that the hydrogen bonding is more relevant compared to the C2-ring interactions. It is not clear yet, what could be the effect of the differences between the electrostatic moments from DFT and those used in force fields. This question is still open and is a topic of ongoing research. The adjustment of the electrostatics in classical MD to match the DFT result might help to improve the classical force fields and the understanding of the influence of these electrostatics on the structure and/or properties of the ionic liquid. The future plans are: to refine the force fields or generate a new one such that the electrostatic properties could be captured. This will at the end lead to either a new model for the ionic liquids or the modification of an existing one. This will then help to understand the properties of ionic liquids on a much broader basis.

6.6 Work in Progress and Outlook

The qualitative results for the ionic liquids so far have to be justified and put on a broader basis. There are several ways to improve the results:

- Most structures from the classical MD show that three cations are connected to one anion, via hydrogen bonding or C2-anion interaction. The same was concluded separately while systematically generating clusters. To the one ion pair one can add either an anion or another cation, which should help to get an idea about the construction of such systems. The anion-cation-anion systems will be calculated, with the same procedure as mentioned above. And the preferred structures from both will be compared. In parallel the cation-anion-cation systems will be studied; first CP-MD calculations to have an idea about the preferred and possible structures show that the system is stable and very flexible. The dominant structures are not the stacked or offset stacked ones but the T-shape configurations. In general chloride has six free sides to attach ligands, the cation-anion-cation system will occupy only four of them. Thus another configuration was constructed. Now the anion was surrounded by three cations and a CP-MD run (at 425K) showed that this system is stable, which in combination with the picture from classical MD implies that the main cluster in these liquids consists of three cations and one anion, if the anion is small enough.

- We have compared the *ab initio* and DFT methods now on the basis of geometries and frequencies. As a next step we will expand the discussion of the comparison *ab initio* and DFT calculations. For this the harmonic frequencies, and the energetic order of the one ion pairs will be discussed on the basis of RI-MP2, RI-CC2 calculations for basis sets up to aug-cc-pV5Z. One expects that this will show that the structures obtained by MP2/aug-cc-pVTZ are accurate enough. Furthermore we will compare the frequencies obtained by RI-CC2 and the larger basis sets with those from our DFT calculations. This procedure will then be repeated for the two ion pairs. We also want to compare the density of states from post Hartree-Fock methods with those obtained from CPMD. This will allow us to compare *ab initio* and DFT calculations even at the very basic electronic level. In this context the technical setup of our DFT calculations could be improved.

- The transition states between the different geometries of the one ion pairs will be calculated by *ab initio* calculations and the characteristic data like height of the energetic barrier for the different methods (RI-MP2, RI-CC2, and DFT) will be collected.

- Parallel to the comparison with *ab initio* larger ionic liquid systems will be treated by long Car-Parrinello MD simulations. There the Wannier functions will be as usual calculated on the fly and the electrostatic moments (dipole and quadrupole moments) will be determined. This should prove that the qualitative results found here are representative for the whole range of ionic liquid systems. From these larger clusters we can also extrapolate the dielectric constant, which will be applied in embedded high level quantum simulation for larger systems. Reaching consistency of all the *ab initio* and DFT methods will then lead (at the very end) to the re-definition of the classical force fields.

- We have used CPMD for all the calculations, now we also want to apply the CP2K program to see if the results can be reproduced. Furthermore we will try to access an even larger system for a longer time than CPMD. This will help to improve the comparison with classical MD.

- Having done all this kind of analysis the setup then will be applied to several other ionic liquids, on the basis of imidazolium. The structures then will be altered by changing the side-chains and the anion. With this the final goal to understand how the ionic liquids are built and to give a general construction scheme for designing molecular structures to obtain certain behaviour could be reached.

7 General Conclusions

The subject of this thesis is the computational study of two systems: (1) one of the most popular solvents, water, and (2) ionic liquids. Water and ionic liquids are important in many processes in chemistry, biology, physics and modern technology. The problem so far is that the experiments only partially capture the different scales like dynamics of whole molecules or the global structuring, or the first shell vibrational spectrum. The goal of this study was to combine the knowledge of the electronic and molecular scales to obtain a general scheme of hydration of ions, which should help to explain also other phenomenas and to help to improve other (classical) simulations. In this work DFT within the CPMD framework is used, thus the atomistic properties and at the same time the electronic properties can be calculated.

The goal of the first part of the thesis was to understand the properties of small ion-water clusters (for the local interactions) then liquid like solutions (for the global interactions). These ion-water clusters have been taken initially from literature and then re-optimized, this is done for monovalent positive ions (Li^+,Na^+,K^+), negative ions (F^-,Cl^-,Br^-) and divalent positive ions (Mg^{2+},Ca^{2+}). With this part the local effects, the direct interaction of the ion with the water can be observed. Additionally, the study for the monovalent and divalent positive ions has been expanded to larger system including 32, 64, and 128 water molecules, which then leads to the understanding of global effects and also the interplay between local and global effects. The dipoles and the angles of the dipole vector with respect to the ion-oxygen vector were calculated for the water molecules for the several clusters and the different solvation shells in the liquid systems. From the collected dipole moments it is concluded that the water-water interaction is more important than the ion-water interaction, because the dipole moment (even in the first shell) approaches a value close to the value obtained for liquid water (3.0 D).[53, 54] This is independent from the size and charge of the ion. From the orientation of the dipoles the influence of the ion on the first solvation shell emerges, the further

shells show no influence of the ion at all. The effect on the water is depending on the size and charge of the ion, i.e. the dipole moments are more aligned along the ion-oxygen vector in case of the divalent ions than for the monovalent ions. This part concerned more the generic properties, however, to understand the electronic details of water-water interactions the electronic contributions to the dipole moment and the thereon based localized Wannier functions have been considered. First, the electronic contributions of the water dipole moments (the lone pair, bonding pair and O-H contributions) were projected on the molecular axis, which was done for the small cluster as well as for the liquid like systems. Each contribution (except the O-H contribution) started at an initial value and approached the bulk value, this behaviour is the same as for the average dipole moments. Then second, the differences of the perturbed water and the unperturbed molecule were calculated, to show the changes of the electronic orbitals. Considering the results from the different approaches, this study has shown that water-water interactions are dominant at the local scale (ion-water) as well as on larger scales (bulk effect). In the small clusters the water-water orbital repulsion is important, the effect of the ion is only the geometrical arrangement of water around the ion. With this study a deeper insight about the processes of solvation can be achieved.

For water we have looked at the possible scales using the CPMD framework and linked the results from each scale to get an overall picture of the solvation of ions. This multiscale modeling approach is then applied to the ionic liquids. Described in Chapter 6.1 is the first step of the multiscale modeling for the ionic liquids, for simplicity the starting system was chosen to be 1,3-dimethyl-imidazolium chloride (the simplest room-temperature ionic liquid). The electronic scale is captured by the *ab initio* methods (very accurate but computationally very costly) and DFT calculations(less accurate and computationally less expensive). The atomistic scale is treated using the planewave pseudopotential approach of DFT in CPMD and classical MD. The results are compared and the models are iteratively improved until certain consistency between quantum and classical results is reached. However, the goal of this study presented (see Chapter 6.1) was to provide more insight into the electronic description and partly of the atomistic level of 1,3-dimethylimidazolium chloride. For this reason several geometries, total energies and harmonic frequencies of selected one ion pairs of 1,3-dimethylimidazolium chloride were calculated. The agreement regarding the geometries is very good and the order of the total energy for the different structures could be reproduced. The harmonic frequencies

were calculated and both methods gave the same spectrum. The comparison of high level quantum chemistry with DFT was the first part of the study, and a step towards a deeper understanding of the ionic liquids on electronic level. Also 2 ion pairs (initial configurations from MD) optimized with MP2 and DFT were compared. The MP2 structure and the one obtained by DFT agree very well. This assures us that the DFT setup is trustable and ready to approach 4 and 8 ion pairs. Next step would be that of comparing the results with those from MD simulations. For this reason the electrostatic moments (dipole and quadrupole moments; with respect to the center of mass (COM) and center of ring (COR)) were used. First the dipole moments compared with those available in literature show good agreement. The results show that the dipole moments obtained by assigning the charges from classical force fields one finds a large discrepancy (about 1 D) between the DFT and the MD results. The dipoles of the classical force fields are designed to match the values of the isolated cation in vacuum. To go further quadrupole moments were discussed. They are more sensitive to changes in the electronic density and from the values obtained it is concluded that also another aspect arises that is the hydrogen bonding is more important than to the C2-ring interactions. According to the discussions above, the comparison of the dipole and quadrupole moments from DFT and MD shows that the description of the electrostatic properties of the two force fields do not agree. The modification of the current force fields to match the dipole and quadrupole moments in larger systems might help to improve the classical force fields and to understand the electrostatic interactions even better.

These results of the project to describe the ionic liquids will be in the future used to refine the classical force field, such that the electrostatic properties could be better captured. The description at the electronic level will be expanded by looking at transition states from geometry 1 to geometry 2 (for one ion pairs) by MP2, coupled cluster methods and DFT (as comparison). Also larger (more liquid like) systems should be accessed via CPMD and CP2K. The final goal of the project on ionic liquids is to have a consistent multiscale description, which describes the ionic liquids and its properties on the electronic and the atomistic level. This will then help to understand the properties of ionic liquids on a much broader basis.

8 Appendix 1: Geometry Data for Ion-water clusters

	1	2	3	4	5
r(Li^+-O_1)	1.821(1.823)	1.857(1.860)	1.899(1.901)	1.954(1.942)	1.948(1.928)
r(Li^+-O_2)		1.853(1.860)	1.893(1.901)	1.974(1.942)	1.957(1.938)
r(Li^+-O_3)			1.896(1.901)	1.949(1.942)	1.952(1.938)
r(Li^+-O_4)				1.953(1.942)	1.953(1.928)
r(Li^+-O_5)					3.7051
$\theta_{12}/^o$		179.4(180.0)	120.0(120.0)	111.9(109.4)	112.0(109.4)
$\theta_{23}/^o$			118.87(120.0)	110.61(109.4)	113.3(109.4)
$\theta_{34}/^o$				104.07(109.4)	112.8(109.4)
$\theta_{45}/^o$					50.4
$\theta_{31}/^o$			121.0(120.0)	113.8(109.4)	110.0(109.4)
$\theta_{41}/^o$				113.7(109.4)	100.9
$\theta_{51}/^o$					50.6

Table 8.1: The solvation structure of the Li^+-H_2O clusters. The distances r(Li^+-O_n) are in Å. The angles are defined as :$\theta_{nm} = \theta$(O_n-Li^+-O_m) (n,m = 1..5, in ^{o}). The data are compared with those, in parenthesis, of Müller et al.[33]

	1	2	3	4	5
$r(Na^+\text{-}O_1)$	2.245(2.252[50])	2.253(2.258[50])	2.298(2.290[50])	2.346(2.330[50])	2.315(2.350[50])
$r(Na^+\text{-}O_2)$		2.252(2.258[50])	2.323(2.290[50])	2.348(2.330[50])	2.360(2.350[50])
$r(Na^+\text{-}O_3)$			2.312(2.290[50])	2.361(2.330[50])	2.360(2.350[50])
$r(Na^+\text{-}O_4)$				2.363(2.330[50])	2.321(2.350[50])
$r(Na^+\text{-}O_5)$					4.07 (4.20[50])
$\theta_{12}/^o$		175.3(180.0[119])	120.0(120.0[119])	114.4	116.5
$\theta_{23}/^o$			119.3(120.0[119])	107.4	106.6(102.0[119])
$\theta_{34}/^o$				116.4	112.2
$\theta_{45}/^o$					44.8(44.3[119])
$\theta_{31}/^o$			120.6(120.0[119])	115.9	121.8
$\theta_{41}/^o$				91.2	88.7(88.7[119])
$\theta_{51}/^o$					43.9(44.3[119])

Table 8.2: As the table before for the Na^+-H_2O cluster. The data are compared with those, in parenthesis, of Ramaniah et al.[50] and Hashimoto et al.[119].

	1	2	3	4	5
$r(K^+\text{-}O_1)$	2.623(2.600[68]/2.620[69])	2.718	2.680	2.733	2.722
$r(K^+\text{-}O_2)$		2.721	2.681	2.753	2.716
$r(K^+\text{-}O_3)$			2.680	2.736	2.676
$r(K^+\text{-}O_4)$				2.724	2.682
$r(K^+\text{-}O_5)$					4.188
$\theta_{12}/^o$		171.9	119.9	113.1	109.0
$\theta_{23}/^o$			120.00	110.1	112.5
$\theta_{34}/^o$				116.6	88.3
$\theta_{45}/^o$					44.6
$\theta_{31}/^o$			120.1	116.7	117.1
$\theta_{41}/^o$				87.9	117.7
$\theta_{51}/^o$					43.7

Table 8.3: As the table before for the K^+-H_2O cluster. The data are compared with those, in parenthesis, of Glending et al.[68] and Džidić et al. [69] (experimental).

	1	2	3	4	5^a	5^b	5^c	6
r(Mg^{2+}-O_1)	1.921	1.951	1.982	2.013	2.010	2.094	2.094	2.132
r(Mg^{2+}-O_2)		1.953	1.984	2.030	2.032	2.071	2.116	2.104
r(Mg^{2+}-O_3)			1.986	2.016	1.994	2.085	2.081	2.111
r(Mg^{2+}-O_4)				2.027	2.009	2.085	2.073	2.134
r(Mg^{2+}-O_5)					3.707	2.048	2.038	2.110
r(Mg^{2+}-O_6)								2.132

Table 8.4: Calculated Mg^{2+}-O distances (in Å) for several water clusters, structures are analogous to Fig. 5.2. ^{a}: 4 water first shell and 1 second shell; ^{b}: 5 water in form of a pyramide; ^{c}: 5 water with trigonal-bipyramidal structure; The results are with maximally 3 % difference consistent with geometries in literature obtained by different level of theory[30, 28, 27].

	1	2	3	4	5^a	5^b	5^c	6	7	8
r(Ca^{2+}-O_1)	2.226	2.285	2.296	2.337	2.295	2.380	2.393	2.415	2.419	2.547
r(Ca^{2+}-O_2)		2.286	2.296	2.332	2.298	2.387	2.390	2.415	2.468	2.543
r(Ca^{2+}-O_3)			2.295	2.331	2.343	2.382	2.376	2.413	2.446	2.562
r(Ca^{2+}-O_4)				2.333	2.347	2.383	2.356	2.414	2.541	2.537
r(Ca^{2+}-O_5)					3.895	2.358	2.380	2.415	2.419	2.560
r(Ca^{2+}-O_6)								2.414	2.541	2.543
r(Ca^{2+}-O_7)									2.487	2.548
r(Ca^{2+}-O_8)										2.537

Table 8.5: The Ca^{2+}-oxygen distances for the several structures see Fig. 5.2. They show good agreement when they are compared to literature [29, 35, 31, 30, 34, 37]. ^{a}: 4 water in the first shell+1water second shell ^{b}: 5 water in a pyramide ^{c}: 5 water trigonal-bipyramidal

n	r(F-H)	θ(H-F-H)	θ(F-H-O)
1	1.454(1.406[75])		176.81
1+1	1.573	159.07	173.87
	1.574		172.84
3	1.645(1.591 Kim et al. [73])	120.54	176.70
	1.636(1.591 Kim et al. [73])	117.55	175.39
	1.644(1.591 Kim et al. [73])	121.80	176.38
3+1	1.714(1.751[75])	117.97	175.26
	1.711(1.661[75])	119.23	175.09
	1.712(1.738[75])	97.06	174.98
	1.734(1.741[75])	96.93	173.35
4+1	1.756(1.821[75])	125.85	157.65
	1.886(1.821[75])	71.48	156.30
	1.880(1.821[75])	72.76	151.61
	1.852(1.821[75])	72.28	156.81
	2.006	126.80	176.33

Table 8.6: Distances (in Å) for the F^--H hydrogen bond and angles (in ^{o}) for the H-F^--H angles are reported. In parenthesis are given the corresponding values found in literature. The meaning of the symbol 1+1, 3, 3+1 and 4+1, is pictorially explained in Fig.5.3.

n	r(Cl-H)	θ(H-Cl-H)	θ(Cl-H-O)
1+1	2.201(2.425[74])	176.6	171.9
	2.201(2.425[74])		170.3
2+1	2.176	71.3	167.8
	2.342		155.5
	2.697		114.7
3^a	2.237	119.9	172.0
	2.230	120.0	172.1
	2.237	120.1	172.1
3+1	2.391(2.550[74])	66.7	151.0
	2.472(2.550[74])	67.2	147.9
	2.409(2.550[74])	67.7	151.3
	2.295(2.478[74])	136.6	173.0
4+1	2.482(2.640[74])	62.2	145.9
	2.513(2.640[74])	63.1	144.3
	2.431(2.640[74])	62.9	147.5
	2.527(2.640[74])	62.1	143.0
	2.252(2.486[74])	122.8	169.5
4+2	2.557	62.6	145.2
	2.446	62.8	147.2
	2.660	60.9	137.0
	2.778	93.9	135.2
	2.465	64.5	155.9
	2.225	126.6	168.0

Table 8.7: Distances (in Å) for the Cl^--H hydrogen bond and angles (in ^{o}) for the H-Cl^--H angles are reported. In parenthesis are given the corresponding values found in literature.

n		r(Br-H)	θ(H-Br-H)	θ(Br-H-O)
1		2.386(2.378[73])		164.4
1+1		2.429		168.0
		2.428	179.4	173.3
2+1	3.294(3.300[76])	2.321	159.8	168.3
	3.528(3.600[76])	2.634	64.8	152.7
	3.335(3.400[76])	2.705	135.2	123.1
3+1	3.453 (3.400[76])	2.481	147.8	149.1
	3.474 (3.500[76])	2.625	64.1	149.5
	3.498 (3.500[76])	2.567	64.6	150.8
	3.453 (3.500[76])	2.597	139.0	171.1
4+1	3.436 (3.400[76])	2.466	132.4	144.3
	3.508 (3.500[76])	2.767	58.4	137.0
	3.526 (3.500[76])	2.850	59.1	142.7
	3.590 (3.600[76])	2.670	60.0	144.6
	3.621 (3.600[76])	2.687	131.8	170.6
4+2		2.603	63.1	141.5
		2.402	128.0	132.3
		2.668	59.6	141.0
		2.809	57.8	145.2
		2.993	58.6	160.9
		2.728	118.1	174.9

Table 8.8: Distances (in Å) for the Br^--H hydrogen bond and angles (in ^{o}) for the H-Br^--H angles are reported. In parenthesis are given the corresponding values found in literature.

9 Appendix 2: Radial Distribution Functions of $M^{n+}(H_2O)_m$

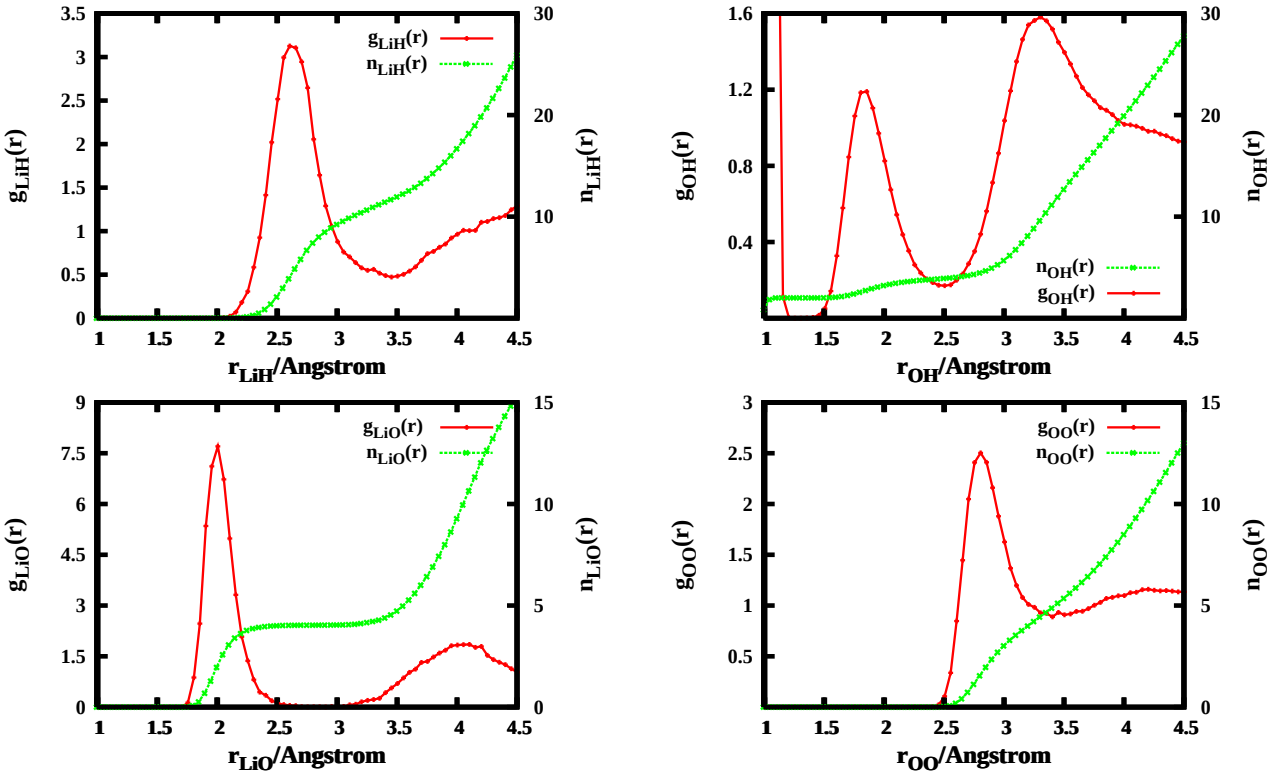

Figure 9.1: Radial distribution function calculated for Li^+-O, Li^+-H, O-O, and O-H in 32 water molecules;

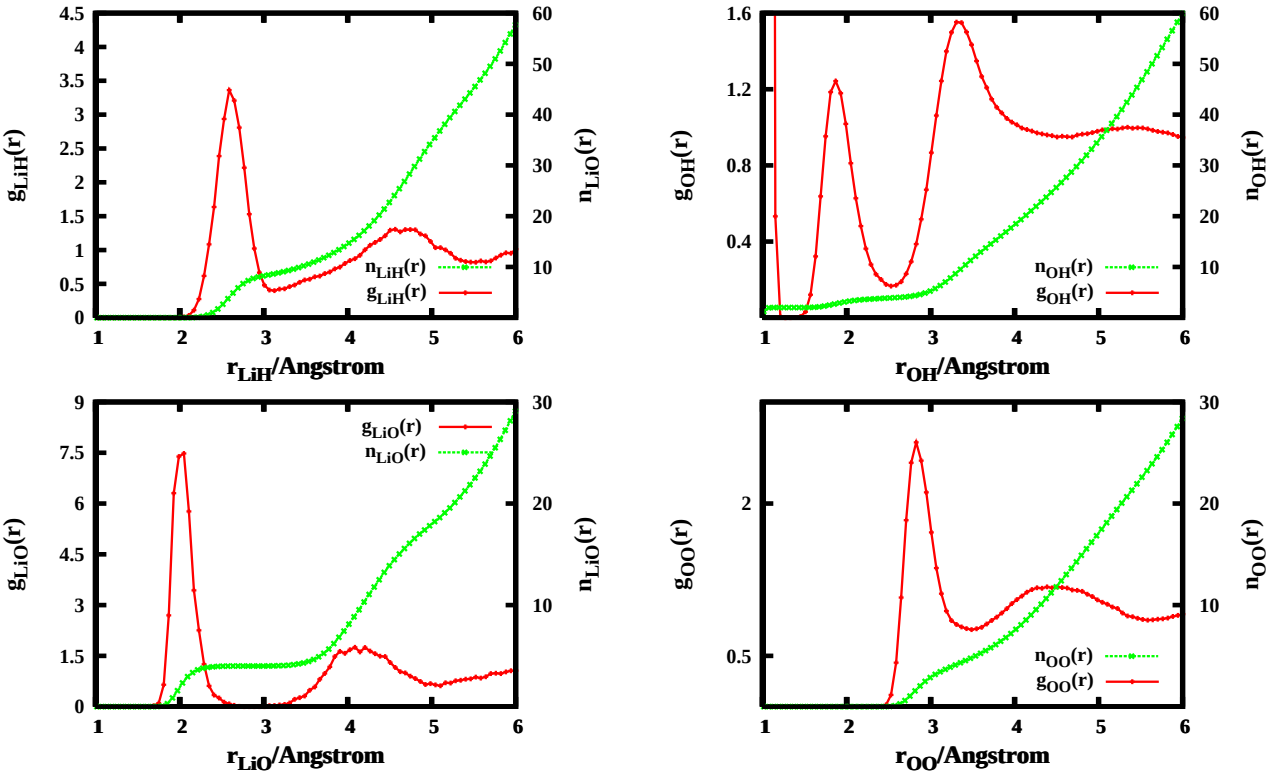

Figure 9.2: Radial distribution function calculated for Li^+-O, Li^+-H, O-O, and O-H in 64 water molecules;

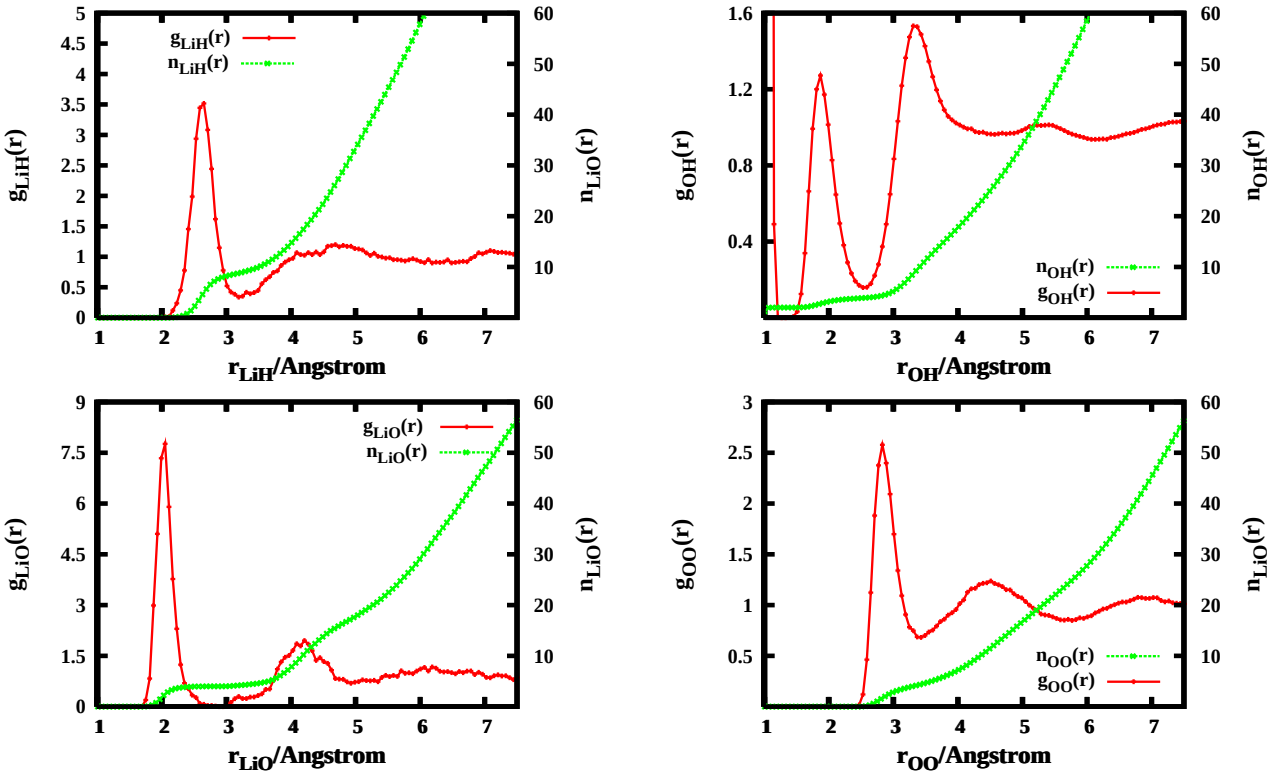

Figure 9.3: Radial distribution function calculated for Li^+-O, Li^+-H, O-O, and O-H in 128 water molecules;

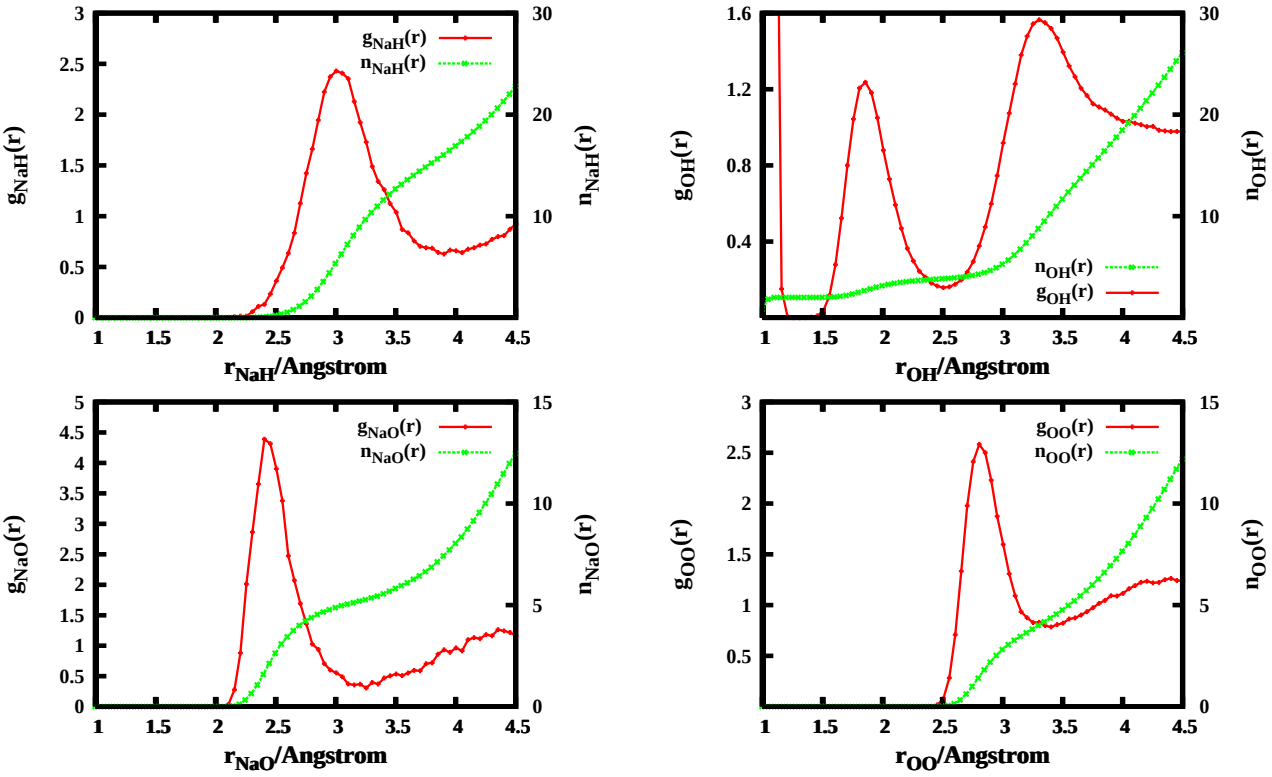

Figure 9.4: Radial distribution function calculated for Na^+-O, Na^+-H, O-O, and O-H in 32 water molecules;

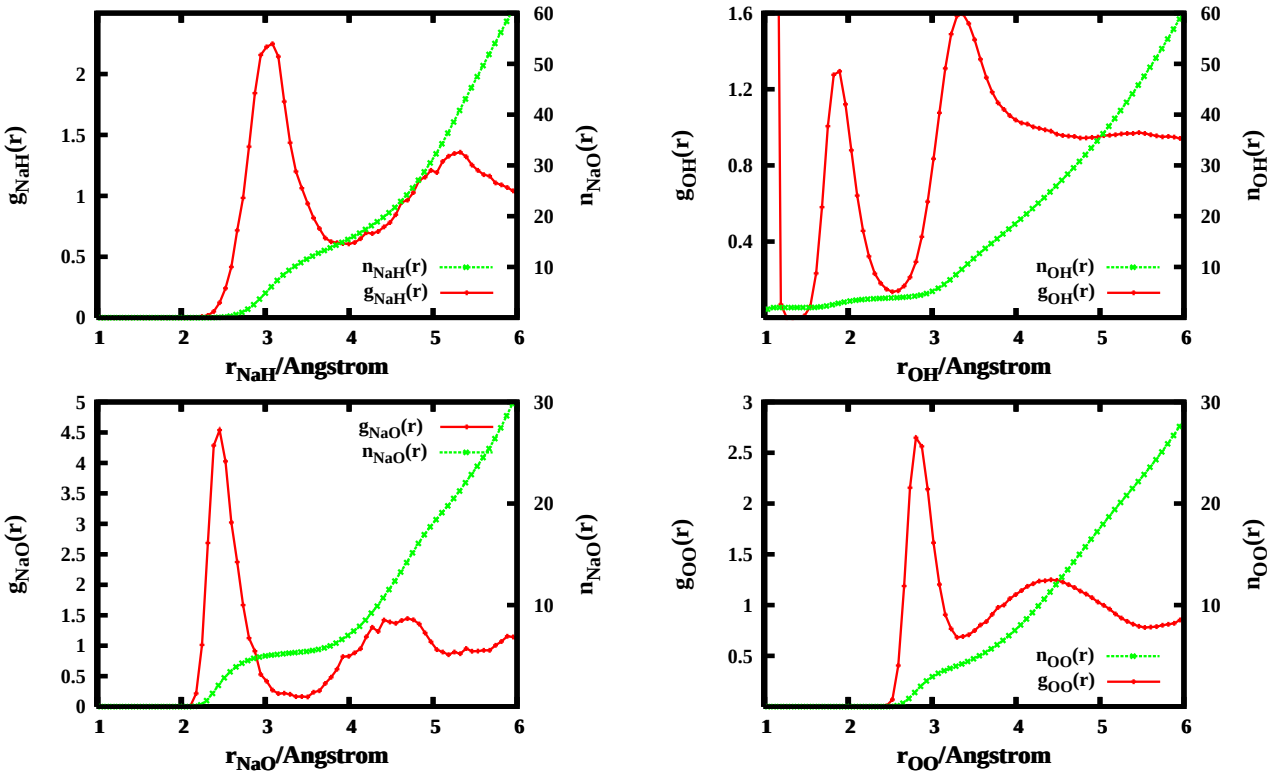

Figure 9.5: Radial distribution function calculated for Na^+-O, Na^+-H, O-O, and O-H in 64 water molecules;

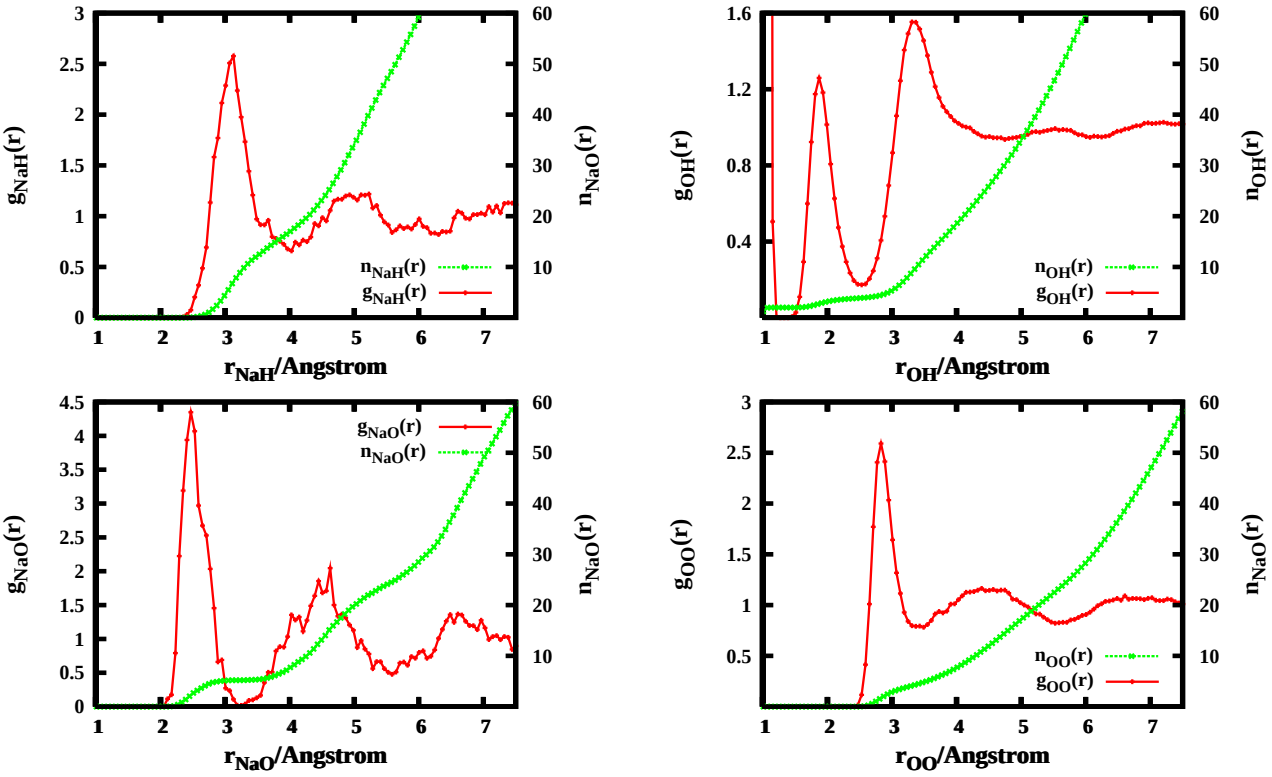

Figure 9.6: Radial distribution function calculated for Na^+-O, Na^+-H, O-O, and O-H in 128 water molecules;

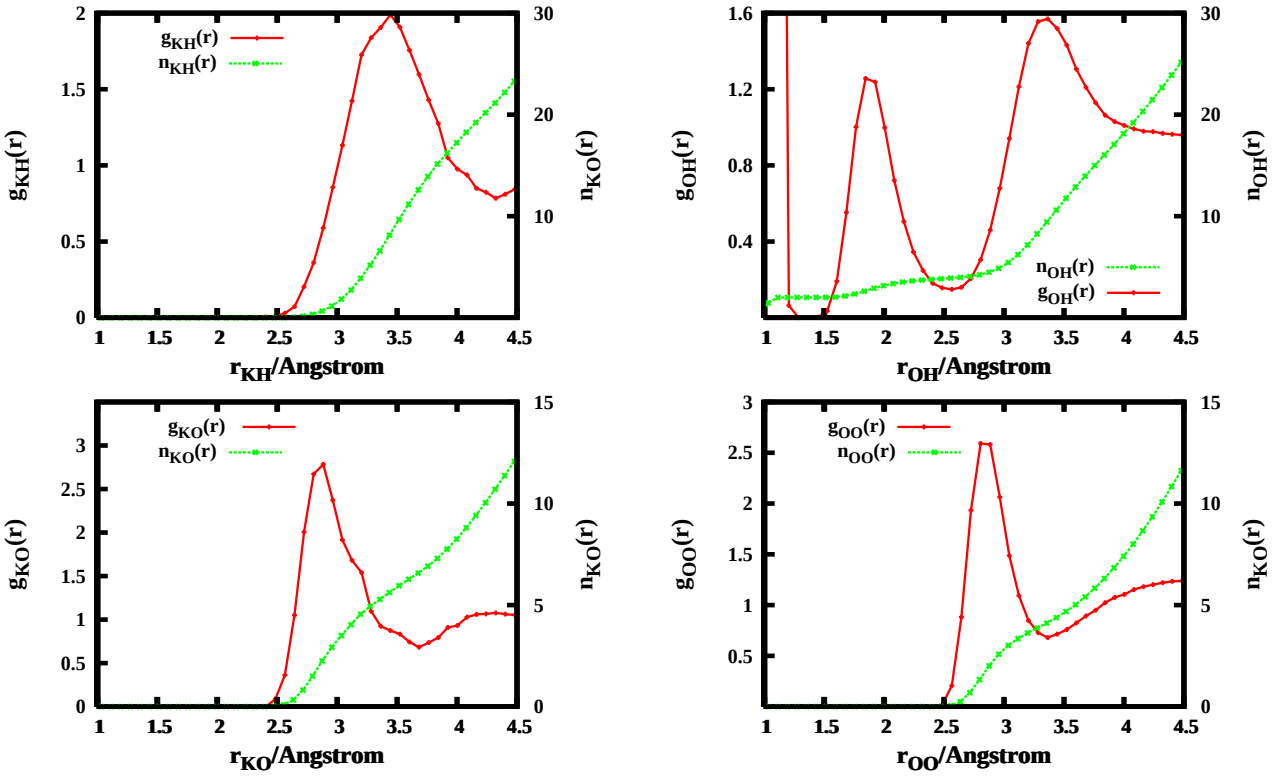

Figure 9.7: Radial distribution function calculated for K^+-O, K^+-H, O-O, and O-H in 32 water molecules;

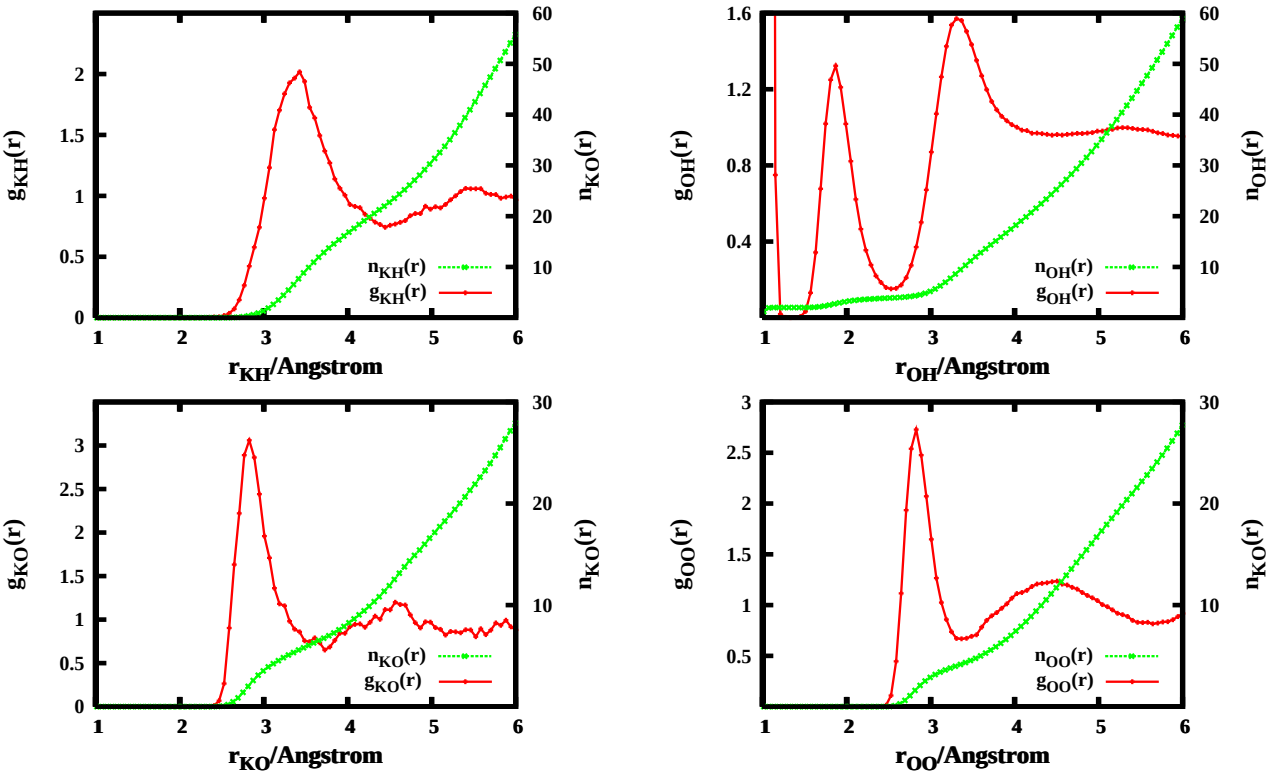

Figure 9.8: Radial distribution function calculated for K^+-O, K^+-H, O-O, and O-H in 64 water molecules;

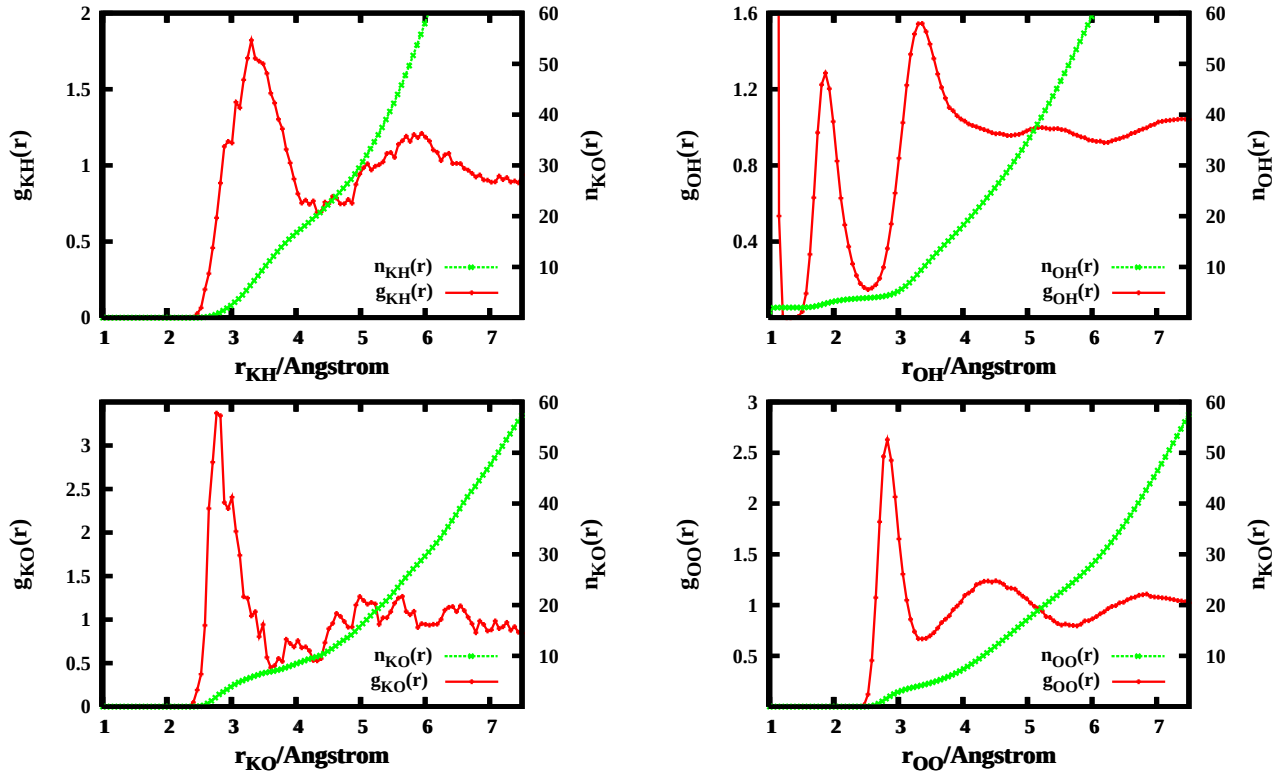

Figure 9.9: Radial distribution function calculated for K^+-O, K^+-H, O-O, and O-H in 128 water molecules;

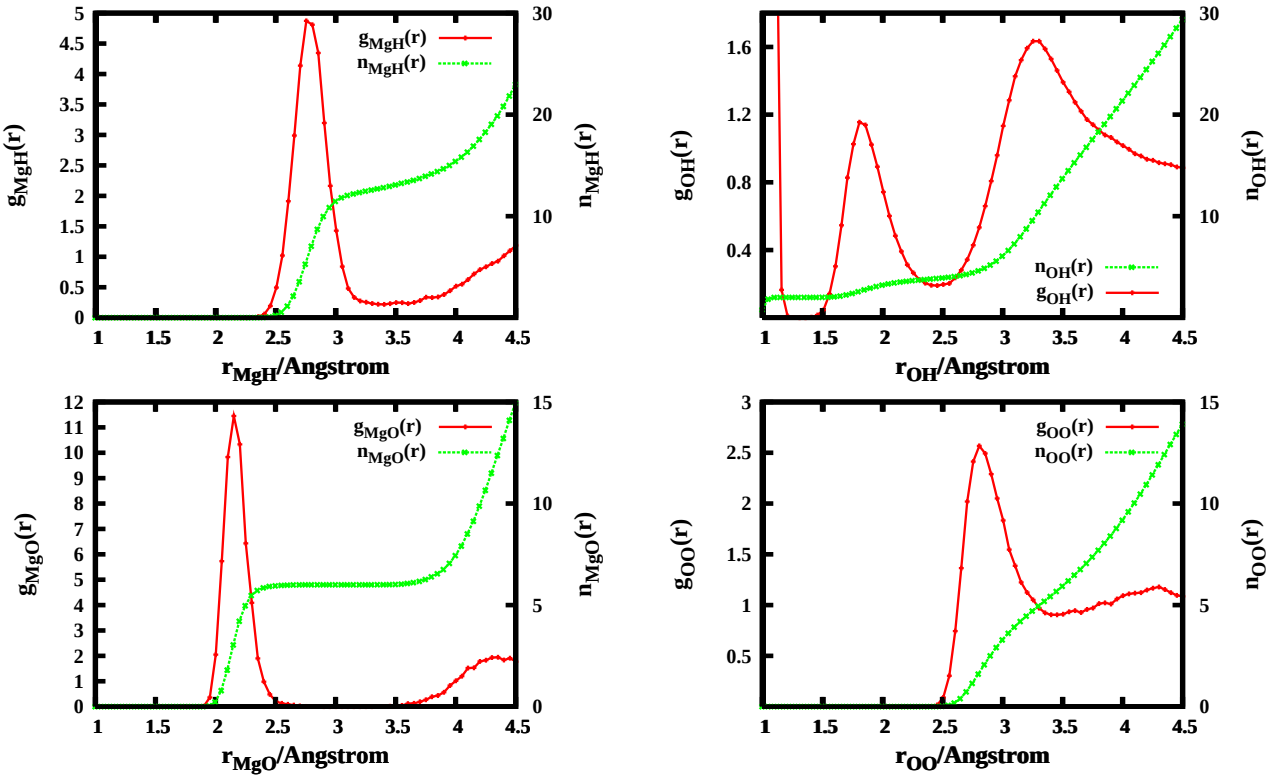

Figure 9.10: Radial distribution function calculated for Mg^{2+}-O, Mg^{2+}-H, O-O, and O-H in 32 water molecules;

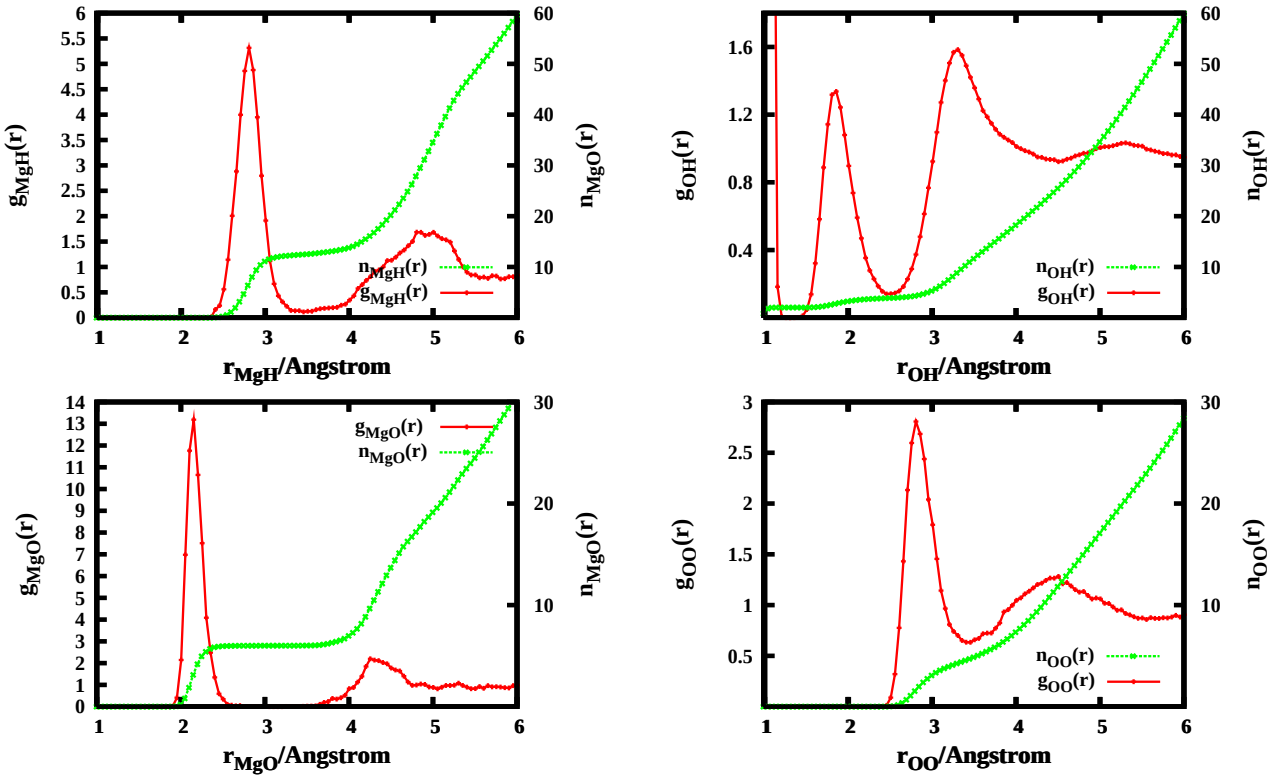

Figure 9.11: Radial distribution function calculated for Mg^{2+}-O, Mg^{2+}-H, O-O, and O-H in 64 water molecules;

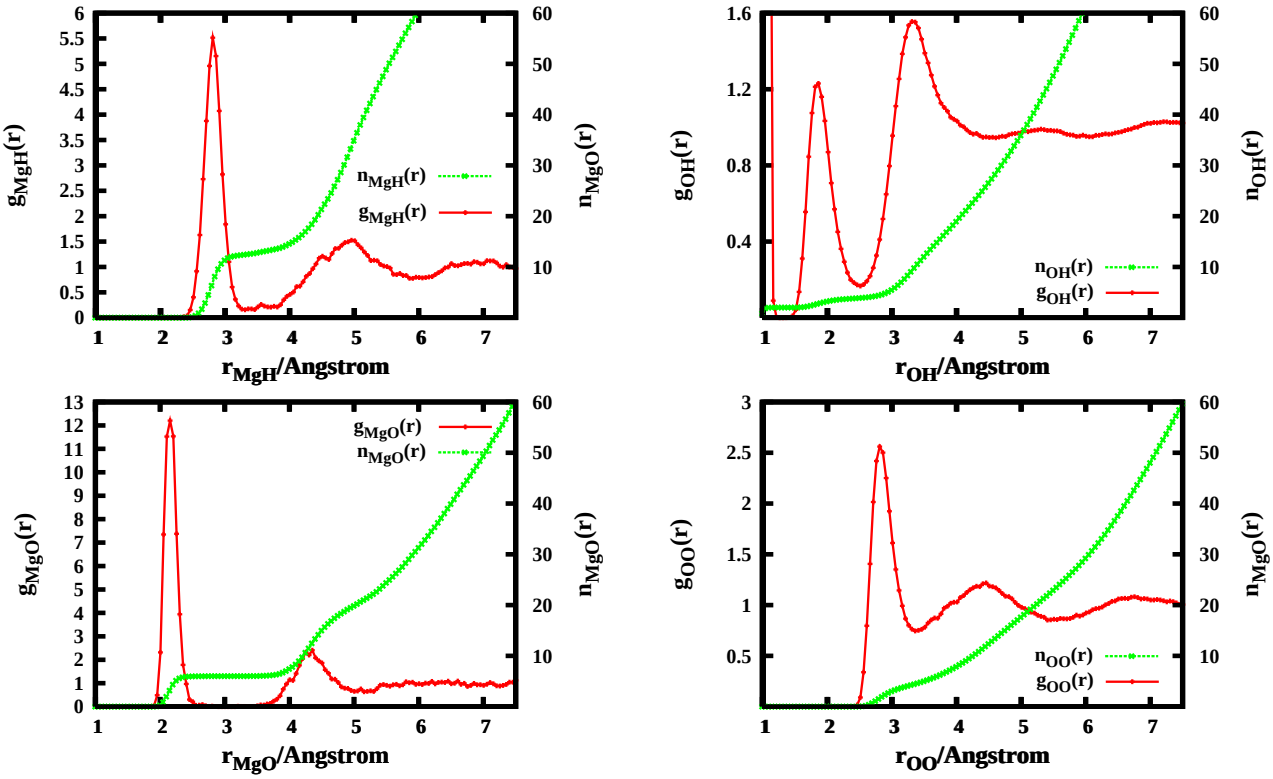

Figure 9.12: Radial distribution function calculated for Mg^{2+}-O, Mg^{2+}-H, O-O, and O-H in 128 water molecules;

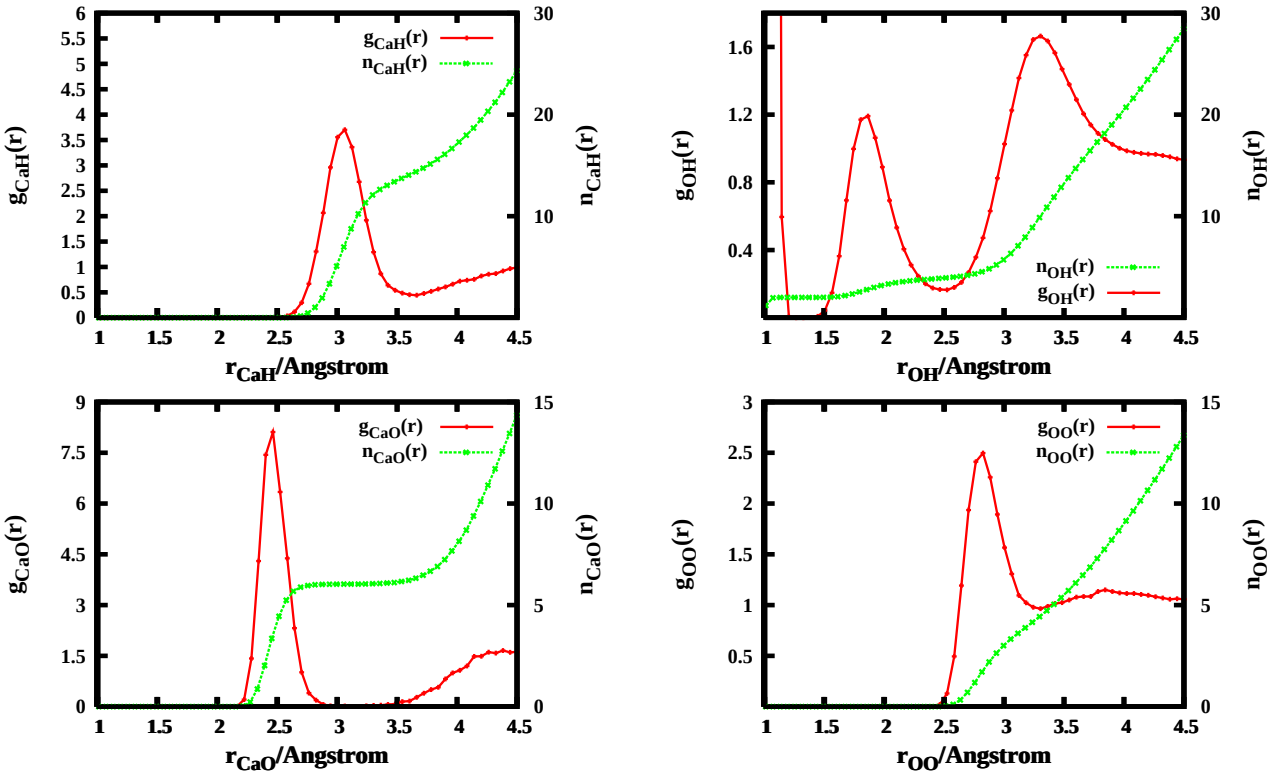

Figure 9.13: Radial distribution function calculated for Ca^{2+}-O, Ca^{2+}-H, O-O, and O-H in 32 water molecules;

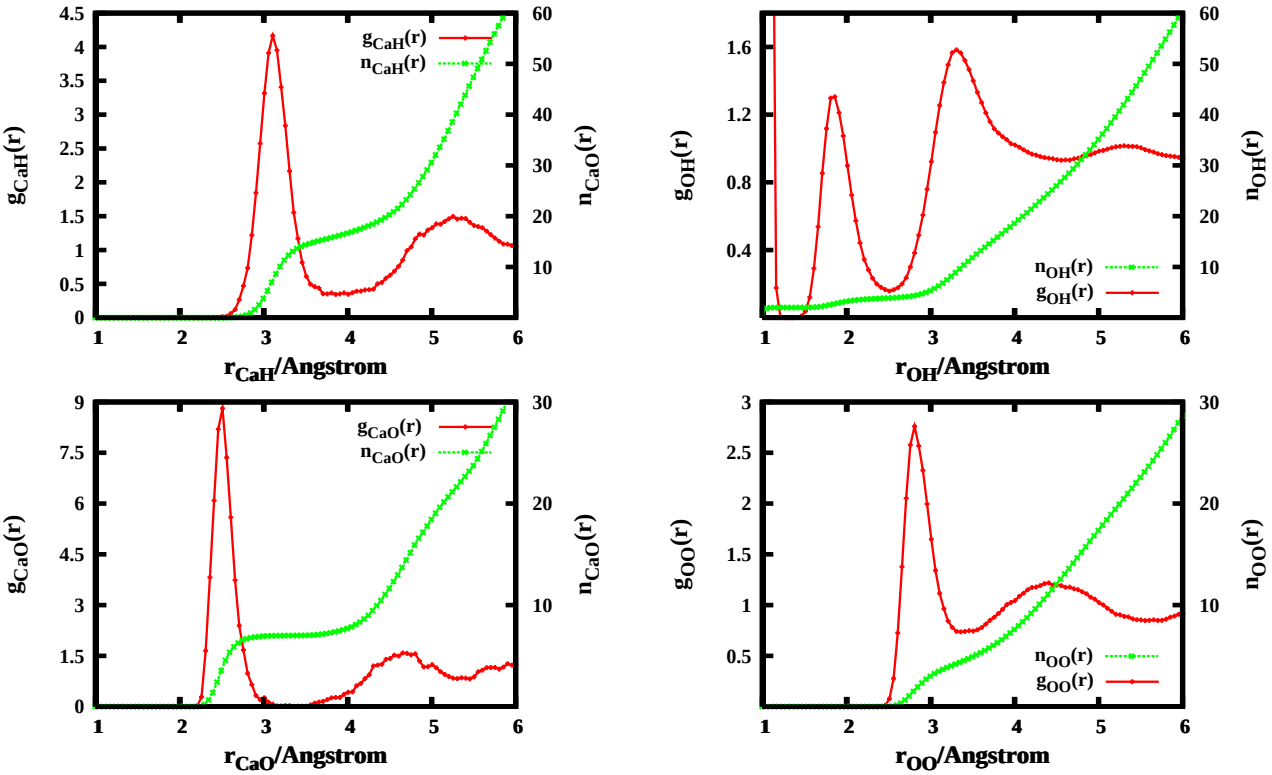

Figure 9.14: Radial distribution function calculated for Ca^{2+}-O, Ca^{2+}-H, O-O, and O-H in 64 water molecules;

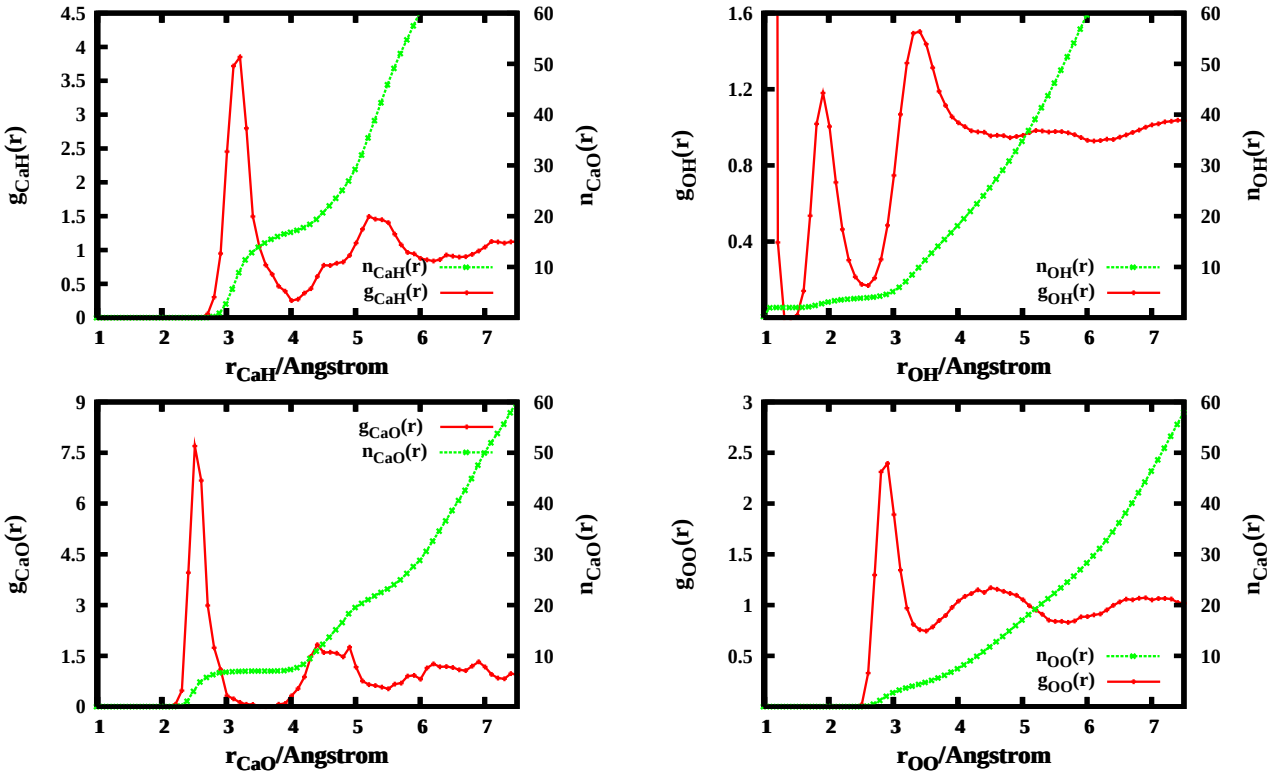

Figure 9.15: Radial distribution function calculated for Ca^{2+}-O, Ca^{2+}-H, O-O, and O-H in 128 water molecules;

Bibliography

[1] A. Szabo and N. S. Ostlund, *Modern Quantum Chemistry*, DOVER PUBLICATIONS, INC., Mineola, New York, 1982.

[2] F.Coester and H. Kümmel, *Nuc.Phys.* **17**, 477 (1960).

[3] J. Čížek, *Adv. Chem. Phys.* **14**, 35 (1969).

[4] G. P. Purvis and R. J. Bartlett, *J. Phys. Chem.* **76**, 1910 (1982).

[5] R. J. Bartlett, *J. Chem. Phys.* **93**, 1697 (1989).

[6] K. Raghavachari, G. W. Trucks, J. A. Pople and M. Head-Gordon, *Chem. Phys. Lett.* **157**, 479 (1989).

[7] R. G. Parr and W. Yang, *Density-Functional Theory of Atoms and Molecules*, Oxford University, 1972.

[8] D. Marx and J. Hutter, Ab initio molecular dynamics: Theory and Implementation, in *Modern Methods and Algorithms of Quantum Chemistry*, volume 1, p. 301, J Grotendorst (Ed.), John von Neumann Institute for Computing,Jülich, NIC Series, 2000, www.fz-juelich.de/nic-series/.

[9] P. Hohenberg and W. Kohn, *Phys.Rev.* **136**, B 864 (1964).

[10] W. Kohn and L. J. Sham, *Phs.Rev.* **140**, A 1133 (1965).

[11] N. Marzari and D. Vanderbilt, *Phys.Rev.B* **56**, 12847 (1997).

[12] I. Souza, N. Marzari and D. Vanderbilt, *Phys.Rev.B* **65**, 035109 (1997).

[13] R. Resta, *Phys.Rev.Lett.* **80**, 1800 (1998).

[14] S. K. Ghosh and B. M. Deb, *Physics Reports* **92**, 1 (1982).

[15] D. M. Ceperley and B. J. Alder, *Phys. Rev. Lett.* **45**, 566 (1980).

[16] R. G. Parr and W. Yang, *Density-Functional Theory of Atoms and Molcules*, Oxford University Press, 1989.

[17] J.P.Perdew, *Phys. Rev. B* **33**, 8822 (1986).

[18] A. D. Becke, *J. Chem. Phys.* **84**, 4524 (1986).

[19] C. Lee, W. Yang and R. G. Parr, *Phys.Rev.B* **37**, 785 (1987).

[20] J. P. Perdew, K. Burke and M. Ernzerhof, *Phys. Rev. Lett.* **77**, 3865 (1996).

[21] For this work we used the version 3.9.2 of the CPMD code. CPMD, J. Hutter, A. Alavi, T. Deutsch, M. Bernasconi, St. Goedecker, D. Marx, M. Tuckerman, M. Parrinello, MPI für Festkörperforschung and IBM Zurich Research Laboratory 1995-1999. / http://www.cpmd.org.

[22] J. J. R. Frausto da Silva and R. J. P. Williams, Nature **263**, 237 (1976); J. H. Seinfeld and S. N. Pandis, Atmospheric Chemistry and Physics, Wiley, New York, 1998; D. L. Blaney and T. B. McCord, J. Geophys. Res. **100**, 14433 (1995); P. Wersin and E. Curti, and C. A. J. Appelo, Applied Clay Science **26**, 249 (2004); R. A. Mickiewicz and A. M. Mayes and D. Knaack, J. Biomed. Mat. Res **61**,581 (2002); C. S. Adams and K. Mansfield, R. L. Perlot, I. M. Shapiro, J. Bio. Chem. **276**(23), 20316 (2001); T. C. Südhof J. Bio. Chem. **277** (10), 7629 (2002); K. Suzuki and H. Sorimachi, FEBS Lett. **1-4**, 433 (1998); Q. Huang and M. Yan, Z.Jiang, J.Pow.Sources **156**, 541 (2006); P. B. Balbuena and E. J. Lamas and Y. Wang, Electrochimica Acta **50**, 3788 (2005); S. Bieller and F. Zhang and M. Bolte and J. W. Bats, H.-W. Lerner, M. Wagner, Organometallics **23**, 2107 (2004); E. Totu and A. M. Josceanu and A. K. Covington, Mat.Sci.ENg. C-Bio. S **18**, 87 (2001).

[23] F. Jalilihvand, D. Spångberg, P. Lindqvist-Reis, K. Hermansson, I. Persson and M. Sandström, *J. Am. Chem. Soc.* **123**, 431 (2001).

[24] S. McLain, S. Imberti, A. K. Soper, A. Botti, F. Bruni and M. A. Ricci, *Phys. Rev. B* **74**, 094201 (2006).

[25] H. Ohtaki and T. Radnal, *Chem. Rev.* **93**, 1157 (1993).

[26] D. Feller, E. D. Glending, R. A. Kendall and K. A. Peterson, *J. Chem. Phys.* **100**, 4981 (1993).

[27] M. Adrian-Scotto, G. Mallet and D. Vasilescu, *J. Mol. Struc.:THEOCHEM* **728**, 231 (2005).

[28] T. Dudev and C. Lim, *J. Phys. Chem. A* **103**, 8093 (1999).

[29] M. Alcamí, A. I. González, O. Mó and M. Yáñes, *Chem. Phys. Lett.* **307**, 244 (1999).

[30] M. Pavlov, P. E. M. Siegbahn and M. Sandström, *J. Phys. Chem. A* **102**, 219 (1998).

[31] A. K. Katz, J. P. Glusker, S. A. Beebe and C. W. Bock, *J. Am. Chem. Soc.* **118**, 5752 (1996).

[32] C. W. Bock, A. Kaufmann and J. P. Glusker, *Inorg. Chem.* **33**, 419 (1994).

[33] I. B. Müller, L. S. Cederbaum and F. Tarantelli, *J. Phys. Chem. A* **108**, 5831 (2004).

[34] M. M. Naor, K. Van Nostrand, and C. Dellago, *Chem. Phys. Lett.* **369**, 159 (2003).

[35] I. Bakó, J. Hutter and G. Pálinkás, *J. Chem. Phys.* **117**, 9838 (2002).

[36] F. C. Lightstone, E. Schwegler, R. Q. Hood, F. Gygi and G. Galli, *Chem. Phys. Lett.* **343**, 549 (2001).

[37] F. C. Lightstone, E. Schwegler, M. Allesch, F. Gygi and G. Galli, *Chem. Phys. Chem.* **6**, 1 (2005).

[38] J. A. White, E. Schwegler, and G. Galli, *J. Chem. Phys.* **113**, 4668 (2000).

[39] A. P. Lyubartsev, K. Laaksonen and A. Laaksonen, *J. Chem. Phys.* **114**, 3120 (2001).

[40] B. Hribar, N. T. Southall, V. Vlachy and K. A. Dill, *J. Am. Chem. Soc.* **124**, 12302 (2002).

[41] L. M. Ramaniah, M. Bernasconi and M. Parrinello, *J. Chem. Phys.* **111**, 1587 (1999).

[42] T. Ikeda, M. Boero and K. Terakura, *J. Chem. Phys.* **126**, 034501 (2007).

[43] M. Carrillo-Tripp, H. Saint-Martín and I. Ortega-Blake, *J. Chem. Phys.* **118**, 7062 (2003).

[44] M. I. Bernal-Uruchurtu and I. Ortega-Blake, *J. Chem. Phys.* **103**, 1588 (1995).

[45] D. Asthagiri, L. R. Pratt, M. E. Paulaitis and S. B. Rempe, *J. Am. Chem. Soc.* **126**, 1285 (2004).

[46] S. Varma and S. B. Rempe, *Biophysical Chemistry* **124**, 192 (2006).

[47] M. Patra and M. Karttunen, *J.Comput.Chem.* **25**, 678 (2004).

[48] N. Troullier and J. Martins, *Phys. Rev. B* **43**, 1993 (1993).

[49] L. Delle Site, A. Alavi and R. M. Lynden-Bell, *Mol.Phys.* **96**, 1683 (1999).

[50] L. M. Ramaniah, M. Bernasconi and M. Parrinello, *J. Chem. Phys.* **109**, 6839 (1998).

[51] J. L. Li, R. Car, C. Tang and N. S. Wingreen, *Proc. of Nat. Academic of Sciences* **104**, 2626 (2007).

[52] S. F. Boys, *J. Chem. Phys.* **59**, 2254 (1973).

[53] P. L. Silvestrelli and M. Parrinello, *J. Chem. Phys.* **111**, 3572 (1999).

[54] P. L. Silvestrelli and M. Parrinello, *Phys.Rev..Lett.* **82**, 3308 (1999).

[55] L. Delle Site, R. M. Lynden-Bell and A. Alavi, *J.Mol.Liq.* **98-99**, 79 (2002).

[56] L. Delle Site, *Mol. Sim.* **26**, 217 (2001).

[57] L. Delle Site, *Mol. Sim.* **26**, 353 (2001).

[58] M. Kohout and A. Savin, *Int. J. Quantum Chem.* **60**, 875 (1996).

[59] A. D. Becke and K. E. Edgecombe, *J. Chem. Phys.* **92**, 5397 (1990).

[60] B. Silvi and A. Savin, *Nature* **371**, 683 (1994).

[61] R. S. Mulliken, *J. Chem. Phys.* **23**, 1833 (1955).

[62] K.P. Huber and G. Herzberg, 'Constants of Diatomic Molecules' (data prepared by J.W. Gallagher and R.D. Johnson, III) in NIST Chemistry WebBook, NIST Standard Reference Database Number 69, Eds. P.J. Linstrom and W.G. Mallard, June 2005, National Institute of Standards and Technology, Gaithersburg MD, 20899 (http://webbook.nist.gov).

[63] A. K. Soper and M. G. Phillips, *Chem. Phys.* **107**, 47 (1986).

[64] A. K. Soper, F. Bruni and M. A. Ricci, *J. Chem. Phys.* **106**, 247 (1997).

[65] A. P. Lyubartsev, K. Laaksonen and A. Laaksonen, *J. Chem. Phys.* **114**, 3120 (2001).

[66] C. P. Schulz, C. Boppert, T. Shimosato, K. Daigoku, N. Miura and K. Hashimoto, *J. Chem. Phys.* **119**, 11620 (2003).

[67] C. W. Bauschlicher,Jr., S. R. Langhoff, H. Partridge, J. E. Rice and A. Komornicki, *J. Chem. Phys.* **95**, 5142 (1991).

[68] E. D. Glendening and D. Feller, *J. Phys. Chem.* **99**, 3060 (1995).

[69] I. Džidić and P. Kebarle, *J. Phys. Chem.* **74**, 1466 (1970).

[70] H. M. Lee, P. Tarakeshwar, M. R. K. J. Park, Y. J. Yoon, H.-B. Yi, W. Y. Kim and K. S. Kim, *J. Phys. Chem. A* **108**, 2949 (2004).

[71] S. Raugei and M. L. Klein, *J. Chem. Phys.* **116**, 196 (2002).

[72] R. W. Gora, S. Roszak and J. Leszczynski, *Chem. Phys. Lett.* **325**, 7 (2000).

[73] J. Kim, H. M. Lee, S. B. Suh, D. Majumdar and K. S. Kim, *J. Chem. Phys.* **113**, 5259 (2000).

[74] J. E. Combariza, N. R. Kestner and J. Jortner, *J. Chem. Phys.* **100**, 2851 (1993).

[75] J. Baik, J. Kim, D. Majumdar and K. S. Kim, *J. Chem. Phys.* **110**, 9116 (1999).

[76] R. Ayala, J. M. Martineź, R. R. Papparlardo and E. S. Marcos, *J. Phys. Chem. A* **104**, 2799 (2000).

[77] J. K. Gregory, D. C. Clary, K. Liu, M. G. Brown and R. J. Saykally, *Science* **275**, 814 (1997).

[78] C. Krekeler and L. D. Site, *J. Phys.: Condens. Matter* **19**, 192101 (2007).

[79] J. A. Boon, A. Levisky, J. L. Pfug and J. S. Wilkes, *J. Org. Chem.* **51**, 480 (1986).

[80] K. Swiderski, A. McLean, C. M. Gordon and D. H. Vaughan, *Chem. Comm.* , 590 (2004).

[81] P. Wasserscheid, T. Weiss, F. Agel, C. Werth, A. Jess and R. Forster, *Angew. Chem. Int. Ed.* **46**, 7281 (2007).

[82] P. S. Schulz, N. Müller, A. Bösman and P. Wasserscheid, *Angew. Chem. Int. Ed.* **46**, 1293 (2007).

[83] A. Bösman, G. Francio, E. Janssen, M. Solinas, W. Leitner and P. Wasserscheid, *Angew. Chem. Int. Ed.* **40**, 2697 (2001).

[84] C. F. Weber, R. Puchta, N. J. R. van Eikema Hommes, P. Wasserscheid and R. van Eldik, *Angew. Chem. Int. Ed.* **44**, 6033 (2005).

[85] P. Wasserscheid and W. Keim, *Angew. Chem. Int. Ed. Engl.* **39**, 3772 (2000).

[86] P. Wasserscheid, R. van Hal and A. Bösman, *Green Chemistry* **4**, 400 (2002).

[87] L. A. Blanchard, D. Hancu, E. J. Beckman and J. F. Brennecke, *Nature* **399**, 28 (1999).

[88] J. Ešer, A. Jess and P. Wasserscheid, *Green Chemistry* **6**, 316 (2004).

[89] A. P. Abbott, P. M. Cullis, M. J. Gibson, R. C. Harris and E. Raven, *Green Chemistry* **9**, 868 (2007).

[90] I. Billard, G. Moutier, A. Labet, A. E. Azzi, C. M. C. Gaillard and K. Lützenkirchen, *Inorg. Chem.* **42**, 1726 (2003).

[91] W. Xu and C. A. Angell, *Science* **302**, 422 (2003).

[92] J.-P. Belieres, D. Gervasio and C. A. Angell, *Chem. Comm.* , 4799 (2006).

[93] C. Cadena, J. L. Anthony, J. K. Shah, T. I. Morrow, J. F. Brennecke and E. J. Maginn, *J. Am. Chem. Soc.* **126**, 5300 (2004).

[94] P. Wasserscheid, *Nature* **439**, 797 (2006).

[95] R. D. Rogers, *Nature* **447**, 917 (2007).

[96] A. Taubert and Z. Li, *Dalton Trans.* , 723 (2007).

[97] R. D. Rogers and K. R. Seddon, *Science* **302**, 792 (2003).

[98] P. Wasserscheid, *Ionic Liquids in Synthesis*, Wiley-VCH, Weinheim, 2007.

[99] J. Dupont, R. F. de Souza and P. A. Z. Suarez, *Chem. Rev.* **102**, 3667 (2002).

[100] P. Wasserscheid and W. Keim, *Angew. Chem. Int. Ed. Engl.* **39**, 3772 (2000).

[101] T. Welton, *Chem. Rev.* **99**, 2071 (1999).

[102] K. R. Seddon, A. Stark and M.-J. Torres, *Pure Appl. Chem.* **72**, 2275 (2000).

[103] W. L. Hough, M. Smiglak, H. Rodriguez, R. P. Swatloski, S. K. Spear, D. T. Daly, J. Pernak, J. E. Grisel, R. D. Carliss, M. D. Soutullo, J. H. Davis, Jr. and R. D. Rogers, *New J. Chem.* **31**, 1429 (2007).

[104] M. Bühl, A. Chaumont, R. Schurhammer and G. Wipff, *J. Phys. Chem. B* **109**, 18591 (2005).

[105] M. G. Del Pópolo, R. M. Lynden-Bell and J. Kohanoff, *J. Phys. Chem. B* **109**, 5895 (2005).

[106] Z. Lui, S. Huang and W. Wang, *J. Phys. Chem.B* **108**, 12978 (2004).

[107] S. Kossmann, J. Thar, B. Kirchner, P. A. Hunt and T. Welton, *J. Chem. Phys.* **124**, 174506 (2006).

[108] E. A. Turner, C. C. Pye and R. D. Singer, *J. Phys. Chem. A* **107**, 2277 (2003).

[109] C. E. Resende Prado, M. G. Del Pópolo, T. G. A. Youngs and J. K. R. M. Lynden-Bell, *Mol. Phys.* **104**, 2477 (2006).

[110] personal communication with Robert Berger, FIAS, Frankfurt a.M.

[111] personal communication with Christian Holm, FIAS, Frankfurt a.M.

[112] For this work we used the version 3.11.1 of the CPMD code. CPMD, J. Hutter, A. Alavi, T. Deutsch, M. Bernasconi, St. Goedecker, D. Marx, M. Tuckerman, M. Parrinello, MPI für Festkörperforschung and IBM Zurich Research Laboratory 1995-1999. / http://www.cpmd.org.

[113] C. Krekeler, B. Hess and L. D. Site, *J. Chem. Phys.* **125**, 053405 (2006).

[114] (a) J. N. C. Lopes, J. Deschamaps, A. A. H. Pádua, J. Phys. Chem. B **108**, 2038-2047 (2004); (b) J. N. C. Lopes, J. Deschamaps, A. A. H. Pádua, J. Phys. Chem. B **108**, 11250 (2004); (c) J. N. C. Lopes, J. Deschamaps, A. A. H. Pádua, J. Phys. Chem. B **108**, 16893-16898 (2004); (d) J. N. C. Lopes, J. Deschamaps, A. A. H. Pádua, J. Phys. Chem. B **110**, 7485-7489 (2006); (e) J. N. C. Lopes, J. Deschamaps, A. A. H. Pádua, J. Phys. Chem. B **110**, 19586-19592 (2006).

[115] Y. Wang, S. Izvekov, T. Yan and G. A. Voth, *J. Phys. Chem. B* **110**, 3564 (2006).

[116] T. H. Dunning JR., *J. Chem. Phys.* **90**, 1007 (1989).

[117] supplementary data can be provided.

[118] B. Qiao, C. Krekeler, R. Berger, L. Delle Site and C. Holm, *J. Phys. Chem. B* **112**, 1743 (2008).

[119] K. Hashimoto and K. Morokuma, *J.Am.Chem.Soc.* **116**, 11436 (1994).